Oxidation of Tetrahydropyridines by MAO B Biomimetics: Mechanistic Studies

Nathan James Price

Dissertation submitted to the faculty of the Virginia Polytechnic Institute and State University in partial fulfillment of the requirements for the degree of

Doctor of Philosophy
In
Chemistry

James M. Tanko – Chair
Andrew N. Lowell
Webster L. Santos
Pablo Sobrado

September 19, 2024
Blacksburg VA, 24061

Keywords: biomimetic, oxidation, nuclear magnetic resonance (NMR), electron paramagnetic resonance (EPR), persistent radicals, proton-coupled electron transfer (PCET)

Oxidation of Tetrahydropyridines by MAO B Biomimetics: Mechanistic Studies

Nathan J. Price

Abstract

The Parkinsonian Syndrome-inducing effects of 1-methyl-4-phenyl-1,2,3,6-tetrahydropyridine (MPTP) on the body have been well-documented since its discovery. However, its mechanism of oxidation by monoamine oxidase B (MAO B) has been debated for just as long. Proponents of the single electron transfer (SET) pathway of oxidation faced severe critiques in that the hypothesized radical intermediates arising from the SET pathway were never directly observed. Work performed herein provides that exact evidence using biomimetics of MAO B.

The first section of the dissertation will highlight the ability of one such biomimetic, 3-methyllumiflavin (3MLF), to provide a chemical model for the oxidation of β-unsaturated tetrahydropyridines. Using a nontoxic analog of MPTP, 1-methyl-4-(1-methyl-1-H-pyrrol-2-yl)-1,2,3,6-tetra-hydropyridine (MMTP), reactions with 3MLF were performed under both aerobic and anaerobic conditions. The anaerobic studies of these reactions proved to be the key to the direct observations (by ^{1}H NMR and EPR) of flavin-derived radical behavior.

Armed with the knowledge of how to prepare reactions for the direct observation of flavin radical intermediates, studies of *N*-cyclopropyl substrate derivatives were subsequently conducted to gather evidence for the formation of radical substrate intermediates. If the hypothesized SET is the first step of the reaction mechanism, then the resulting aminyl radical cation could undergo a cyclopropyl ring opening. Several products derived from the substrate were observed; among them were ring-opened variations

suggesting that the reaction does begin with a SET. Thermodynamically, this process is unfavorable, leading to the hypothesis that this reaction step may be better described as a proton-coupled electron transfer (PCET). The kinetics of this process were studied at length.

Finally, to provide a more compelling argument for the fundamental reactivities, two other flavin biomimetics are investigated. Their reactions with tetrahydropyridines were put under the same scrutiny as 3MLF, leading to the conclusion that the chemistry discussed herein is not unique to 3MLF, but is much more broadly applicable to other flavin biomimetics and MAO B.

Oxidation of Tetrahydropyridines by MAO B Biomimetics: Mechanistic Studies

Nathan J. Price

General Audience Abstract

First reported in 1982, Parkinsonian Syndrome related to the injection of the designer drug meperidine was linked to an impurity in the drug, 1-methyl-4-phenyl-1,2,3,6-tetrahydropyridine, MPTP. That compound was able to be oxidized in the brain by the enzyme monoamine oxidase B (MAO B) to form the neurotoxin 1-methyl-4-phenylpyridinium (MPP^+). For many years, the way that oxidation occurred remained a mystery as MPTP is chemically very different than typical substrates of MAO B. One type of reaction, single electron transfer (SET), which involves the production of high-energy intermediates called radicals, was largely overlooked as it seemed chemically implausible, especially in a biological system.

This dissertation will focus on providing evidence for the SET oxidation of MPTP-like molecules using a class of compounds called flavins. Flavins are biomimetics of MAO B, meaning they behave in reaction vessels the same way that MAO B behaves biologically. Evidence for the SET pathway comes primarily in two forms: nuclear magnetic resonance (^{1}H NMR) and electron paramagnetic resonance (EPR). Each of these techniques allow us to "see" exactly what species are present in solution. In the case of ^{1}H NMR, we will be able to see the "normal" molecules, while EPR allows us to see the high energy radical species in solution. Using these techniques, several substrate and flavin analogs were investigated to uncover a universal reaction mechanism by which MPTP and related compounds are oxidized by MAO B.

Dedication

This dissertation is dedicated to my parents, Brian and Christy Price, to my sister, Allison Smith, and to my wife, Megan Price.

Acknowledgements

First and foremost, I would like to thank my Ph. D. advisor, Dr. Tanko. The choice to join your group was the single best decision that I made during my time at Virginia Tech. Your constant support and patience as I worked through struggles both personal and professional has been second to none. Even through a pandemic, you served as a beacon of joy and a constant reminder that there is a light at the end of the tunnel. Thank you for giving me the space to grow as a person when I needed it (and for bearing down on me when I needed that). I will always cherish your mentorship.

To my committee members, Dr. Lowell, Dr. Santos, and Dr. Sobrado, thank you all for agreeing to learn with me as this project has blossomed. I know that physical organic chemistry isn't the most exciting (to some), but your willingness to challenge me with your unique perspectives on my research has encouraged me to grow as a scientist. I hope that I have managed to capture those perspectives herein and that you see some of yourselves reflected in this work. I hope to be able to share my own perspective with others as I progress in my career.

To my friends who have undeniably struggled with me throughout graduate school, thank you all for the reminder that things really aren't so bad. Chase, Emma, and Clark, you all have been a constant in my life for far too long not to get a shout out here. The three of you help keep me grounded, reminding me that it's okay to be a real person even when my professional life is in turmoil. Thank you all for the space that you've granted me. I hope I have been and will continue to be able to do the same for you. To my chronically online friends, thank you for the distraction from reality that you provided. Often, I found

that a welcome distraction helped me refocus myself, leading to more than its fair share of breakthroughs. I will continue to welcome distractions in my life.

To my parents, thank you from the bottom of my heart for raising me to ask questions and always be curious. That desire to learn more is at the core of this thesis and everything that I do. You have both been nothing but supportive, always there to lean on if needed but (usually) not overbearing. I love you both dearly and hope that you actually read this whole thing. To my sister, thank you for showing me that it's okay to be unapologetically myself. Your example has taught me that life is too short to conform to every expectation; thanks Al.

To my wife, I sincerely cannot describe the depths of my love and appreciation for you in a single paragraph. You have been here for every step of this journey, and your support has dragged me through to the finish line. I hope that I am able to provide you the same support that you have shown me for the rest of our lives. Megan, the long con is finally up.

To anyone that has been with me through this process who went without mention, know that you have my deepest thanks and appreciation for the support that you have shown.

Table of Contents

Abstract ii
General Audience Abstract iv
List of Figures x
List of Schemes xiii
List of Tables xiv
Attributions xv
Chapter 1: How MPTP Provided Fresh Perspective on the Monoamine Oxidase Catalytic Cycle 1
- **1.1 Introduction and Motivation** 1
- **1.2 Biochemistry of Monoamine Oxidase** 2
- **1.3 The MPTP Model of PD** 4
- **1.4 Proposed Mechanisms for MAO Catalysis** 6
  - **1.4.1 Polar Nucleophilic Pathway** 6
  - **1.4.2 Hydride Transfer Pathway** 8
  - **1.4.3 Single Electron Transfer (SET) Pathway** 10
- **1.5 Proton Coupled Electron Transfer (PCET)** 17
- **1.6 Silent NMR** 19
- **1.7 Scope of Dissertation** 24
- **1.8 References** 25

Chapter 2: Why Does Monoamine Oxidase (MAO) Catalyze the Oxidation of Some Tetrahydropyridines? 28
- **2.1 Abstract** 28
- **2.2 Introduction** 28
- **2.3 Results** 35
  - **2.3.1 Reaction of MMTP and 3MLF in the Presence of O_2** 35
  - **2.3.2 Reaction of MMTP and 3MLF in the Absence of O_2** 37
- **2.4 Discussion** 44
- **2.5 Conclusions** 47
- **2.6 References** 50

Chapter 3: Using Cyclopropyl Spin Traps as Radical Probes for the Oxidation of MPTP 53
- **3.1 Abstract** 53
- **3.2 Introduction** 53
- **3.3 Anaerobic Reactions of Cyc-MPTP with 3MLF** 56
- **3.4 Aerobic Reactions of Cyc-MPTP with 3MLF** 59
- **3.5 Physical Organic Studies of MMTP and MPTP Reactivities** 68
- **3.6 Conclusions** 73
- **3.7 References** 76

Chapter 4: Exploration of Alternative Flavins for Biomimetic Studies 77
- **4.1 Abstract** 77
- **4.2 Introduction** 77
- **4.3 10-ethyl-3-methyllumiflavin (ETD)** 79
- **4.4 5,10-diethyl-3-methyllumiflavinium perchlorate (5-Et-ETD$^+$)** 85
- **4.5 Future Work** 92
- **4.6 Conclusions** 94

4.7 References **95**
Appendix A: *Why Does Monoamine Oxidase (MAO) Catalyze the Oxidation of Some Tetrahydropyridines?* **96**
Appendix B: *Using Cyclopropyl Spin Traps as Radical Probes for the Oxidation of MPTP* **108**
Appendix C: *Exploration of Alternative Flavins for Biomimetic Studies* **130**

List of Figures

Figure 1.1: General metabolism scheme for oxidation of primary amines to aldehydes
Figure 1.2: Flavin redox couple
Figure 1.3: MAO B catalyzed oxidation of MPTP to generate the neurotoxic metabolite, MPP^+
Figure 1.4: Proposed mechanism for the polar nucleophilic pathway using a benzylamine substrate
Figure 1.5: Single-electron transfer redox forms of flavin moiety.
Figure 1.6: Proposed mechanism for the hydride transfer pathway using a general amine substrate
Figure 1.7: The proposed reaction schemes for SET
Figure 1.8: SET mechanisms first proposed by Silverman using *N*-cyclopropylbenzylamine as substrate
Figure 1.9: Proposed reaction scheme for the oxidation of 1-phenylcyclobutylamine
Figure 1.10: General thermodynamic square scheme to represent PCET reactions
Figure 1.11: Overall reaction of MMTP with Fl^+ to produce MMP^+ with $MMTPH^+$ byproduct
Figure 1.12: Time dependence on reaction mix for the oxidation of MMTP by 3-methyllumiflavinium perchlorate under aerobic conditions (A) and anaerobic conditions (B)
Figure 1.13: Proposed mechanism highlighting the potentially important early role of molecular oxygen in the reaction of 3-MLF^+ with MMTP
Figure 2.1: MAO B catalyzes the oxidation of MPTP to MMP^+
Figure 2.2: Proposed concerted mechanisms for MAO catalysis
Figure 2.3: Use of a single electron transfer probe to examine the mechanism of MAO-catalyzed oxidations
Figure 2.4: The reaction mechanism for the oxidation of MMTP by 5-ethyl-3-methyllumiflavinium perchlorate (Fl^+) proposed by Nakamura, et al.
Figure 2.5: Modified single electron transfer (SET) hypothesis
Figure 2.6: Structures of 5-ethy-3-methyllumiflavinium perchlorate and 3-methyllumiflavin
Figure 2.7: A plot of concentration vs. time for an aerobic 8:1 MMTP:3MLF reaction
Figure 2.8: ^1H NMR spectrum of a reaction mixture of 3MLF and MMTP (1:1) under anaerobic conditions at t = 4 hours (top) demonstrates the disappearance of 3MLF from the ^1H NMR
Figure 2.9: ^1H NMR spectra of 1:1 reaction of MMTP and 3MLF (2.50 mM each) in CD_3CN recorded as a function of time
Figure 2.10: The EPR spectrum of a 1:1 MMTP:3MLF (2.50 mM each) reaction at t = 225 minutes
Figure 2.11: M06-2X/6-311G* calculated spin density surfaces of several flavin radicals
Figure 2.12: Proposed self-exchange reactions for flavin radicals with neutral 3MLF starting material
Figure 2.13: ^1H NMR spectrum of a 1:1 (MMTP:3MLF, 2.05 mM) reaction, taken after approximately four hours, is shown at two different temperatures
Figure 2.14: Proposed mechanism for the reaction of 3MLF with MMTP
Figure 2.15: Tertiary amines that interact with MAO B

Figure 3.1: Proposed mechanism for the reaction of 3MLF with MMTP
Figure 3.2: Left: Classical cyclopropylcarbinyl rearrangement probe. Right: Use of a single electron transfer probe to examine the mechanism of MAO-catalyzed oxidations
Figure 3.3: The ^{1}H NMR spectra for a 1:1 anaerobic reaction of cyc-MPTP and 3MLF
Figure 3.4: The 1:1 aerobic reaction of 3MLF and cyc-MPTP (5.00 mM each) was monitored as a function of time by ^{1}H NMR
Figure 3.5: The reaction distillate (top) is compared directly with pure propionaldehyde (bottom)
Figure 3.6: The aerobic 1:1:1 reaction of cyc-MPTP-d4, MPTP, and 3MLF
Figure 3.7: A mechanistic hypothesis for the oxidation of cyc-MPTP by 3MLF
Figure 3.8: Two pathways of initial oxidation of MPTP
Figure 3.9: Spectra demonstrating the overlap of MPTP and MPTP-d4 ^{1}H NMR signals in the 1:1:1 reaction of MPTP, MPTP-d4, and 3MLF
Figure 3.10: The plot of ln[substrate] vs time for the oxidation of MPTP and MPTP-d4 with 3MLF
Figure 3.11: Proposed mechanism for the oxidation of MMTP and MPTP by 3MLF
Figure 4.1: The structures of 3MLF, ETD, 5-Et-3MLF^{+}, and 5-Et-ETD^{+}
Figure 4.2: The time resolved ^{1}H NMR spectra for the 8:1 (MMTP:ETD) aerobic reaction of MMTP and ETD with a benzene internal standard
Figure 4.3: Time-resolved ^{1}H NMR spectra for the 1:4 (MMTP:ETD) anaerobic reaction of ETD and MMTP
Figure 4.4: The EPR spectra for the anaerobic 1:1 reactions of ETD and MMTP (left) and the 1:1 reaction of 3MLF and MMTP (right) after 4 hours of reaction
Figure 4.5: The time-resolved ^{1}H NMR spectra for the 1:3 (5-Et-ETD^{+}:MMTP) aerobic reaction of 5-Et-ETD^{+} and MMTP
Figure 4.6: The reference ^{1}H NMR spectra for MMTPH^{+}•Cl^{-} (top) and MMTP (bottom)
Figure 4.7: Time-resolved ^{1}H NMR spectra for the 1:2 (5-Et-ETD^{+}:MMTP) reaction of 5-Et-ETD^{+} and MMTP
Figure 4.8: The liquid chromatogram (top) associated with the 1:2 (5-Et-ETD^{+}:MMTP) reaction of 5-Et-ETD^{+} and MMTP
Figure 4.9: The hypothesized reaction mechanism for the oxidation of MMTP by 5-Et-ETD^{+}
Figure 4.10: The hypothesized mechanism for the reaction of cyclopropyl MMTP and 5-Et-ETD^{+}
Figure A.1: Reference spectra for 3MLF (top), MMP^{+} (middle), and MMTP (bottom)
Figure A.2: ^{1}H NMR spectral assignments for MMTP, MMP^{+}, and 3MLF
Figure A.3: The complete 1:1 aerobic reaction of MMTP and 3MLF
Figure A.4: An 8:1 aerobic reaction of MMTP and 3MLF was allowed to occur with sporadic monitoring for 11 days
Figure A.5: The 1:1 anaerobic reaction of MMTP and 3MLF demonstrates little significant change after the first 48 hours
Figure A.6: This reaction, begun anaerobically and exposed to air after 1 hour, proceeded normally as an aerobic reaction
Figure A.7: The EPR spectrum of a 1:1 (MMTP:3MLF, 2.05 mM) reaction at t = 30 minutes.

Figure A.8: The EPR spectrum of a 1:1 (MMTP:3MLF, 2.05 mM) reaction at t = 40 minutes.
Figure A.9: The EPR spectrum of a 1:1 (MMTP:3MLF, 2.05 mM) reaction at t = 60 minutes.
Figure A.10: The EPR spectrum of a 1:1 (MMTP:3MLF, 2.05 mM) reaction at t = 90 minutes.
Figure A.11: The EPR spectrum of a 1:1 (MMTP:3MLF, 2.05 mM) reaction at t = 120 minutes.
Figure A.12: The EPR spectrum of a 1:1 (MMTP:3MLF, 2.05 mM) reaction at t = 150 minutes.
Figure A.13: The EPR spectrum of a 1:1 (MMTP:3MLF, 2.05 mM) reaction at t = 225 minutes.
Figure B.1: The reference ^{1}H NMR spectrum for 3MLF
Figure B.2: The reference ^{1}H NMR spectrum for cyc-MPTP
Figure B.3: ^{1}H NMR spectral assignments for the hypothesized dihydropyridinium intermediate
Figure B.4: ^{1}H NMR spectral assignments for the hypothesized iminium intermediate
Figure B.5: Mass spectra for the hypothesized intermediates and products for the reaction of 3MLF with cyc-MPTP
Figure B.6: Total ion (top) and selected ion chromatograms for the hypothesized intermediates and products for the reaction of 3MLF with cyc-MPTP
Figure B.7: Anaerobic 1:1 reaction of 3MLF and cyc-MPTP shown as a function of time
Figure B.8: Time-resolved ^{1}H NMR spectra from the aerobic 1:1 reaction of 3MLF and cyc-MPTP
Figure B.9: The time-resolved ^{1}H NMR spectra from the aerobic 1:1 reaction of 3MLF and cyc-MPTP-d4
Figure B.10: Time resolved ^{1}H NMR spectra for the aerobic 1:2 (3MLF:MPTP) reaction of 3MLF and MPTP
Figure B.11: Time resolved ^{1}H NMR spectra for the aerobic 1:2 (3MLF:MPTP-d4) reaction of 3MLF and MPTP-d4
Figure B.12: Time resolved ^{1}H NMR spectra for the aerobic 1:2 (3MLF:MMTP) reaction of 3MLF and MMTP
Figure B.13: Time resolved ^{1}H NMR spectra for the aerobic 1:2 (3MLF:MMTP-d4) reaction of 3MLF and MMTP-d4
Figure B.14: Plot of ln[MPTP-d4] and ln[MPP^{+}] vs. time
Figure B.15: Plot of ln[MPTP] and ln[MPP^{+}] vs. time
Figure B.16: Plot of ln[MPTP-d4] and ln[MPP^{+}] vs. time
Figure B.17: Plot of ln[MPTP] and ln[MPP^{+}] vs. time
Figure B.18: Plot of ln[MMTP-d4] and ln[MMP^{+}] vs. time
Figure B.19: Plot of ln[MMTP] and ln[MMP^{+}] vs. time
Figure B.20: Plot of ln[MMTP-d4] and ln[MMP^{+}] vs. time
Figure B.21: Plot of ln[MMTP] and ln[MMP^{+}] vs. time
Figure C.1: Several ^{1}H NMR spectra for the 1:1 aerobic reaction of MMTP and 5-Et-ETD^{+} in the presence of water
Figure C.2: Several ^{1}H NMR spectra for the aerobic 1:1 reaction of 5-Et-ETD^{+} and MMTP in the presence of water

List of Schemes

Scheme 3.1: Proposed anaerobic radical equilibrium of 3MLF from Price et al.
Scheme 3.2: The proposed hydrolysis of iminium intermediate resulting from ring opening to form propionaldehyde and secondary amine
Scheme 3.3: Proposed hydrolysis step
Scheme 3.4: Hypothesized HAT processes to form the ring-opened intermediate
Scheme 3.5: The reaction of cyc-MPTP-d4, MPTP, and 3MLF is hypothesized to have two possible aldehydic product distributions
Scheme 3.6: Fate of ring-opened intermediate
Scheme 4.1: The reaction of MMTP and ETD is expected to produce the oxidized form of the substrate, MMP^+
Scheme 4.2: The hypothesized reaction mechanism for the oxidation of MMTP by ETD
Scheme A.1: The synthetic pathway to form MMTP

List of Tables

Table 3.1: Concentrations of Reactants and Products for the Aerobic Reaction of 3MLF and cyc-MPTP
Table 3.2: Average rate constants for the oxidation of H/D substituted MMTP and MPTP

Attributions

Chapter 1: Nathan Price (graduate student, Department of Chemistry, Virginia Tech) performed the writing and editing of this chapter. James M. Tanko (Ph.D., Department of Chemistry, Virginia Tech) is the advisor who provided guidance, writing, and editing of this chapter.

Chapter 2: Nathan Price (graduate student, Department of Chemistry, Virginia Tech) performed the experimentation, writing, and editing of this chapter. Akiko Nakamura (Ph. D., Department of Chemistry, Colorado State) and Neal Castagnoli (Ph. D., Department of Chemistry, Virginia Tech) are collaborators who provided preliminary evidence and guidance for this chapter. James M. Tanko (Ph.D., Department of Chemistry, Virginia Tech) is the advisor who provided guidance, writing, and editing of this chapter.

Chapter 3: Nathan Price (graduate student, Department of Chemistry, Virginia Tech) performed most of the experimentation, writing, and editing of this chapter. Bradley Engels (undergraduate student, Department of Chemistry, Virginia Tech) provided experimental assistance for this chapter. James M. Tanko (Ph.D., Department of Chemistry, Virginia Tech) is the advisor who provided guidance, writing, and editing of this chapter.

Chapter 4: Nathan Price (graduate student, Department of Chemistry, Virginia Tech) performed the methodology, writing, and editing of this chapter. Thomas Robbins (undergraduate student, Department of Chemistry, Virginia Tech) and Bradley Engels (undergraduate student, Department of Chemistry, Virginia Tech) performed most of the experimentation for this chapter. James M. Tanko (Ph.D., Department of Chemistry, Virginia Tech) is the advisor who provided guidance, writing, and editing of this chapter.

Chapter 1. How MPTP Provided Fresh Perspective on the Monoamine Oxidase Catalytic Cycle

1.1 Introduction and Motivation

Parkinson's disease (PD) is a neurodegenerative disease first identified by James Parkinson who described it in "*An Essay on the Shaking Palsy*" in 1817.[1] Among its symptoms are gait instability and tremor.[2] Pathologically, PD is known to be linked to the deterioration of nigrostriatal neurons, leading to a decrease in the neurotransmitter dopamine in the dopaminergic nigrostriatal region of the brain. As with other neurodegenerative diseases, PD is associated with the production of microglia-derived neurotoxins, specifically reactive oxygen species (ROS).[3] Among these are superoxide anion radicals and hydroxyl radicals.

Dopamine belongs to a class of neurotransmitters called catecholamines; other members of this group include epinephrine and norepinephrine. The metabolism of catecholamines and the indolylalkylamine serotonin is catalyzed by the mitochondria through the action of flavoenzymes monoamine oxidase-A and B (MAO A and MAO B). After the catalytic oxidation of amines by MAO, one equivalent of molecular oxygen (O_2) is consumed to re-oxidize the flavin moiety, producing H_2O_2 as a byproduct. Hydrogen peroxide is a well-established ROS precursor. In high concentrations, reactive oxygen species are known to trigger the release of cytochrome c from the mitochondrial membrane, beginning a cascading effect which eventually results in cellular apoptosis.[36] Dopamine deficiency resultant from the loss of nigrostriatal neurons was linked to PD in a paper published by Carlsson *et al*.[4] It has been estimated that once striatal dopamine levels decrease by 20%, symptoms of PD begin appearing.[5]

In addition to its role in PD, MAO has recently been linked to heart disease.[6-9] The oxidative stress caused by the production of reactive oxygen species by peripheral MAO activity is believed to cause both structural and functional issues in cardiac tissue.[6] The primary indicators

for this increased stress are believed to be the aldehyde-bearing intermediates generated by metabolic MAO activity, and ROS produced as a byproduct of MAO oxidation as these species are known to target mitochondria.[7,8] As a result, monoamine oxidase inhibitors (MAOIs) are actively being pursued as potential treatments for heart disease.

1.2 Biochemistry of Monoamine Oxidase

As stated above, MAO is a mitochondrial flavoenzyme that catalyzes the oxidative deamination of amine-containing neurotransmitters and xenobiotics (4) into iminyl metabolites (5) as shown in Figure 1.1.[13] These intermediates then leave the enzyme active site where they undergo non-enzymatic hydrolysis to yield the corresponding aldehydes (6).[14] Given the role MAO plays in neurotransmitter regulation, the enzyme is often targeted to treat neurological disorders such as PD and depression.

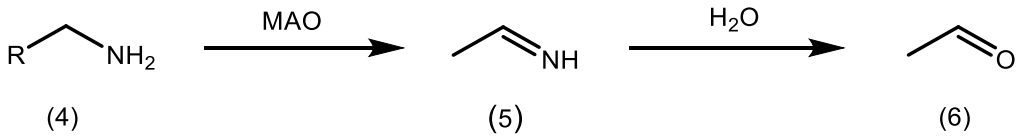

Figure 1.1: General metabolism scheme for oxidation of primary amines to aldehydes

Divided into the isoforms A and B, MAO is primarily found in the CNS, though both are prevalent in peripheral tissues with the A isoform in particularly high concentrations in the gastrointestinal tract and the B isoform in the liver. However, the use of ladostigil, a multi-target cholinesterase and MAO inhibitor, has led to the enhancement and better understanding of drug localization to the brain to avoid peripheral side effects.[16] Efforts to isolate and purify these enzymes for study *in vitro* have proven fruitful. MAO B has been successfully isolated from the fungus *Pichia pastoris*.[18]

The A and B isoforms share only about 70% of their sequence identities, resulting in a slight difference in both substrate and inhibitor selectivities.[13] In general, MAO B preferentially

binds bulkier substrates while MAO A binding depends more on the electronic parameters of the substrate.[17] One instance of this behavior is noted with the affinities of the enzymes for benzylamines. Specifically, the A isoform has a significantly lower K_m value (~6 μM) than observed for MAO B (K_m = 240 μM).[17] However, neither is entirely specific for one class of amine over another. This has led to ambiguity in understanding the mechanisms by which each oxidizes substrates. Some believe it is unlikely that the two react by different mechanisms of α-C-H bond cleavage due to the similarity of their binding pockets.[13] The active site of MAO, as with all flavoenzymes, features a flavin moiety that accepts the two electrons from the aminyl substrate. The isoalloxazinyl ring of the flavin, shown in Figure 1.2, is considered one of the more versatile cellular redox cofactors.[15] While effective for catalysis, this versatility further complicates the understanding of its associated oxidative mechanism.

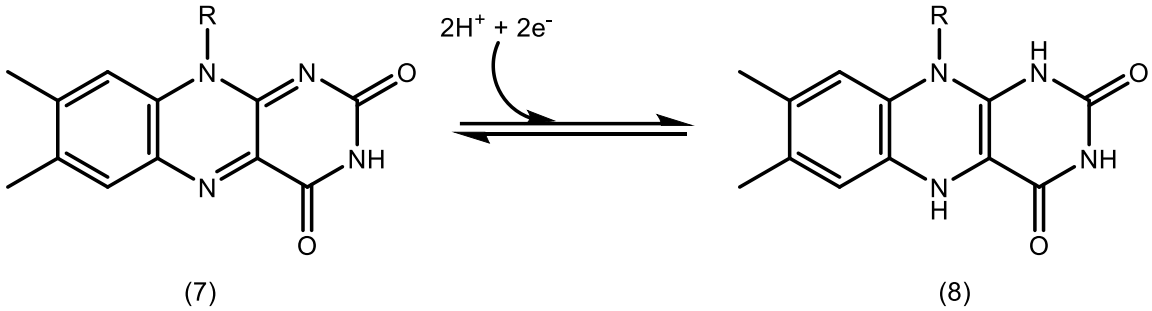

(7) (8)

Figure 1.2: Flavin (isoalloxazinyl) redox couple. The oxidized form (left) is present in the active site of MAO A and B and is responsible for oxidizing amine substrates. Post-catalysis, the reduced form of the flavin (right) is oxidized by O_2 to form H_2O_2 and the oxidized flavin.

Arising from seemingly contradictory results, competing hypotheses for the reaction mechanism are an unfortunate reality for studies conducted with MAO. In work done by Miller *et al.*,[17] anaerobic reductive titrations using a clorgyline substrate suggested only one equivalent of substrate (two reducing equivalents) is required for full oxidation via MAO A, meaning a redox-active disulfide group is likely not involved in the process. This contradicts previous work done by Sablin and Ramsay[17] who suggested that four reducing equivalents would be necessary for the

complete oxidation of substrate. A QSAR study of *para*-substituted benzylamine substrates showed a strong positive correlation (ρ = 1.89 ± 0.40) between the rate of flavin reduction and electron-withdrawing properties of the substituent, suggesting H^+ abstraction as the mode of C-H bond cleavage for the MAO A-catalyzed oxidation of benzylamine (the positive ρ-value suggests a buildup of negative charge in the transition state). A kinetic isotope effect (KIE) study showed the C-H bond cleavage is rate-limiting for substrates of MAO A (k_H/k_D ~7-10), also consistent with a H^+ abstraction.[17]

Brown et al. found what they believed to be a persistent radical form of MAO B. It was later determined that the radical residue was an artifact of the purification process and did not have any bearing on the activity of the enzyme.[18] However, recent work on the tyrosine-398 (Y398) residue has revealed a possible radical sink within the enzyme that may be of relevance to its activity.[26] The presence of radical species in MAO further complicates the already confusing state of research on the matter.

1.3 The MPTP Model of PD

An important part of the PD story relates to a small molecule, 1-methyl-4-phenyl-1,2,3,6-tetrahydropyridine (MPTP) (Figure 1.3). This cyclic tertiary allylamine, produced as a hydrolytic degradation product of the designer drug meperidine, unexpectedly proved to be an excellent and selective MAO B substrate.[10] Humans who intravenously injected this compound subsequently developed symptoms linked to PD. It has been shown that subjection to MPTP in humans and susceptible animals leads to the selective destruction of nigrostriatal dopaminergic neurons, a consequence of which is the emergence of Parkinsonian syndrome. We propose that an increased understanding of the mechanism of action of this compound may prove fruitful in gaining a better

understanding of the chemical causes of Parkinsonian syndrome and the development of potential therapeutic and/or neuroprotective agents or potential treatments for PD.

The MAO B catalyzed oxidation of MPTP leads eventually to the formation of the neurotoxic compound 1-methyl-4-phenylpyridiniumyl (MPP^+) (3) via the intermediate dihydropyridiniumyl species, $MPDP^+$ (2). The potency of MPTP as a neurotoxic precursor is directly related to its relative hydrophobicity and associated ease of transport through the blood-brain barrier. After oxidation by MAO B, the toxin, MPP^+, can be taken up into nigrostriatal nerve terminals via the action of the dopamine transporter (DAT). There, MPP^+ inhibits the electron transport chain and blocks the formation of ATP, leading to apoptosis.[11]

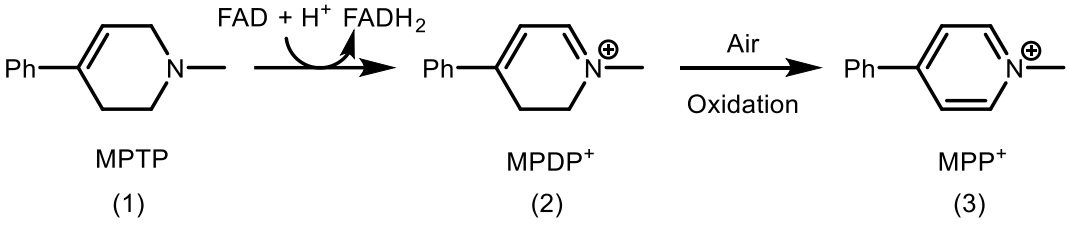

Figure 1.3: MAO B catalyzed oxidation of MPTP to generate the neurotoxic metabolite, MPP^+.

Because of a lack of evidence supporting a genetic link to PD,[12] environmental factors are considered by some to be a major cause of the disease. As such, studies of known initiators of the MAO B catalyzed oxidation of MPTP could prove invaluable to improving our understanding of the etiology of PD. Although there is a well-substantiated link between MAO and diseases that lead to the deterioration of nigrostriatal neurons, the chemical mechanism by which oxidation occurs in the enzyme is not fully understood.

The lack of agreement on the mechanism by which MAO oxidation occurs, has led to the proposal of three possible pathways (Figures 1.4, 1.6, 1.7). The first is a polar nucleophilic pathway in which a substrate proton transfer from the α-carbon position mediates the formation of an adduct

(Figure 1.4). The second is a direct hydride transfer from the same position on the adduct, resulting in direct oxidation to form an iminiumyl product with the corresponding flavinyl anion (Figure 1.6). The last proposed mechanism is a single electron transfer (SET) pathway in which the loss of an electron from the substrate results in the formation of an aminyl radical cation and semiquinone intermediate. Subsequent loss of a proton from the substrate results in a carbon-centered radical (Figure 1.7). Currently, the most widely accepted is the polar nucleophilic pathway, though it alone cannot account for all observed reaction phenomena.

1.4 Proposed Mechanisms for MAO Catalysis

1.4.1 Polar Nucleophilic Pathway

Brown *et al.* originally proposed a polar nucleophilic pathway for the MAO-catalyzed oxidation of amines by MAO in 1970.[19] They proposed a nucleophilic attack by the nitrogen lone pair of the aminyl substrate (10) directly to the C4a position of the flavin moiety (9) to generate an anionic adduct (11). The reduced flavin (12) and imine (13) are subsequently produced as products of the reaction. Several groups have provided support for this mechanism.

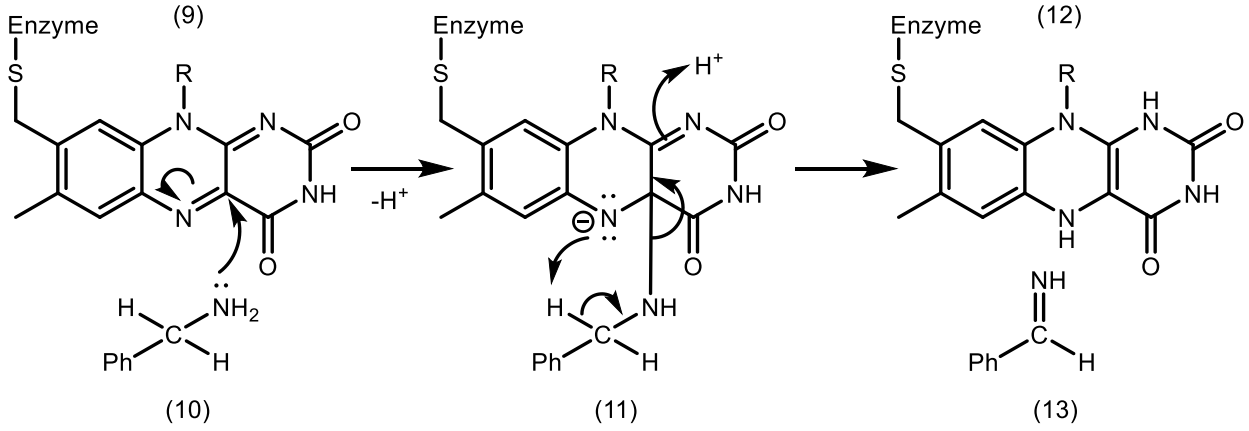

Figure 1.4: Proposed mechanism for the polar nucleophilic pathway using a benzylamine substrate (10). The nucleophilic amine (10) attacks the electrophilic C4a position (9) to form a covalent intermediate (11), followed by the cleavage of the oxidized imine product (13) to produce the fully reduced flavin (12).

For example, Miller *et al.* employed recombinant human liver MAO A to study reaction rates as a function of amine nucleophilicity.[17] Using substituted benzylaminyl substrates, they challenged the results of earlier QSAR studies performed by Strickland that suggested substrate α-C-H bond cleavage happens by direct hydrogen atom transfer (HAT) to a non-radical flavin moiety followed by electron transfer (ET) to the flavin. Miller found support for the polar mechanism for MAO A using QSAR involving a concerted C4a addition and proton abstraction by N5. This mechanism was consistent with observed electronic effects in QSAR studies with para- and meta-substituted benzylamines, KIEs, and the apparent lack of radicals via EPR spectroscopy. The consistency within these results suggests that a polar mechanism is able to account for the oxidations of many substrates by MAO.

This mechanism, however, cannot account for the oxidation of MPTP. The steric bulk of MPTP and other tertiary amines provides too high of an energetic barrier to form a covalent bond between the amine of the substrate and the C_4 position of the flavin moiety. So, to account for tertiary amine reactivity, alternative pathways that do not involve direct N_{amine}-C_4 bond formation became necessary. The two major contenders are hydride transfer and single-electron transfer (SET).

However, as discussed at length below, each of these mechanisms have their own faults. For the hydride transfer mechanism, evidence has relied primarily in the field of computational results, leading to questions about reliability as there is only scarce direct experimental support. Similarly, while SET is a plausible mechanism of oxidation, a lack of convincing experimental evidence is a long-standing detraction. Strong evidence for the SET mechanism would come from the detection of a semiquinone radical intermediate (14, Figure 1.5). Stopped flow experiments using 1-amino-1-benzoylcyclobutane spin trapping provided evidence for substrate radical

formation via EPR spectroscopy but not semiquinone formation. UV-Vis detection in the visible range only suggested the existence of a hydroquinone (8) in MAO B catalysis.[22] Due to an underwhelming lack of evidence for alternative pathways, the polar nucleophilic has become the de facto mechanism for these oxidations.

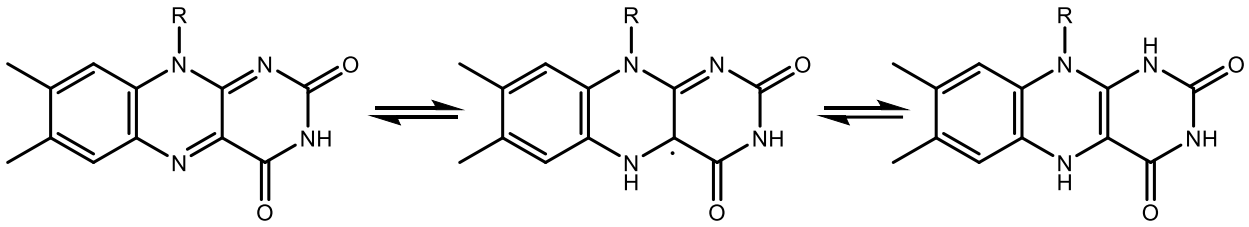

Figure 1.5: Single-electron transfer redox forms of flavin moiety.

1.4.2 Hydride Transfer Pathway

Recent evidence has suggested the hydride transfer pathway as a possible explanation for the observations made specifically with oxidations involving human MAO B. This pathway involves a direct hydride transfer from the substrate molecule (10) to the flavin moiety (9) to produce the iminium (16) with the corresponding flavin anion (15) as shown in Figure 1.6.

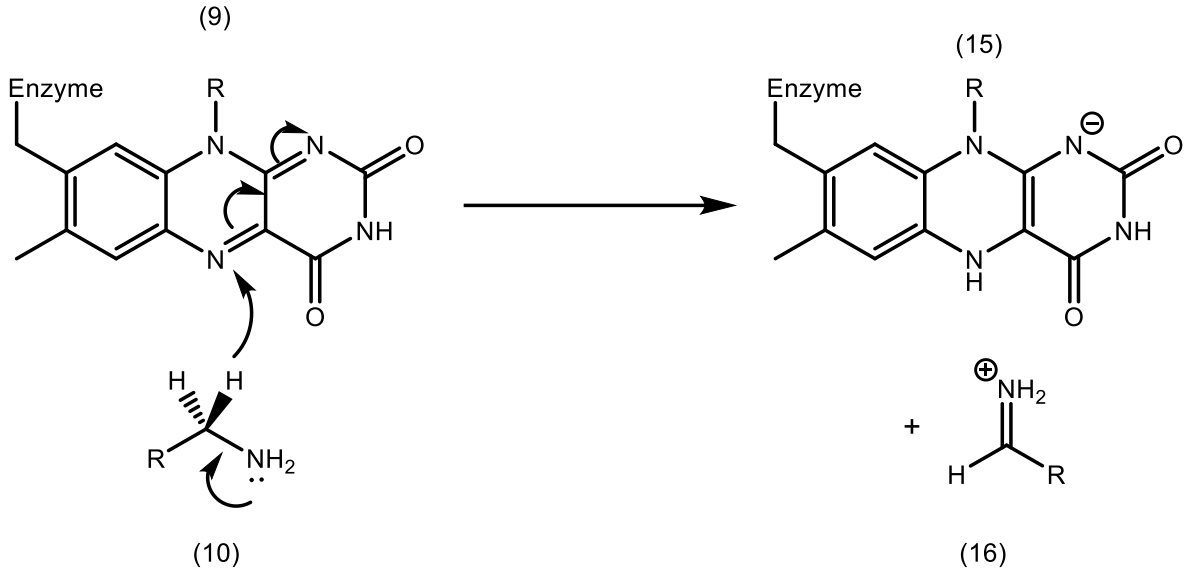

Figure 1.6: Proposed mechanism for the hydride transfer pathway using a general amine substrate (10). The hydride derived from the α-carbon directly attacks the N5 position on the flavin moiety (9), causing a cascading electron movement and resulting in the anion/cation pair shown (15/16). This is followed by a quick deprotonation facilitated by water trapped in the protein.[13]

Orru et al. studied the reaction parameters for the catalytic oxidation of substituted benzylamines at pH 9.0 by MAO B. Results of the QSAR study suggested that hydride transfer is the most reasonable explanation for the reaction due to a strong, negative ρ correlation (ρ = -0.9 ± 0.1).[35] This is directly contrary to results gathered previously by Wang et al. in previous studies using the same reaction conditions and substrates with MAO A (ρ = +0.8 ± 0.1).[35] Additionally, computational work done by Vianello et al. suggests that the hydride transfer mechanism is the most kinetically viable due to a lower transition state energy (24.4 kcal mol^{-1}) compared to the polar nucleophilic pathway (37.3 kcal mol^{-1}).[13] Instead of C4a addition, their proposed mechanism relies on direct hydride transfer to N5 which is posited to have a lower free energy of activation.[13] This study, however, is limited in substrate scope, only analyzing dopamine, ethylamine, and the ethylaminium cation, limiting its applicability to other known MAO substrates and inhibitors. Again, the limited evidence in support of this mechanism is its largest drawback at present.

1.4.3 Single Electron Transfer (SET) Pathway

The SET pathway, first proposed by Silverman, begins with the loss of an electron from the amine nitrogen to generate an aminyl radical cation (17) and flavin radical anion in the rate limiting step. The α-deprotonation of the aminyl radical cation is believed to be favorable due to the relative acidity of the α-proton whose pK_a is estimated to be ~10.[20]

There are two important arguments in favor of the polar pathway over SET. For SET, the proposed electron transfer is thermodynamically unfavorable. Oxidation of a primary amine by a ground state flavin moiety (Figure 1.7) is estimated to have a ΔG of 1.3 - 1.5 V (30 - 35 kcal/mol), based upon redox potentials. Additionally, no semiquinone has been observed via EPR spectroscopy.[17]

Kim et. al. published a paper using 3-methyllumiflavin (3MLF) as a biomimetic which suggested the polar nucleophilic mechanism is more appropriate than SET. However, the reaction conditions (wet acetonitrile heated to 80°C for 7 days to convert only 30% of benzylamine to its corresponding imine form) are so distant from biological conditions that this finding appears to be of limited relevance to the question of the MAO mechanism. Further, *N*-methylbenzylamine did not react under these conditions, despite being a known substrate for MAO.[21] One major conclusion from Kim was that steric hindrance played a very significant role in the reactivity of amines with MAO, to the extent that tertiary amines were completely nonreactive--consistent with the proposed polar pathway. In response to this, Silverman created a new series of *N*-cyclopropylbenzylamines to demonstrate that, at least for some inhibitors, the sterics of the amines are not of importance. In the reaction of MAO with *N*,α-dimethyl-N-(1-methylcyclopropyl)benzylamine $k_{inactivation}$ = 0.71 min^{-1}, despite being an extremely hindered amine.[21]

It was further posited that the resulting radical cation (17) could decompose in three distinct routes. The radical cation (17) could undergo a hydrogen atom transfer (HAT) with the flavin semiquinone (14) to directly produce the iminium product (16) alongside the fully reduced flavin (12, Figure 1.7A). The first step in either remaining path is a fast deprotonation from the α-C-H position of the radical cation to generate a neutral carbon-centered radical (18/19). From there, direct single electron transfer between the amine and the flavin yields the iminium product (16, Figure 1.7B). The final mechanism is a radical coupling between the carbon-centered radical and a single-electron donor/acceptor (20) to form a covalent adduct (21). This is followed by a two-electron transfer to the flavin to decouple the reactants, generating the same products (Figure 1.7C).[20]

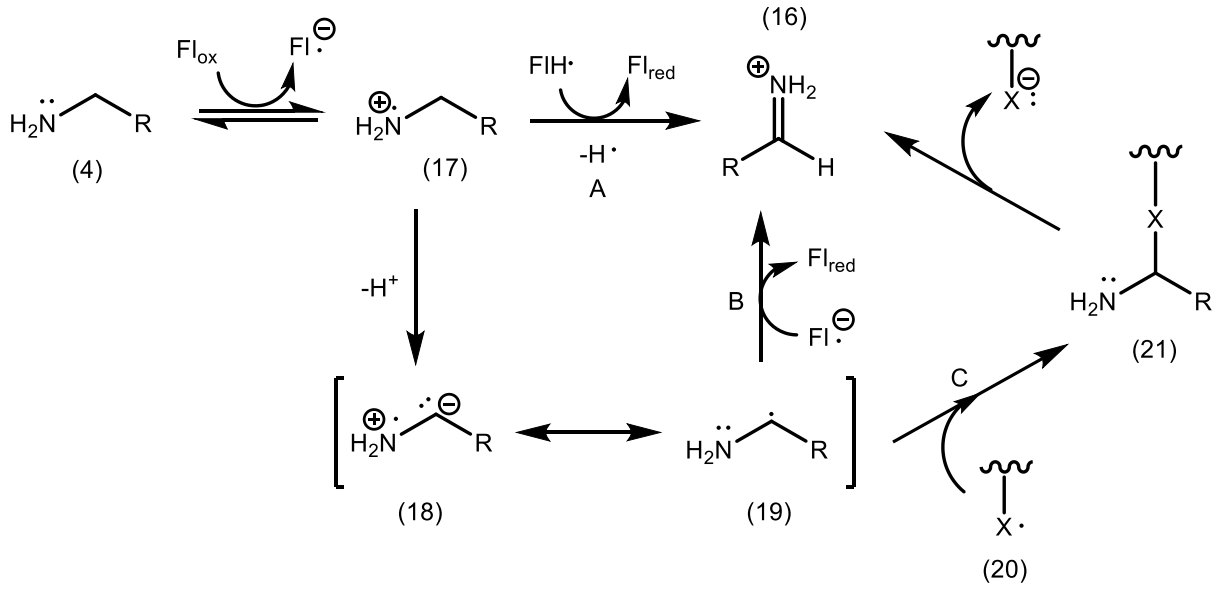

Figure 1.7: The proposed reaction schemes for SET all begin with the formation of the aminyl radical cation (17) then diverge: a) a direct HAT occurs between the aminyl radical (17) and the partially reduced semiquinone (14) b) deprotonation at the α position results in a neutral carbon-centered radical (18/19) which then undergoes SET with the partially reduced flavin (14) c) the neutral carbon-centered radical (18/19) couples to another radical species (20) to form an adduct (21), quickly decoupling afterward to form the iminium product.

Generally, the consensus is that the first step in a SET mechanism to produce the aminyl radical cation (17) is unfavorable, explaining the failure to detect the semiquinone (14) intermediate. The oxidized form of flavin is highly rigid and aromatic, but its reduced form must bend to avoid antiaromaticity. This bending may lower the LUMO energy, making SET to the enzyme a more facile process.[22] It is also suggested that distortion of the substrate and/or flavin geometry by binding, perturbation of reduction potential via binding, and/or endergonic tunneling over relatively short distances might facilitate this otherwise unfavorable electron transfer.[23]

Magnetic field effects (MFEs), which are typically used to detect radicals, have not been observed with MAO B, but that does not rule out the possibility of the SET mechanism. MFEs require a pair of spin-correlated radicals in at least one reaction step (allows for intersystem crossing between singlet and triplet states so the radicals must exist long enough for intersystem crossing to occur before relaxing). The reaction rate must be significantly sensitive with respect to the fraction of enzyme-substrate complex that requires spin correlation, and the conformational and binding steps which precede the reaction step of interest must be reversible.[23]

The lack of observed radical intermediates would suggest that any radicals produced are low in concentration, very short-lived, or spin-paired if they exist. To address this, cyclopropylamine and its derivatives (e.g. 22) were chosen as potential mechanism-based inhibitors in work done by Silverman.[20] Using this approach, it was expected that a flavin-bound ring-opened product would lead to MAO inactivation (Figure 1.8, Pathway c).[20,21,24]

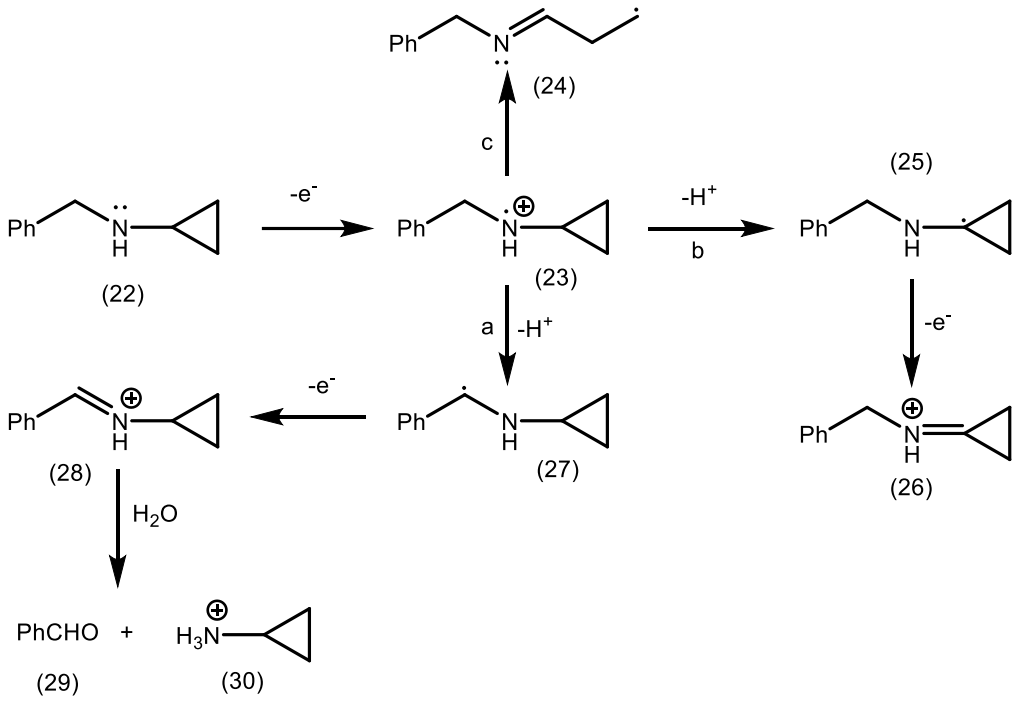

Figure 1.8: SET mechanisms first proposed by Silverman using *N*-cyclopropylbenzylamine as substrate. The anticipated ring-opened product (Pathway c) was not observed.

Similarly, in reactions with 2-phenylcyclobutylamine (31), it was expected that the formation of an imine (34/36) by the oxidation of the primary amine would initiate a radical ring-opening process, eventually leading to the formation of 2-phenyl-1-pyrroline (36) as shown in Figure 1.9.[24] Upon incubation of MAO with 2-phenylcyclobutylamine, a time-dependent amount of the pyrroline product (36) was formed (confirmed by HPLC-MS), supporting a radical mechanism.[24]

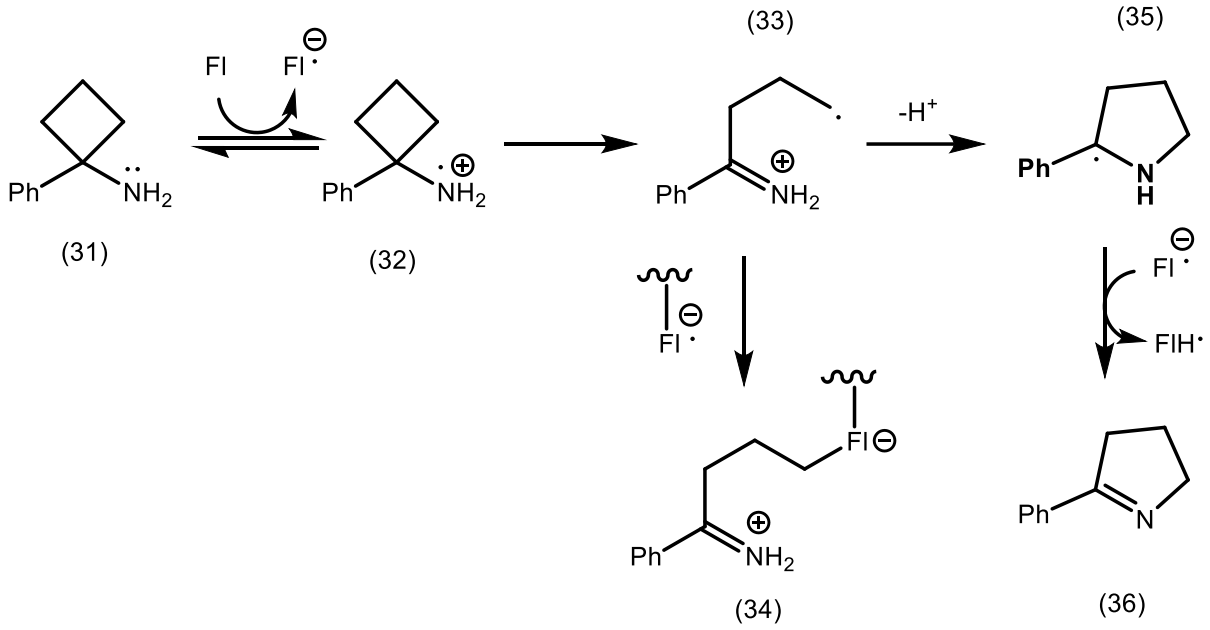

Figure 1.9: Proposed reaction scheme for the oxidation of 1-phenylcyclobutylamine

The work by Silverman and Krantz has provided evidence for the SET mechanism; however, they had thus far been unable to provide direct evidence of a radical intermediate. Yelekci et al. posited that this could be due to either a thermodynamic or kinetic problem.[22] They hypothesized that either the benzylamine radicals were not sufficiently thermodynamically stable (making them very short-lived) or that the oxidation of benzylamine is so efficient that all radical intermediates are processed rapidly. By enhancing radical stabilization via electron-donating/withdrawing groups on benzylamine, spin-trapping techniques proved to be effective. Using the spin trap and noncompetitive MAO inhibitor α-phenyl-*N*-*tert*-butyl nitrone (PBN), Yelekci et al. were able to capture an EPR spectrum as a result of its addition to 1-phenylcyclobutylamine radical in the presence of MAO B at room temperature over the course of 17 hours. This suggested that the SET between the benzylamine and the flavin was relatively slow. Notably, no EPR spectrum was observed in the absence of enzyme or in the presence of inactive

enzyme, when flavin mononucleotide is substituted for enzyme, when pargyline (an inactivator) is present, if the substrate is omitted, or if benzylamine is used instead of the chosen substrate.[22]

Although highly supported by model studies on lumiflavins in terms of kinetics, the highly unfavorable thermodynamics of electron transfer required for production of the aminyl radical cation has proven to be a great barrier to the acceptance of the SET pathway for MAO catalysis. Rigby proposed a single electron oxidant could be accounted for by the presence of a tyrosyl residue proximal to the active site of MAO. After reduction of MAO A by sodium dithionite under anaerobic conditions, absorbance bands at 365 nm and 412 nm indicated the presence of a flavin semiquinone and tyrosyl radical, respectively.[25] Similarly, an absorbance band at 412 nm was present in the reduction of MAO B, indicating a possible similarity in mechanism. Further, researchers hypothesize that the tyrosyl radical is transient, because of the lack of its observation in the past. This would suggest a fast equilibrium with $FADH_2$ and the tyrosyl radical, and reversible electron transfer from substrate to flavin with the reverse reaction being fast.[25]

Murray *et al.* sought to provide further evidence for the involvement of the tyrosyl radical by creating a model system to reflect its involvement in the catalytic cycle. This reaction involved a flavin biomimetic as well as alloxan and Me_2S with benzylaminyl substrates.[26] *In situ* NMR studies were performed, and the inability to find a lock on the signal suggested paramagnetic behavior from the sample, which was subsequently confirmed by EPR spectroscopy. Further studies confirmed the paramagnetic signal to be localized to the N5 position on the model flavin. It is also suggested that the use of a hydrogen-bonding solvent such as trifluoroethanol could help further stabilize the semiquinone intermediate. To probe the viability of the model compounds, kinetic isotope studies were performed with para-substituted $ArCD_2NH_2$. The observed KIE was $k_H/k_D = 1.9$ with a Hammett correlation of -2.[26] Additionally, rates were shown to be independent

of Me_2S concentration and were first-order with respect to flavin concentration. Finally, the reduction potential of the model flavin (+66 mV) was shown to be similar to that of MAO (+40 mV), leading researchers to believe that the compound is a viable model to study.[26] The purpose of the Me_2S and alloxan in the reaction mixture is to emulate the presence of Y398 that is hypothesized to be a single-electron acceptor in the active site of MAO, which initiates the catalytic cycle of MAO oxidation. The proposed mechanism involves a rate-determining C-H substrate bond cleavage mediated by a semiquinone followed by a series of single-electron transfer events to eventually form the imine product and reproduce the semiquinone species. Notably, this reaction is performed under aerobic conditions in order to regenerate the alloxan species.[26]

Recent EPR and ENDOR studies on partially reduced MAO A have revealed the presence of a stable tyrosyl radical in the enzyme. The tyrosyl radical has been shown to be able to undergo a proton transfer to form a radical centered on the α-carbon of the substrate via QSAR studies as shown in Figure 1.7 (pathways B & C). The absence of an absorption band in rapid stopped-flow experiments suggests that this tyrosyl radical species is short lived, indicating a reversible electron transfer from substrate to flavin and rapid establishment of equilibrium with $FADH_2$ and the tyrosyl radical species.[23]

The β,γ-unsaturation of allyl amines should increase the acidity of α-protons, making the deprotonation of the corresponding radical cation much more facile. As the barrier to deprotonation is decreased, there is increased likelihood that the electron transfer and proton transfer might occur simultaneously. This phenomenon, referred to as concerted proton-coupled electron transfer (PCET) has yet to be explored with regard to MAO catalysis.

1.5 Proton-Coupled Electron Transfer (PCET)

Classically, PCET refers to an elementary process in which the concerted transfer of both a proton and electron occur from different orbitals. More recently, the term PCET has also become associated with separate H^+ and e^- transfer mechanisms that result in intermediate formation.[34] The discussion of thermodynamics in the context of PCET is often dominated by reduction potentials (E) and pK_a values, both of which are free energy measurements. If bond strength is constant, then any shift in E that results from solvent effects or placement within a protein must have an equally compensating opposite shift in pK_a.[28] Marcus theory is applicable to the kinetics of PCET reactions by its analysis of the intrinsic barrier to reaction. Although most directly applicable to self-exchange reactions, it has led to further insights on HAT reactions, specifically that C-H abstraction is several orders of magnitude slower than analogous O-H or N-H abstraction.[28] Simply stated, the PCET mechanism is usually more thermodynamically favorable than the associated stepwise mechanisms. However, there is a sense that the intrinsic barrier to the PCET reaction is higher than those of the stepwise mechanisms which is not supported by experimental data for most systems. When considering the intrinsic barriers to reaction for PCET and stepwise PT/ET or ET/PT, the thermodynamic favorability of PCET should make it the kinetically favored mechanism.[28, 34]

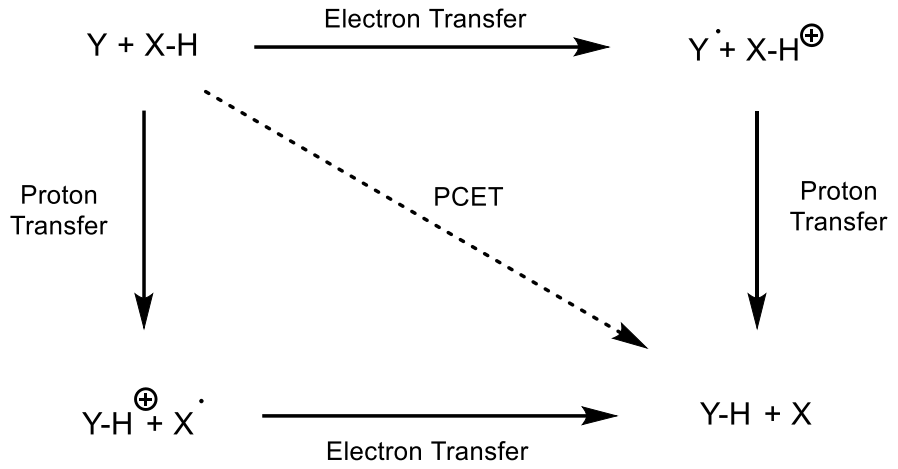

Figure 1.10: General thermodynamic square scheme to represent PCET reactions

PCET reactions are most often depicted as thermodynamic square schemes (Figure 1.10). Bond dissociation free energies should be used when working through a thermodynamic square as opposed to bond dissociation enthalpies because the use of BDEs implies that the entropy term is negligible (which it often is for organic systems, but often is not for transition metal complexes). When the free energy of activation calculated by the Eyring equation are lower than free energy change for stepwise ET/PT, then a concerted mechanism can be assumed. A "shortcut" for predicting PCET behavior can be drawn from studying pK_a and E^o. The difference in pK_a between the oxidized and reduced forms is equivalent to the difference between E^o of the protonated and deprotonated forms. When the difference is large (e.g. toluene), concerted reactions are preferred. When the difference is small (e.g. ascorbate), stepwise mechanisms are preferred. For those systems in which the difference is middling, chemical environment plays a key role in determining which process will occur. Perturbations in the chemical environment tend to have a large influence over the reaction mechanism. For a biological system such as an enzyme, key factors include hydrophobicity, hydrogen bonding, and dielectric tuning from residues within the binding pocket. These particularities make biomimetic studies of enzymes difficult. In solutions with hydrogen

bonding, phenols showed characteristics of PCET due to the diffusion-controlled rate of proton transfer.[29]

The mechanism for PCET is as follows: 1) a reorganization of the environment leads to the crossing point of proton vibrational states 2) a transition occurs between the reactant and product degenerate vibronic states while the proton and electron simultaneously tunnel from their donors to their acceptors 3) reorganization of the environment to further stabilize the products.[30]

1.6 Silent NMR

The term "silent NMR" refers to a situation in which a diamagnetic compound does not exhibit an NMR spectrum because it is in equilibrium with paramagnetic species (radicals) that cause significant changes in chemical shift in NMR signals and line-broadening. It has been long believed that due to the paramagnetic character of radicals, NMR spectroscopy is not a useful technique for their study. This is because paramagnetic interference distorts ^{1}H and ^{13}C signals and shifts them far downfield.

For reactions of TEMPO derivatives, researchers were unable to observe the ^{13}C signals from the piperidine ring but were able to see those of groups opposite the nitroxide radical on the ring. Work previously done on nitroxyl radical species suggested ^{13}C NMR spectroscopy is more useful than ^{1}H spectroscopy because carbon atoms which are sufficiently far from radical centers can be observed.[31] This study posits that atoms sufficiently far from the radical center are able to be detected and are relatively unaffected by the presence of a radical center in the molecule. It is unclear whether it is a proximity effect exhibited by the magnetic field of the radical or one transmitted through bonds that causes the NMR distortion. From this study, the distance between the nitroxide radical and the last missing ^{13}C signal is about four angstroms.[31]

The NMR studies of these radicals in conjunction with oxoammonium salts yielded the same results in a variety of solvents, most notably H_2O and D_2O. Studies performed with TEMPO-containing peptides reported a loss of 5-6 carbon signals in the NMR. It was proposed that those missing signals may be attributable to the carbon atoms local to the nitroxide radical. Even after purification, the radicals persisted in solution at a concentration of 1-2%. The few remaining radicals cause the sample to exhibit paramagnetic behavior in the presence of oxoammonium salts. A fast equilibrium between the TEMPO derivative and the oxoammonium salt on an order much faster than is able to be observed by NMR was suggested, which is hypothesized to cause an observation of peak averages from the equilibrium as opposed to a true snapshot.[31]

It is possible to determine rate constants for the dissociation and association reactions of radical species using NMR assuming there are signals unaffected by the radical center present in the molecule. In work done by Williams et. al, the dimerization of two radical species was studied. The broadening of the dimer's NMR signal was used to calculate the rate constants for the reactions taking place. Changes in the line broadening caused by nonequivalent diamagnetic states would be uniform across the whole spectrum while those caused by paramagnetic species would differ depending on vicinity to the unpaired electron, allowing one to deduce not only the cause of line broadening, but the approximate location of the radical center. Performing these experiments at a variety of temperatures allowed for the determination of an equilibrium constant for the dimerization process.[32]

The issue of "silent NMR" proved to be critical in reviving the SET pathway as a possible mechanism for the MPTP by MAO. Recently, work done by Nakamura *et al.* provided evidence for a SET mechanism in the anaerobic reaction of MMTP (37) with 5-ethyl-3-methyllumiflavinium perchlorate (36), an MAO biomimetic.[33] The reaction resulted in the

formation of two products: $MMTPH^+$ (38) and a small amount of the oxidized MMP^+, as shown in Figure 1.11 (39). Critically, the NMR signals for both starting materials were not present (under anaerobic conditions), likely indicating paramagnetic radical species which have engaged in a fast equilibrium (Figure 1.12).[33]

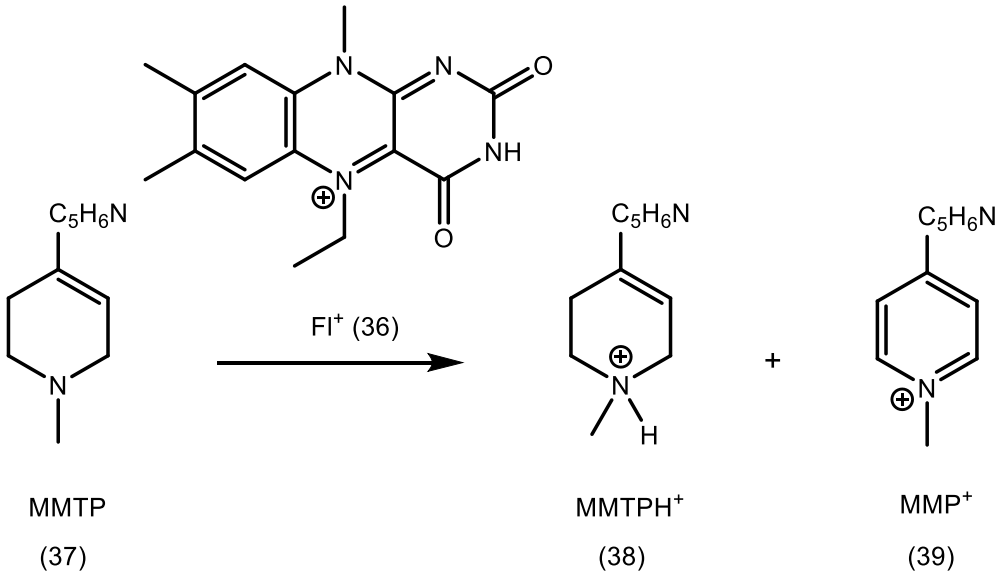

Figure 1.11: Overall reaction of MMTP with Fl^+ to produce MMP^+ with $MMTPH^+$ byproduct

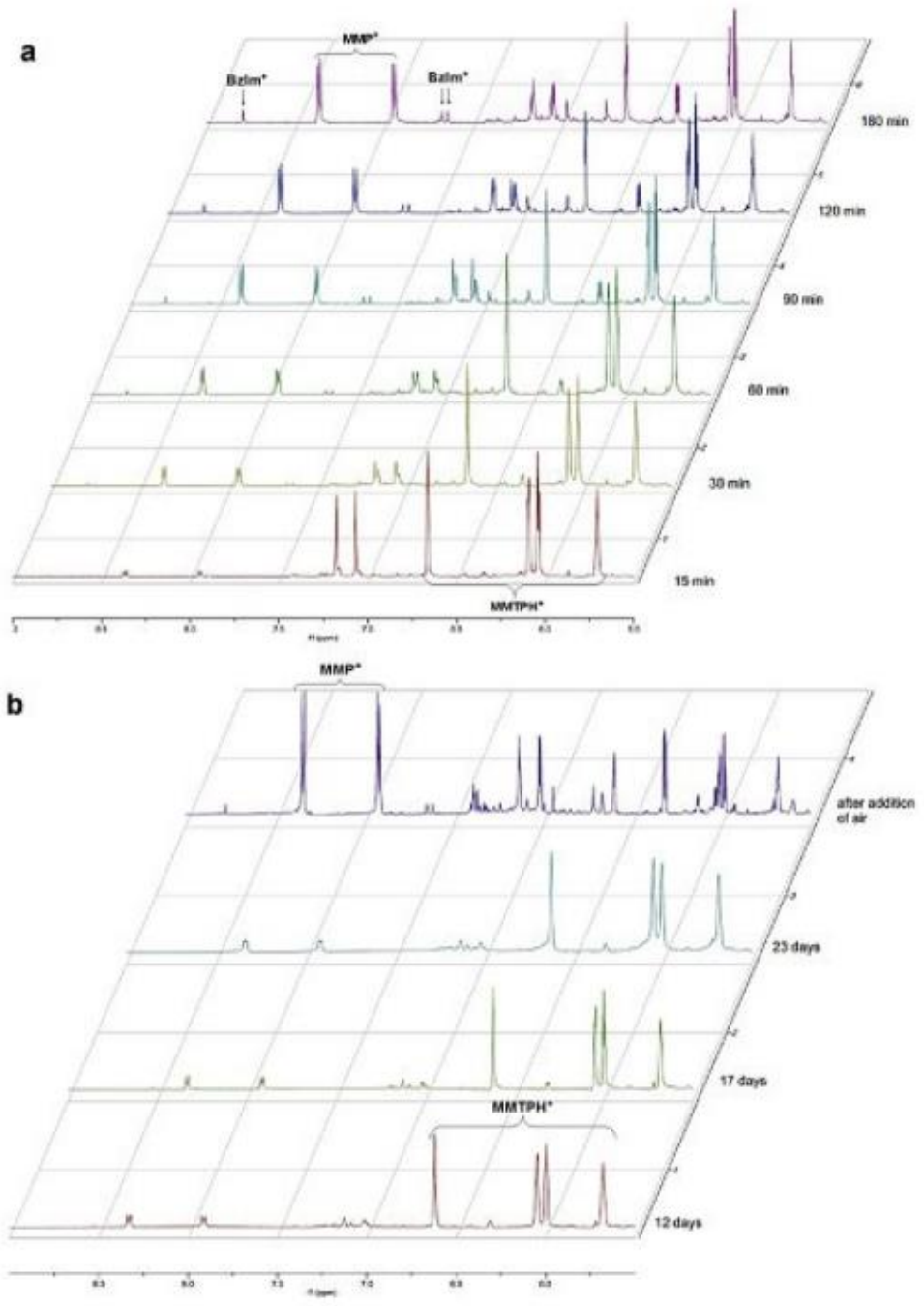

Figure 1.12: Time dependence on reaction mix for the oxidation of MMTP by 3-methyllumiflavinium perchlorate under aerobic conditions (A) and anaerobic conditions (B). The reluctance for reaction progression under anaerobic conditions as well as suppression of MMTP-correspondent peaks around 7.0 ppm suggest the presence of a persistent radical species in solution. Additionally, the presence of $MMTPH^+$ in under both sets of conditions suggests a proton transfer before the formation of a persistent radical.

Further supporting this was that, under anaerobic conditions, an EPR spectrum was observed attributable to a flavin-derived radical resulting from a single electron reduction. Notably, the reaction under anaerobic conditions did not proceed to product regardless of the amount of time that had elapsed. Upon addition of molecular oxygen to the reaction, the reaction seemed to progress to conclusion, which was interpreted in terms of a possible persistent radical effect in solution stored in the absence of O_2.[33] This suggests a possible early role of O_2 in the mechanism wherein the molecular oxygen provides a second, fast single electron transfer to the substrate.

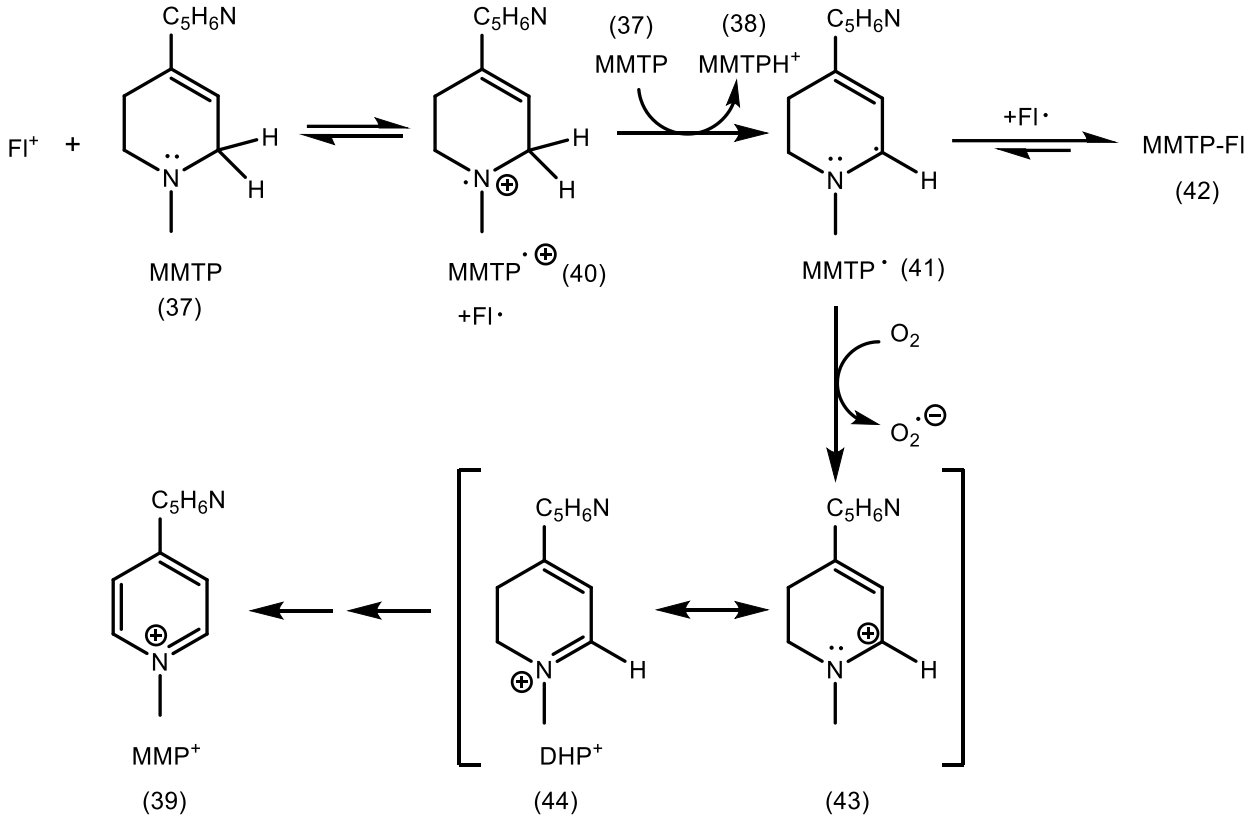

Figure 1.13: Proposed mechanism highlighting the potentially important early role of molecular oxygen in the reaction of 3-MLF$^+$ with MMTP.

In order to rationalize these results, a new mechanism for the oxidation mechanism was proposed. It was suggested that the single electron transfer step could be coupled to an extremely

favorable proton transfer from the α position on the allylamine. PCET had not been considered as a possibility for the MAO oxidation reaction until this point.

1.7 Scope of Dissertation

Herein, we aim to reevaluate and expand upon the work done by Nakamura et al. to provide further evidence for the SET mechanism of oxidation of MPTP and similar compounds. The selection of a neutral biomimetic to better reflect biological conditions was first completed, and its reactivity was fully mapped (Chapter 2). The substrate scope was subsequently expanded to include the study of the N-cyclopropyl derivative of MPTP to provide evidence for substrate radical behavior (Chapter 3). Finally, an expansion of flavin biomimetics is discussed in the context of MMTP to demonstrate the broader applicability of the mechanisms hypothesized to underline the oxidation of MPTP (Chapter 4).

1.8 References

1) Parkinson, J., *J. Neuropsychiatry Clin. Neurosci.* **2002**, *14* (2), 223-36.

2) Savitt, J. M.; Dawson, V. L.; Dawson, T. M., *J. Clin. Invest*. **2006**, *116* (7), 1744-54

3) Reynolds, A.; Laurie, C.; Mosley, R. L.; Gendelman, H. E., *Int. Rev. Neurobiol.* **2007**, *82*, 297-325.

4) Carlsson, A.; Lindqvist, M.; Magnusson, T., *Nature* **1957**, *180* (4596), 1200.

5) Bernheimer, H.; Birkmayer, W.; Hornykiewicz, O.; Jellinger, K.; Seitelberger, F., *J. Neurol. Sci.* **1973**, *20* (4), 415-55.

6) Kaludercic, N.; Carpi, A.; Menabo, R.; Di Lisa, F.; Nazareno, P., *Biochim. Biophys. Acta* **2011**, *1813* (7), 1323 - 1332.

7) Costiniti, V.; Spera, I.; Menabo, R.; Palmieri, E. M.; Menga, A.; Scarcia, P.; Porcelli, V.; Gissi, R.; Castegna, A.; Canton, M., *BBA - Molecular Basis of Disease* **2018**, *1864*, 3050 - 3059.

8) Kaludercic, N.; Carpi, A.; Nagayama, T.; Sivakumaran, V.; Zhu, G.; Lai, E. W.; Bedga, D.; De Mario, A.; Chen, K.; Gabrielson, K. L.; Mindsey, M. L.; Pacak, K.; Takimoto, E.; Shih, J. C.; Kass, D. A.; Di Lisa, F.; Paolocci, N., *Antioxidants & Redox Signaling* **2014**, *20*, 267 - 280.

9) Villeneuve, C.; Caudrillier, A.; Ordener, C.; Pizzinat, N.; Parina, A.; Mialet-Perez, J., *Am. J. Physiol. Heart Circ. Physiol.* **2009**, *297*, H821 - H828.

10) Yu, J.; Castagnoli, N., Jr., *Bioorg. Med. Chem.* **1999**, *7* (12), 2835-42.

11) Vila, M.; Przedborski, S., *Nature Rev. Neurosci.* **2003**, *4* (5), 365-75.

12) Elbaz, A.; Bower, J. H.; Maraganore, D. M.; McDonnell, S. K.; Peterson, B. J.; Ahlskog, J. E.; Schaid, D. J.; Rocca, W. A., *J. Clin. Epideiol*. **2002**, *55* (1), 25-31.

13) Vianello, R.; Repič, M.; Mavri, J., *Eur. J. Org. Chem.* **2012**, No. 36, 7057–7065.

14) Edmondson, D. E.; Bhattacharyya, A. K.; Walker, M. C., *Biochemistry* **1993**, *32* (19), 5196–5202.

15) Fitzpatrick, P. F. *Arch. Biochem. Biophys.* **2010**, *493* (1), 13–25.

16) Ramsay, R. R.; Albreht, A., *J. Neural. Transm.* **2018**, *125* (11), 1659–1683.

17) Miller, J. R.; Edmondson, D. E., *Biochemistry* **1999**, *38* (41), 13670–13683.

18) Newton-Vinson, P.; Hubalek, F.; Edmondson, D. E., *Protein Expr. Purif.* **2000**, *20* (2), 334–345.

19) Brown, L. E.; Hamilton, G. A., *J. Am. Chem. Soc*. **1970**, *92* (24), 7225-7227.

20) Silverman, R. B.; Hoffman, S. J.; Catus, W. B., III, *J. Am. Chem. Soc*. **1980**, *102* (23), 7126-7128.

21) Silverman, R. B.; Lu, X., *J. Am. Chem. Soc.* **1994**, *116* (9), 4129–4130.

22) Yelekci, K.; Lu, X.; Silverman, R. B., *J. Am. Chem. Soc.* **1989**, *111* (3), 1138–1140.

23) Scrutton, N. S., *Nat. Prod. Rep.* **2004**, *21* (6), 722–730.

24) Silverman, R. B., *Acc. Chem. Res.* **1995**, *28* (8), 335–342.

25) Rigby, S. E. J.; Hynson, R. M. G.; Ramsay, R. R.; Munro, A. W.; Scrutton, N. S., *J. Biol. Chem.* **2005**, *280* (6), 4627–4631.

26) Murray, A. T.; Dowley, M. J. H.; Pradaux-Caggiano, F.; Baldansuren, A.; Fielding, A. J.; Tuna, F.; Hendon, C. H.; Walsh, A.; Lloyd-Jones, G. C.; John, M. P.; Carbery, D. R., *Angew. Chemie - Int. Ed.* **2015**, *54* (31), 8997–9000.

27) Simpson, J. T.; Lewis, F. D.; Krantz, A.; Kokel, B., *J. Am. Chem. Soc.* **1982**, *104* (25), 7155–7161.

28) Mayer, J. M.; Rhile, I. J. *Biochimica et Biophysica Acta*, **2004**, *1655*, 51-58.

29) Warren, J. J.; Mayer, J. M., **2015**, *54* (10), 1863–1878.

30) Hammes-Schiffer, S., *J. Am. Chem. Soc.* **2015**, *137* (28), 8860–8871.

31) Bobbitt, J. M.; Eddy, N. A.; Cady, C. X.; Jin, J.; Gascon, J. A.; Gelpí-Dominguez, S.; Zakrzewski, J.; Morton, M. D., *J. Org. Chem.* **2017**, *82* (18), 9279–9290.

32) Williams, D. J.; Krellick, R., *J. Am. Chem. Soc.* **1967**, *89* (14), 3408–3412.

33) Nakamura, A.; Latif, M. A.; Deck, P. A.; Castagnoli, N.; Tanko, J. M., *Chem. - A Eur. J.* **2020**, *26* (4), 823–829.

34) Mayer, J. M.; Rhile, I. J., *Biochemica et Biophysica Acta* **2004**, *1655*, 51-58.

35) Orrum R.; Aldeco, M.; Edmondson, D. E., *J. Neural Transm.* **2013**, *120*, 847-851.

36) Martindale, J. L.; Holbrook, N. J., *J. Cell. Phys.* **2002**, *192* (1), 1-15.

Chapter 2. Why Does Monoamine Oxidase (MAO) Catalyze the Oxidation of Some Tetrahydropyridines?

2.1 Abstract

Results pertaining to the mechanism of the oxidation of the tertiary amine 1-methyl-4-(1-methyl-1-H-pyrrol-2-yl)-1,2,3,6-tetra-hydropyridine (MMTP, a close analog of the Parkinsonism inducing compound MPTP) by 3-methyllumiflavin (3MLF), a chemical model for the FAD cofactor of monoamine oxidase, are reported. MMTP and related compounds are among the few tertiary amines that are monoamine oxidase B (MAO B) substrates. The MMTP/3MLF reaction is catalytic in the presence of O_2 and the results under anaerobic conditions strongly suggest the involvement of radical intermediates, consistent with a single electron transfer mechanism. These observations support a new hypothesis to explain the MAO-catalyzed oxidations of amines. In general, electron transfer is thermodynamically unfavorable, and as a result, most primary and secondary amines react via one of the currently accepted polar pathways. Steric constraints prevent tertiary amines from reacting via a polar pathway. Those select 3^o amines that are MAO substrates possess certain structural features (e.g., a C-H bond that is α- both to nitrogen and a C=C) that dramatically lower the pK_a of the corresponding radical cation. Consequently, the thermodynamically unfavorable electron transfer equilibrium is driven towards products by an extremely favorable deprotonation step in the context of Le Chatelier's principle.

2.2 Introduction

Monoamine oxidase A (MAO A) and B (MAO B) catalyze the oxidation of various neurotransmitters, including dopamine, norepinephrine, epinephrine and serotonin. The overall reaction is a two-electron a-carbon oxidation, $R'NH\text{-}CH_2R \rightarrow R'N{=}CHR$, that is coupled to the two-electron reduction of the flavin cofactor FAD to $FADH_2$. Several mechanisms have been

proposed to account for the initial stages of the mechanism of MAO-catalyzed oxidations[1] including conventional "two-electron/polar" pathways such as nucleophilic addition[2] and hydride transfer,[3] as well as a single electron transfer (SET) pathway that involves radical intermediates.[3-4] 1-Methyl-4-phenyl-1,2,3,6-tetrahydropyridine (MPTP) is a selective MAO B substrate, and a precursor to the Parkinsonian syndrome-inducing neurotoxic pyridinium species MPP^+ (Figure 2.1).[5] Moreover, MPTP is one of the very few tertiary amines that are MAO substrates.

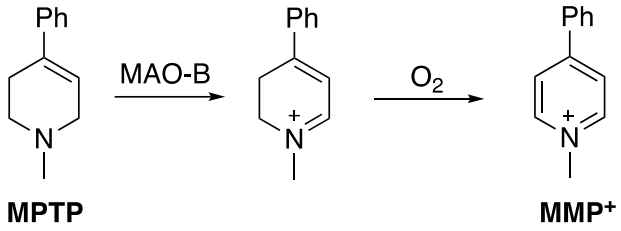

Figure 2.1: MAO B catalyzes the oxidation of MPTP to MMP^+, which induces symptoms of Parkinson's disease in humans. MPTP (and some derivatives) are rare in that they are the only tertiary amines known to be oxidized by MAO.

In general, tertiary amines are not MAO substrates,[6] which makes sense in the context of the currently proposed and generally accepted mechanisms of catalysis. As noted, these mechanisms include a polar, nucleophilic addition pathway (which may be stepwise or concerted), or a hydride transfer pathway.[1a, 1b, 7] Current thinking is that both mechanisms proceed via the same transition state, with the difference being in the direction of electron flow (Figure 2.2).[8] Because of steric issues, tertiary amines cannot react by either of these mechanisms which require the nitrogen lone-pair of the amine, and C_{4a} of the flavin to be in close proximity in the transition state.

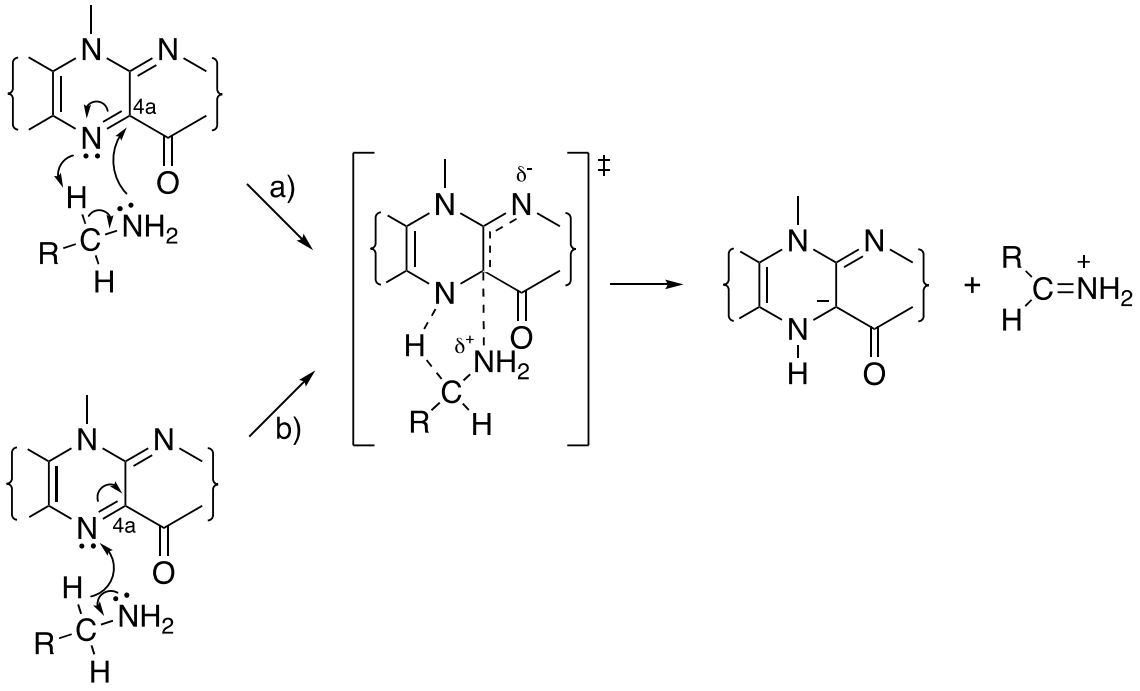

Figure 2.2: Proposed concerted mechanisms for MAO catalysis: a) a polar, nucleophilic pathway where the amine acts as a nucleophile, attacking C_{4a} of the flavin, and b) a hydride transfer pathway. Both mechanisms may proceed through the same five-membered transition state, with the difference being the direction of electron flow.

Single electron transfer mechanisms for MAO catalysis have been proposed by Silverman,[4a] Castagnoli,[9] and others.[10] The most compelling evidence for single electron transfer came from the behavior of MAO substates equipped with a single electron transfer probe essentially a compound with an *N*-cyclopropyl[4a, 4b, 9] or *N*-cyclobutyl group[11] that (because of ring strain) would undergo ring opening when a radical cation was produced. This is illustrated in Figure 2.3 with the *N*-cyclopropyl derivative of MPTP which is an irreversible MAO inhibitor. The rationale for inhibition is that ring opening produces a 1^o radical which disrupts the active site of MAO through covalent bond formation.

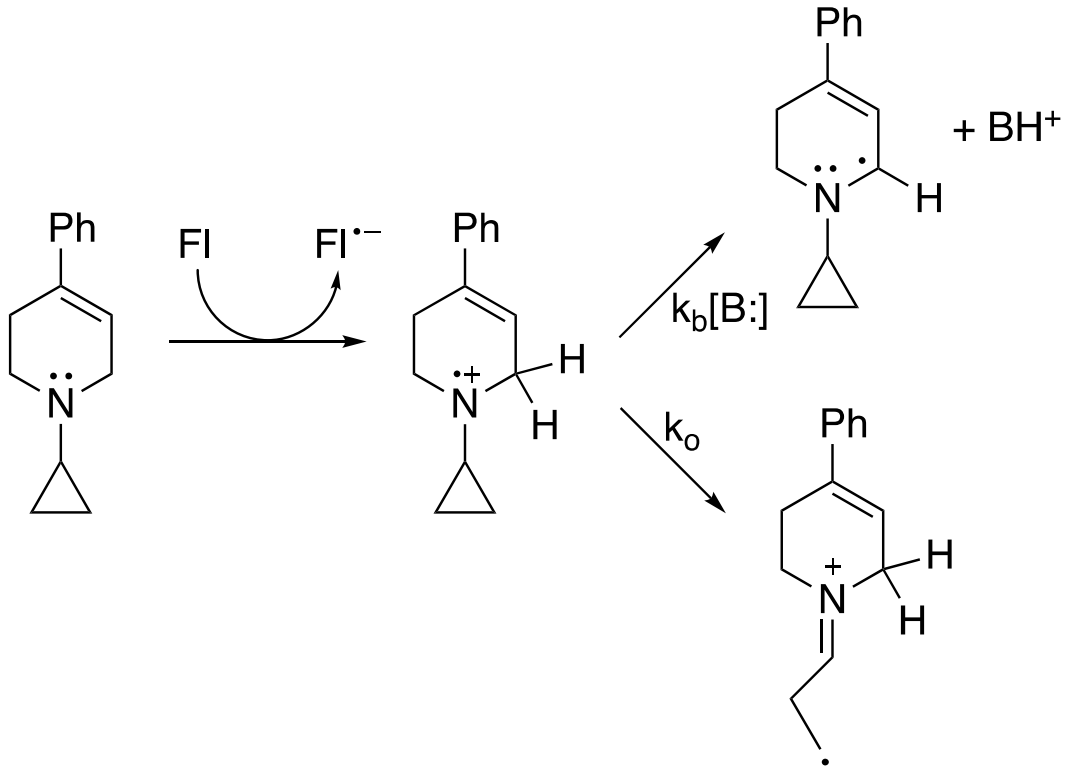

Figure 2.3: Use of a single electron transfer probe to examine the mechanism of MAO-catalyzed oxidations. The *N*-cyclopropyl group diverts the initially produced radical cation forming a 1° radical that disrupts the active site thereby deactivating the enzyme. Fl represents the flavin cofactor in MAO.

One of the classic arguments against the SET pathway is that the initial single electron transfer reaction is thermodynamically unfavorable,[12] and with a few exceptions,[1c, 10] the SET pathway seems to have fallen out of favor.[8a, 13] In 2020, we reported results for the oxidation of 1-methyl-4-(1-methyl-1*H*-pyrrol-2-yl)-1,2,3,6-tetrahydropyridine (MMTP, an MPTP derivative and MAO B substrate with no known human toxicity) using a flavin biomimetic that provided compelling evidence that this class of compounds may react through an SET process. The reaction of 5-ethyl-3-methylumiflavinium perchlorate (Fl^+, Figure 2.4) with MMTP was monitored using NMR and EPR spectroscopy. The results suggested the intermediacy of radicals, an insight that

came from studying this reaction under aerobic--but more importantly, under anaerobic conditions.[14]

In the absence of O_2, the reaction of MMTP with Fl^+ occurred nearly instantaneously and resulted in the disappearance of all ^1H NMR signals corresponding to Fl^+ and MMTP. (The sole species present in the ^1H NMR spectrum was the protonated starting material, $MMTPH^+$). However, no oxidation products were detected, and the reaction became dormant. During this dormant period, however, a persistent flavin radical was detected by EPR. When O_2 was introduced (as much as three weeks later), the reaction resumed and resulted in the formation of the final oxidation product MMP^+. The ^1H NMR spectrum was remarkably similar to that observed when the reaction was conducted under aerobic conditions. To explain what was happening during this dormant period, an extension of the "persistent radical effect"[15] was proposed, wherein the "persistent" neutral flavin radical coupled reversibly to neutral reactive radical derived from MMTP (Figure 2.4).[14]

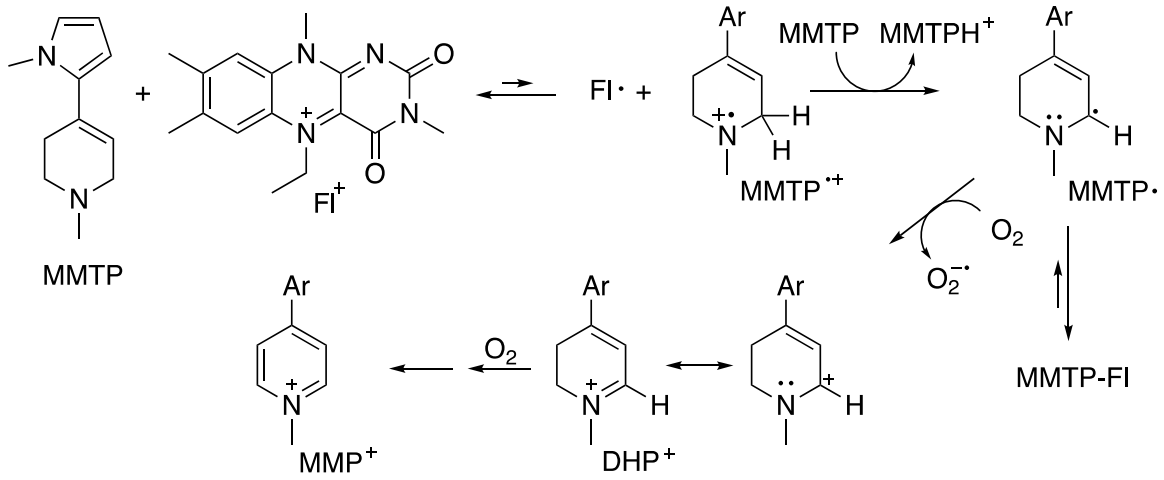

Figure 2.4: The reaction mechanism for the oxidation of MMTP by 5-ethyl-3-methyllumiflavinium perchlorate (Fl^+) proposed by Nakamura, et al.[14] A single electron transfer step is coupled to an extremely favorable proton transfer to a second molecule of MMTP, forming $MMTPH^+$ (detected by ^1H NMR) and MMTP• and Fl• (which are "invisible" in ^1H NMR). MMTP• and Fl• are believed to exist in equilibrium with a covalent adduct (MMTP-Fl), causing the reaction to enter a "dormant" phase. Upon O_2 addition, the equilibrium (MMTP• + Fl• = MMTP-Fl) is shifted towards the left and MMTP• is quickly consumed by O_2 to complete the oxidation of the substrate. Note: Ar refers to the N-methylpyrrole moiety in MMTP.

We believe that it is the unique structure of MPTP and its analogs that makes the electron transfer pathway feasible. Compared to typical tertiary amines (which are not MAO substrates), the additional resonance stability provided by the β-unsaturation makes the radical cation exceptionally acidic. For the oxidation of tertiary amines such as MPTP by monoamine oxidase, we propose that a reversible, thermodynamically unfavorable electron transfer followed by (and potentially coupled to) an extremely favorable deprotonation from the α-position of the aminyl radical cation (pK_a ca. -5) [14, 16] provides the driving force for the single electron transfer mechanism (Figure 2.5).

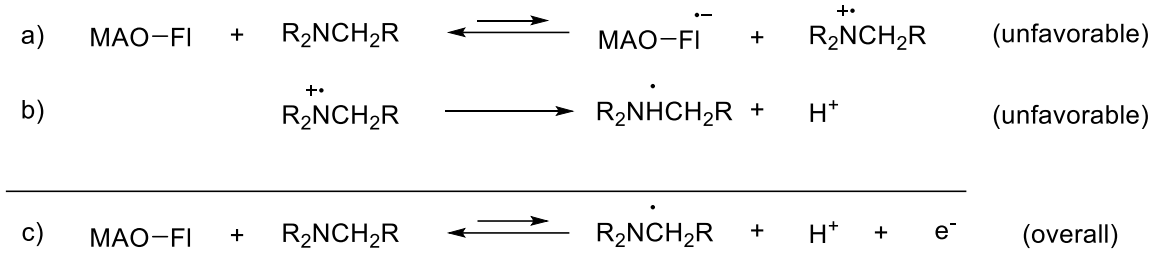

Figure 2.5: Modified single electron transfer (SET) hypothesis. a) Electron transfer between the flavin moiety and an amine is thermodynamically unfavorable. b) For some substrates, the radical resulting from deprotonation is very stable and the pK_a of the radical cation is exceptionally low. c) In the context of Le Chatelier's principle, the overall result of coupling an unfavorable electron transfer (a) and a very favorable proton transfer (b) drives the overall electron transfer/proton transfer process (c).

The biomimetic study discussed above utilized the highly reactive and electrophilic 5-ethyl-3-methyllumiflavinium (Fl^+) perchlorate, rather than a neutral flavin such as 3-methyllumiflavin (3MLF, Figure 2.6). Oxidation potentials reported by Sichula, et al.[17] suggests that an analogous N10-ethyl flavinium species has an oxidation potential of +0.17 V, while the neutral flavin analog has an oxidation potential from -0.95 V (vs. $Ag/AgNO_3$). The increased oxidation potential of the flavinium (vs. neutral flavin moiety) introduces a bias favoring the SET process on the order of 25 kcal/mol!

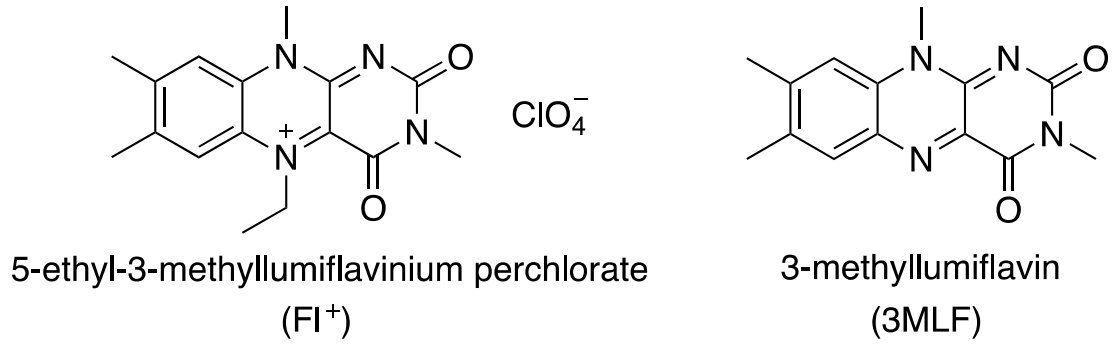

Figure 2.6: Structures of 5-ethy-3-methyllumiflavinium perchlorate and 3-methyllumiflavin.

In addition, the Fl^+/MMTP reaction was not catalytic. Upon reduction, Fl^+ decomposes and much of its fate is unknown. (The only detectable product was a benzimidazolium byproduct,[14]

formed in a low yield). The objective of the present work was to examine the reactivity of a biomimetic that is more closely related to the neutral flavin moiety in MAO, to determine whether an electron transfer process remained feasible, and if so, whether the oxidation was catalytic. Towards this end, we report the results from a study of the reaction of 3-methyllumiflavin (3MLF) with MMTP. Our earlier work with Fl^+ and MMTP demonstrated that O_2 played a critical role in the reaction mechanism. Perhaps more importantly though, it was only possible to detect radicals when O_2 was excluded. Consequently, the 3MLF/MMTP chemistry was studied under both aerobic and anaerobic conditions.

2.3 Results

2.3.1 Reaction of MMTP and 3MLF in the Presence of O_2

The progress of both the aerobic and anaerobic reactions of MMTP and 3MLF was monitored by ^{1}H NMR. Authentic spectra for MMTP, 3MLF, and the reaction product MMP^+ and the observed chemical shifts and multiplicities for these compounds are provided in the supporting information (Figure A.1). The peaks at 8.3, 6.0, and 4.0 ppm were particularly diagnostic, well-resolved and used to monitor relative concentrations of MMP^+, MMTP, and 3MLF, respectively, and for quantification purposes when an internal standard was used.

Aerobic reactions were prepared directly in an NMR tube using stock solutions of 3MLF and MMTP in CD_3CN and monitored by ^{1}H NMR. The solutions were continuously agitated on a mixing table to ensure thorough incorporation of O_2 into the solution and shielded from light to avoid any photo-induced reactions of 3MLF. The reaction of a 1:1 MMTP/3MLF mixture (2.50 mM each) was followed by ^{1}H NMR. In about four hours, all the MMTP was oxidized with ~50% conversion to MMP^+. During this time, there was no apparent change in the 3MLF concentration,

demonstrating that 3MLF behaves as a catalyst in this reaction. Additionally, there was no ^{1}H NMR evidence for the presence of the reduced form of 3MLF at any time during the reaction.

To further probe catalysis, an 8:1 MMTP/3MLF reaction ([MMTP] = 4.80 mM, [3MLF] = 0.60 mM) was monitored by ^{1}H NMR for 240 hours. Again, the concentration of 3MLF remained constant for the duration of the reaction, and the MMTP was oxidized completely, indicating catalytic behavior over multiple turnovers (Figure 2.7). As a control, under identical conditions, it was shown that there was no significant reaction between MMTP and O_2 in the absence of 3MLF.

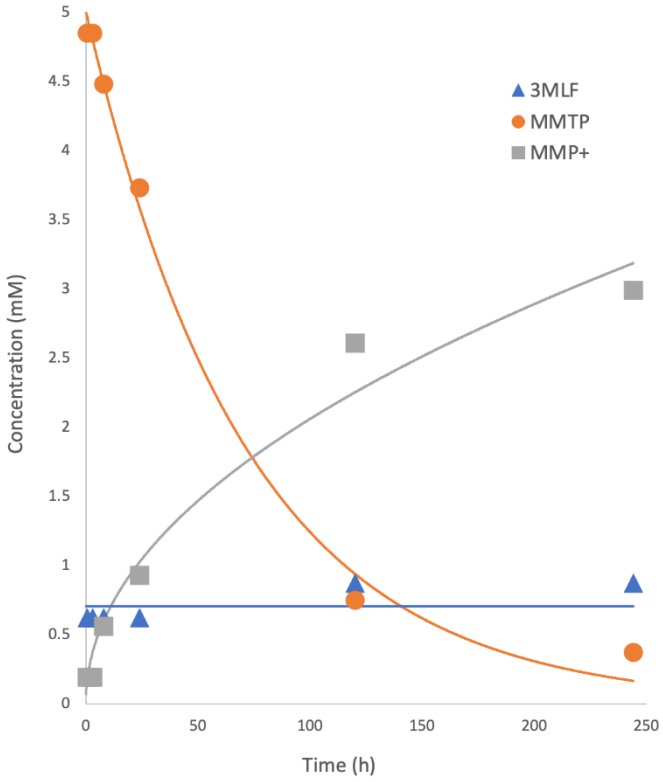

Figure 2.7: A plot of concentration vs. time for an aerobic 8:1 MMTP:3MLF reaction is shown here. The flavin demonstrates catalytic behavior while the substrate achieves ~50% conversion to the fully oxidized product. One turnover is estimated to take 4 hours. Concentrations were monitored by ^{1}H NMR with a benzene internal standard.

In summary, results from the reaction of 3MLF and MMTP under aerobic conditions demonstrated a) that 3MLF was an effective oxidant, b) that the reaction was catalytic, and most significantly c) that 3MLF was a good biomimetic for the flavin in the active site in MAO B. However, as was found earlier with Fl^+/MMTP, important mechanistic features of the reaction became apparent when the reaction was conducted in the absence of O_2.

2.3.2 Reaction of MMTP and 3MLF in the Absence of O_2

Solutions for the anaerobic reactions were also prepared directly in NMR tubes using stock solutions of 3MLF and MMTP in CD_3CN. The solutions were freeze-pump-thaw degassed immediately after mixing (to remove O_2), and the NMR tubes were flame-sealed. The reaction mixtures were kept in the dark unless being actively analyzed by NMR. (Analysis of the mixture shortly after mixing revealed the reaction did not proceed to a significant extent during the time period associated with sample preparation.)

The reaction of 1:1 MMTP and 3MLF (2.50 mM each) in CD_3CN in the absence of O_2 was monitored qualitatively by ^1H NMR for several hours. Within ca. four hours, all peaks corresponding to 3MLF disappeared from the ^1H NMR spectrum, leaving only peaks attributable to solvent, MMTP, and the reaction product MMP^+ (Figure 2.8). This behavior was reminiscent of the work of Nakamura, et al.,[14] but with some notable exceptions and nuances. The signals associated with the aromatic protons of 3MLF at d = 7.7 and 7.9 ppm, and the aromatic methyl groups (2.4 and 2.5 ppm) disappeared "immediately." By immediate, we mean in the time it takes to prepare the sample and record the first spectrum, usually within fifteen minutes. However, as shown in Figure 2.9, rather than disappearing, the peaks associated with the N3- and N10-methyl groups of 3MLF exhibited line broadening at early reaction times, before disappearing into the baseline after about four hours (although the N3 methyl was the last to completely vanish). After

four hours, no peaks attributable to 3MLF (or any derived reduction product) were apparent in the reaction mixture. Nonetheless, the reaction progressed and MMTP was slowly oxidized to MMP^+.

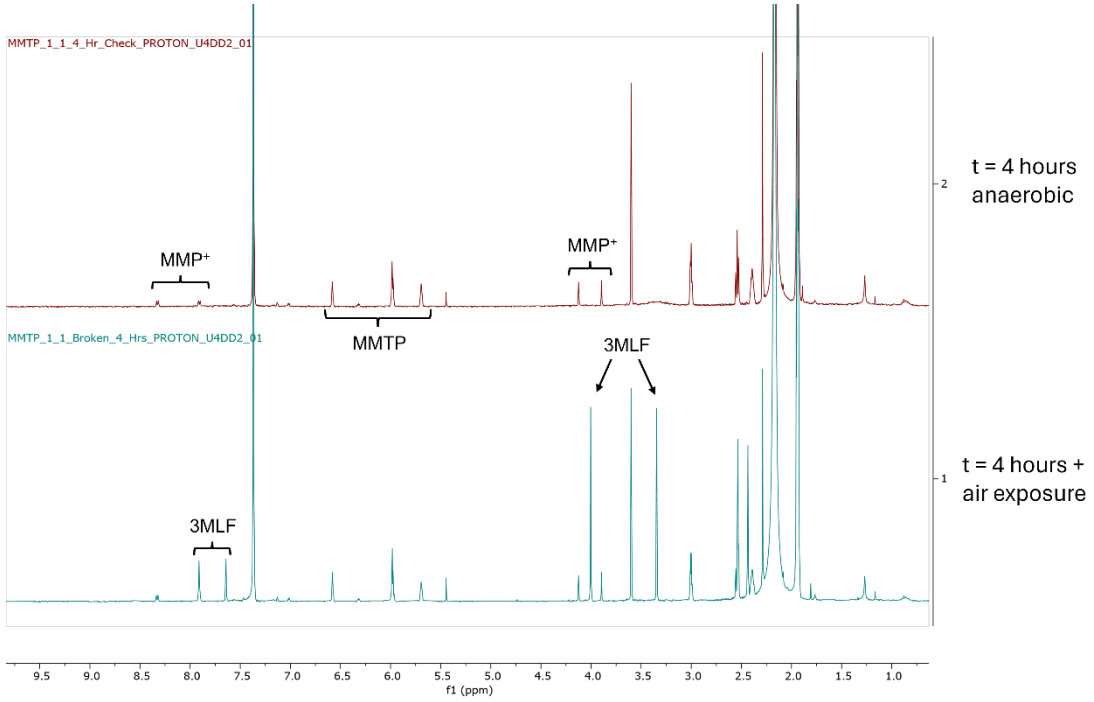

Figure 2.8: ^{1}H NMR spectrum of a reaction mixture of 3MLF and MMTP (1:1) under anaerobic conditions at t = 4 hours (top) demonstrates the disappearance of 3MLF from the ^{1}H NMR. Upon introduction of O_2, the flavin signals quantitatively re-emerge (bottom).

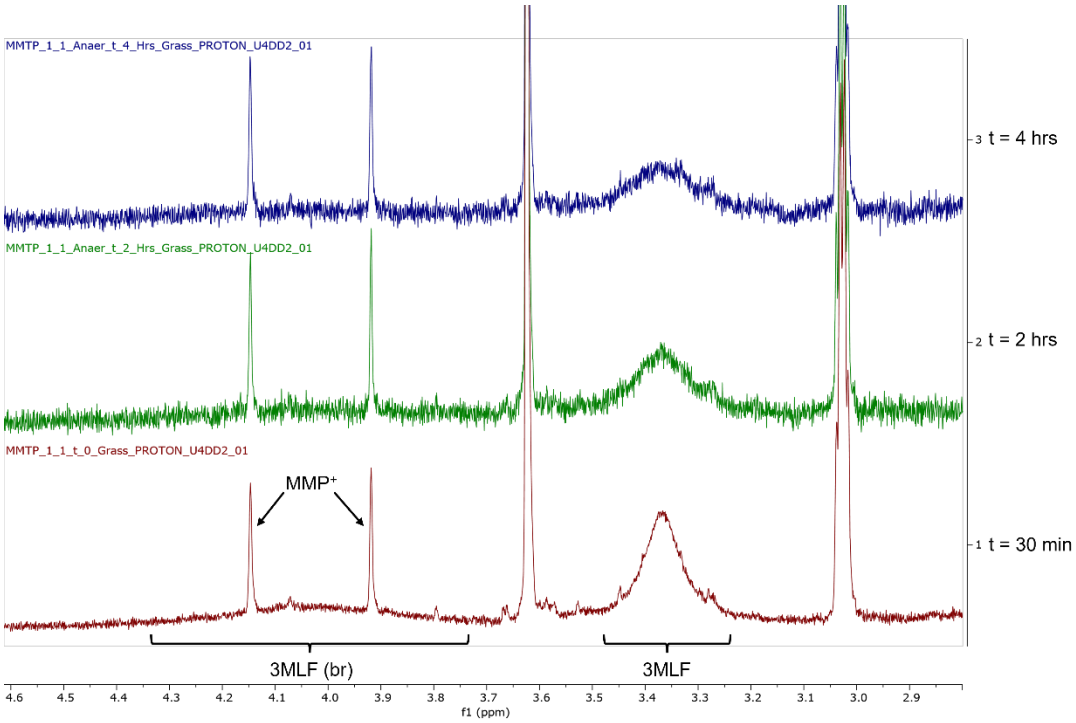

Figure 2.9: ^{1}H NMR spectra of 1:1 reaction of MMTP and 3MLF (2.50 mM each) in CD_3CN recorded as a function of time. The flavin N3 and N10 methyl peaks disappear over the course of 4 hours while the MMTP decreases in intensity and the MMP^+ increases.

If O_2 was introduced at any time during the reaction, 3MLF reappeared in the ^{1}H NMR spectrum quantitatively, Figure 2.8. This phenomenon piqued a particular interest in uncovering the fate of the flavin over the course of the anaerobic reaction. We propose that during this early four hour period that the 3MLF ^{1}H NMR signals were broadening and decreasing in intensity, the concentration of flavin-derived radicals was steadily increasing.

The reaction continued until all the MMTP was consumed. After several days (3 - 5 depending on starting concentrations of MMTP and 3MLF), an orange precipitate formed. To isolate this precipitate, the NMR tube was opened in a glove box (to maintain anaerobic conditions). Direct characterization of this precipitate proved difficult, which was found to be insoluble in D_2O, $CDCl_3$, DMSO, and only sparingly soluble in CD_3CN. However, when suspended in CD_3CN and exposed to air, the precipitate readily dissolved, and the recorded ^{1}H

NMR was a perfect match for 3MLF. This leads to the conclusion that the orange precipitate was a reduced form of the flavin, most likely dihydroflavin ($3MLFH_2$) or its deprotonated form ($3MLFH^-$) either of which upon exposure to O_2, would regenerate 3MLF.

Spectra collected in the absence of O_2 suggest that 3MLF is consumed but not degraded over the course of the reaction with MMTP because when O_2 is added, 3MLF is regenerated. This contrasts with the work done by Nakamura wherein the flavinium compound decomposed into a benzimidazolium ion as a function of time.[14] Unlike this earlier study, peaks attributable to 3MLF do not all disappear from the ^1H NMR spectrum simultaneously. Instead, the disappearance follows a consistent pattern of line broadening into the baseline as a function of time for each unique 3MLF signal.

We suggest that the observed line broadening and disappearance of signals associated with 3MLF provides indirect evidence for formation of a 3MLF derived radical or radical ion resulting from single electron transfer, whose concentration increases during the first few hours or so of reaction. Specifically, we suggest that during this period, approximately one equivalent of electrons have been transferred from MMTP to 3MLF producing 3MLFH• or $3MLF^{\bullet-}$. To confirm this hypothesis, EPR spectroscopy was used to directly probe for the formation of flavin radicals in solution.

A 1:1 MMTP : 3MLF (2.50 mM each) anaerobic reaction solution was prepared and monitored by EPR spectroscopy. Initially, no EPR signals were observed. However, after about 40 minutes, the first sign of a signal appeared, and this signal continued to grow, reaching a maximum intensity after about four hours (Figure 2.10). After several days, the EPR signal vanished, coinciding with the formation of precipitate in the reaction vessel (i.e., a fully reduced

form of 3MLF, vide supra). The shape and linewidth of the observed EPR signal is reminiscent of flavin derived radicals.[18]

It is particularly noteworthy that during the course of this reaction, the growth of the EPR signal associated with the flavin parallels the broadening and disappearance of the 3MLF signals in the ^{1}H NMR. During this same period, signals associated with the fully oxidized product (MMP^{+}) steadily grow in intensity in the ^{1}H NMR spectra. At longer times, the EPR signal diminishes and completely disappears when the reaction is complete (and the orange precipitate is formed).

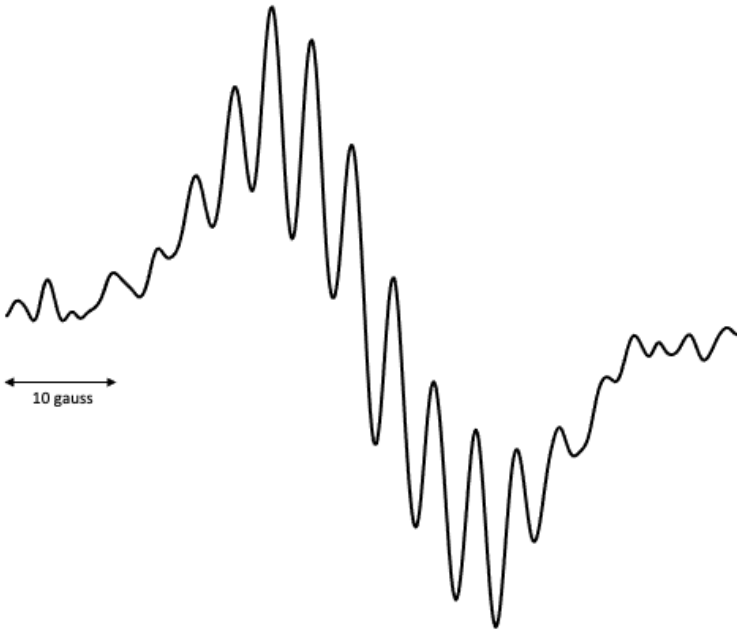

Figure 2.10: The EPR spectrum of a 1:1 MMTP:3MLF (2.50 mM each) reaction at t = 225 minutes. This spectrum matches the line shape and width of a flavin derived radical.

Oxidation of MMTP to MMP^{+} requires a total of four electrons, and 3MLF (or species derived therefrom) are clearly effecting this oxidation. The EPR results and peculiar ^{1}H NMR observations point to the intermediacy of flavin derived radicals. To reconcile these observations,

we propose that single electron transfer is occurring, and that the flavin radical observed by EPR is either 3MLF$^{\bullet-}$, or if protonated, 3MLFH-1• or 3MLFH-2•. The difference between the latter two being the site of protonation. Figure 2.11 illustrates these structures, and also, shows the spin density surface and calculated spin density at hydrogen for each (M06-2X/6-311G*).[19] It is noteworthy that, regardless of which flavin structure is formed, the spin density at the N3-methyl is nearly zero, and these are the last signals in the ^{1}H NMR to disappear. At longer times, the oxidation continues (MMTP → MMP$^+$), the EPR signals vanish, and a precipitate is formed (assigned to the fully reduced flavin 3MLFH$_2$).

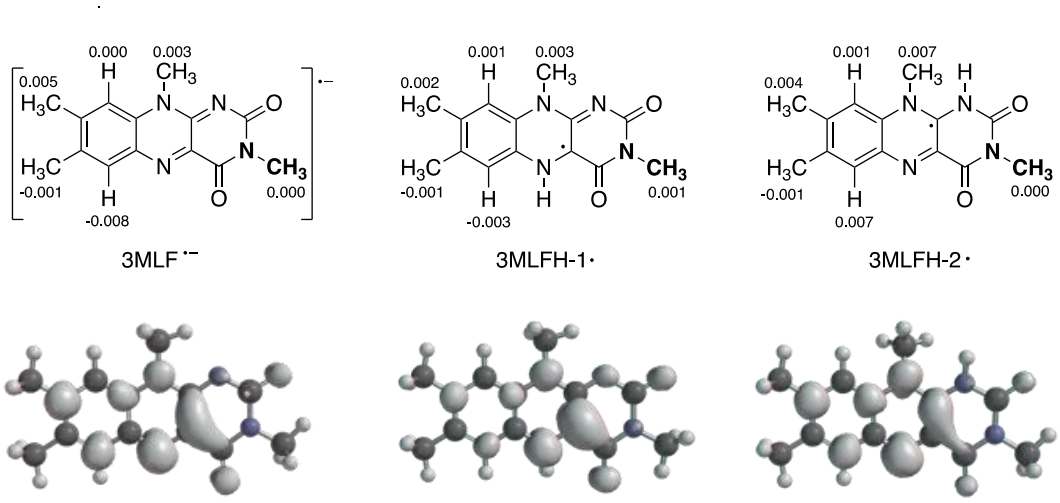

Figure 2.11: M06-2X/6-311G* calculated spin density surfaces of several flavin radicals; the numbers summarize the spin densities at each hydrogen. For all these species, the bulk of the spin density is associated with the left end of the fused-ring system with little to no spin density at the N3-methyl group (boldfaced).

The line broadening observed in the ^{1}H NMR of the *N*-methyl groups of 3MLF during the early stages of the reaction (< 4 hours) is likely the result of a rapid exchange process between unreacted 3MLF and partially reduced 3MLF (3MLF$^{\bullet-}$ or 3MLFH•) as shown in Figure 2.12. Evidence for this rapid exchange was provided by variable temperature ^{1}H NMR and EPR.

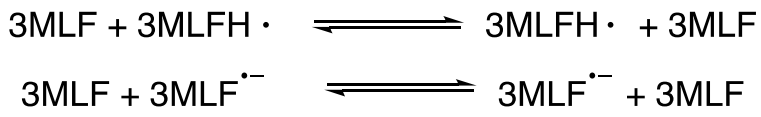

Figure 2.12: Proposed self-exchange reactions for flavin radicals with neutral 3MLF starting material are shown.

The results of the variable temperature NMR experiments for a 1:2 MMTP : 3MLF reaction at three hours are shown in Figure 2.13. At room temperature, the signal for the N10 methyl group is not observed, and that for the N3 is broadened and weak. As the temperature is reduced (10 degree increments to -30 ^{o}C, the N3 and N10 methyl groups start to reappear in the opposite order in which they disappeared (N10, followed by N3). At -30 ^{o}C, even some peaks associated with protons on the aromatic ring appear to be emerging from the baseline. (The results obtained with variable temperature EPR were complementary. As the temperature was lowered, the EPR signal of the flavin radical disappeared, but reappeared when the temperature was brought back to ambient temperature.)

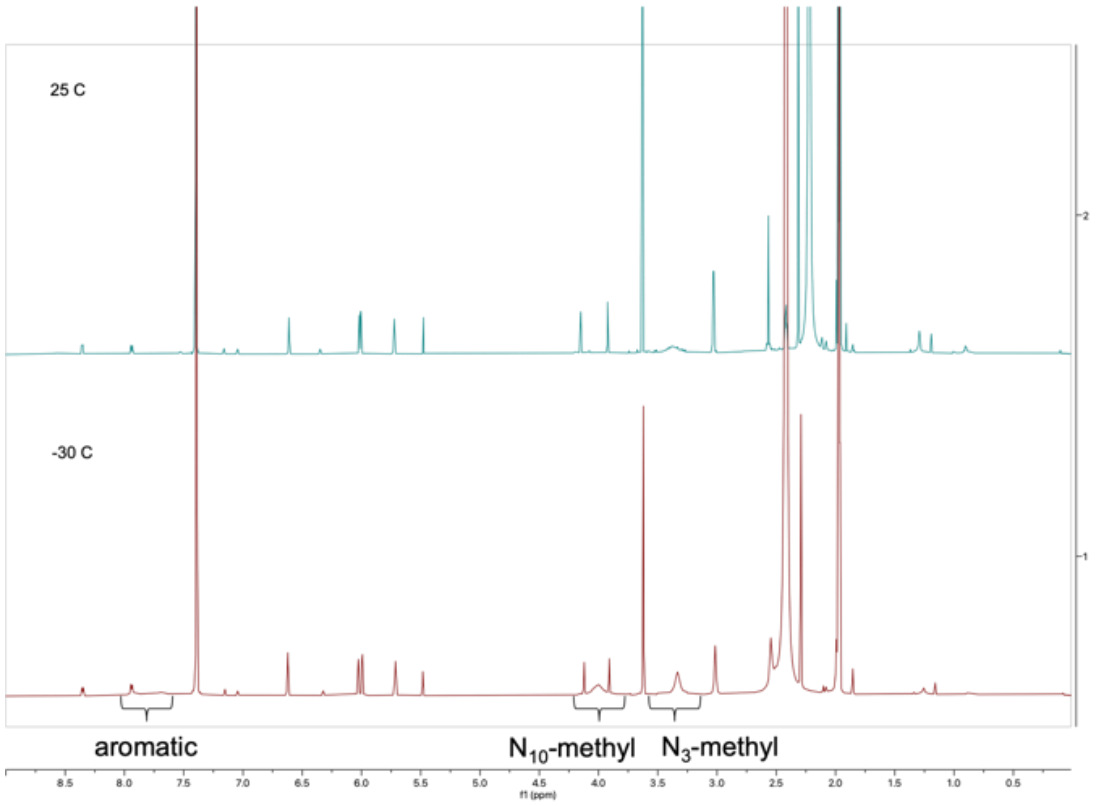

Figure 2.13: ^{1}H NMR spectrum of a 1:1 (MMTP:3MLF, 2.05 mM) reaction, taken after approximately four hours, is shown at two different temperatures, 25 ^{o}C (top) and -30 ^{o}C (bottom). Both the N3- and N10-methyl groups from 3MLF are much sharper and greater in intensity at low temperatures, indicating that the self-exchange reaction of 3MLF and its radical form has slowed down significantly.

2.4 Discussion

The oxidation of MMTP to MMP^{+} is a net four electron process. Under aerobic conditions, the reaction is catalyzed by 3MLF, which requires the reaction stoichiometry shown in Eq. 1. Under anaerobic conditions, the oxidation of MMTP by 3MLF is stoichiometric, requiring the stoichiometry shown in Eq. 2. In both cases, MMP^{+} must be paired with a negatively charged counterion, HOO^{-} in the case of the catalyzed reaction and $3MLFH^{-}$ for the stoichiometric reaction (or hydroxide ion if $3MLFH^{-}$ is protonated by small amounts of water present in the CD_3CN NMR solvent.)

$$MMTP + 2\,O_2 \longrightarrow MMP^+ + H_2O_2 + HO_2^- \quad (\mathbf{1})$$

$$MMTP + 2\,3MLF \longrightarrow MMP^+ + 3MLFH_2 + 3MLFH^- \quad (\mathbf{2})$$

The results unambiguously point to the intermediacy of radical species formed via single electron transfer. We propose the mechanism depicted in Figure 2.14a for the anaerobic reaction. An unfavorable electron transfer between 3MLF and MMTP produces the radical anion/radical cation pair ($3MLF^{\bullet-}$ and $MMTP^{\bullet+}$). $MMTP^{\bullet+}$ is extremely acidic, and $3MLF^{\bullet-}$ is the strongest base in solution, so proton transfer leads to the neutral radicals MMTP• and 3MLFH•, the latter of which is persistent under anaerobic conditions and detected EPR. The 3MLFH• concentration increases steadily during the first few hours of reactions reflected by the intensifying EPR signal. Rapid exchange between 3MLFH• and 3MLF (or $3MLF^{\bullet-}$ and 3MLF) leads to line broadening and disappearance of the 3MLF signals in the ^1H NMR spectrum. These lines reappear and sharpen as the temperature, and thus rate of exchange, is lowered.

Meanwhile, MMTP• is sequentially oxidized in a series of electron transfer/proton transfer steps leading to MMP^+. Figure 2.14a does not explicitly identify the secondary or tertiary one-electron oxidant, but it is most certainly a flavin derived species in its oxidized (3MLF) or partially reduced form (3MLFH•), the latter of which is likely more easily reduced.[20] Similarly, the proton transfers likely involve the partially or fully reduced forms of the flavin, $3MLF^{\bullet-}$ and/or $3MLFH^-$. Over the course of longer time periods (days) the reaction continues until most of MMTP is converted to MMP^+ and a precipitate is formed ($3MLFH_2$ or $3MLFH^-$). The identity of this precipitate is confirmed by the fact that it reverts cleanly to the fully oxidized form (3MLF) when exposed to oxygen.

With oxygen present, the same mechanism operates up to and including the formation of MMTP• and 3MLFH•. Now, however, as suggested in our earlier work,[14] MMTP• reacts with O_2 yielding

DHP^+ (presumably at a diffusion-controlled rate),[21] and further oxidation leads to MMP^+ (Figure 2.14b). Because 3MLF remains at its initial concentration throughout the course of the aerobic reaction (i.e., it is a catalyst), we believe 3MLFH• reacts with O_2 to regenerate 3MLF. (The is no indication of any partially or fully reduced flavin in the ^1H NMR.)

a) Anaerobic oxidation of MMTP by 3MLF

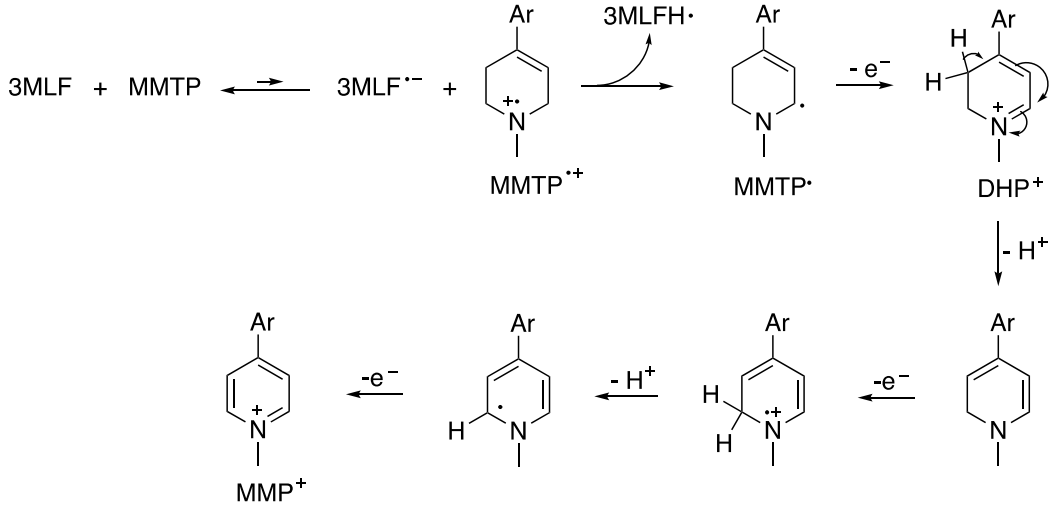

b) When oxygen is present, 3MLF is regenerated and the reaction is catalytic

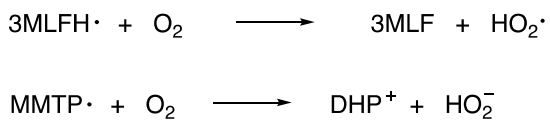

Figure 2.14: Proposed mechanism for the reaction of 3MLF with MMTP. Under anaerobic conditions (a), the reaction is stoichiometric and $3MLFH_2$ is a by-product. (b) In the presence of O_2, the reaction is catalytic; O_2 can also oxidize MMTP• to DHP^+.

It is not clear whether the initially formed $3MLF^{\bullet-}$ and $MMTP^{\bullet+}$ are freely diffusing and can separate, or are formed as a radical anion/radical cation caged pair. If the latter, then electron transfer/proton transfer sequence may not be discrete steps and the overall process may be tending toward a proton coupled electron transfer,[22] where electron transfer and proton transfer are concerted. Future work will address this issue in more detail.

2.5 Conclusions

These results are of direct relevance to oxidations of tertiary amines catalyzed by MAO. Unlike our earlier work with Fl^+ which is strongly oxidizing, 3MLF is a more realistic biomimetic for the neutral flavin in the active site of MAO. Moreover, 3MLF functions as a catalyst for oxidation. These results strengthen our hypothesis (Figure 2.5) that for MAO-catalyzed oxidations, the SET pathway is always available and present, but only becomes important when the resulting radical cation is very acidic. As noted, consistent with currently accepted mechanisms, tertiary amines are not generally MAO substrates. The exceptions are tertiary amines based upon the tetrahydropyridine framework (i.e., MPTP, MMTP, etc.). Assuming that MAO inhibitors interact with the enzyme via a mechanism similar to that of substrates (i.e., mechanism-based inhibition), it may be particularly significant that there are a number of tertiary amines that a) are MAO inhibitors and b) have structural features related to the tetrahydropyridines (i.e., a CH_2 moiety α- both to nitrogen and either a C=C or C≡C, Figure 2.15.) These structural features dramatically lower the pK_a of the corresponding radical cations because they impart resonance stabilization to the resulting free radicals,[16] and we believe, activate the SET pathway.

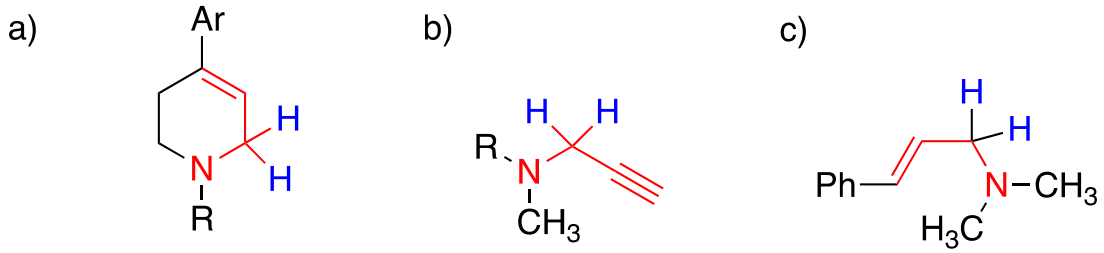

Figure 2.15: Tertiary amines that interact with MAO B. The reactive C-H bonds are depicted in blue, and critical functionality in red: a) tetrahydropyridines and related compounds that are MAO substrates or inhibitors,[6a] b) MAO inhibitors based on 3° propargylic amines such as pargyline and deprenyl,[23] and c) analogs of *N*,*N*-dimethylcinnamylamine that are MAO inhibitors.[24]

Finally, it should be noted that both 5-ethyl-3-methyllumiflavinium perchlorate (Fl^+) and 3MLF have been used previously as biomimetics to better understand the mechanism of MAO-catalyzed oxidations by Mariano, et al.[25] All of their results were consistent with a polar (nucleophilic addition) mechanism. For 3MLF, the reactivity order parallels that of MAO in terms of amine structure, i.e., $1^o > 2^o > 3^o$, which makes sense because of steric effects. Moreover, using Fl^+ and benzylamine as substrate, a nucleophilic addition product was isolated which resulted from nucleophilic addition to the 4a position, as expected for the polar mechanism. However, unlike the present study, none of the amines examined in this earlier work possessed the structural features that we believe activates the electron transfer pathway, specifically a CH_2 moiety α- both to nitrogen and either a C=C or C≡C (Figure 2.15). Based upon our results and this earlier work, it appears that 3MLF faithfully mimics the reactivity patterns found with monoamine oxidase and is an outstanding biomimetic for understanding the mechanism of MAO-catalyzed oxidations.

In the recent MAO literature, there appears to be an (almost) general consensus that some sort of polar mechanism explains the catalytic pathway(s) by which MAOs convert 1^o and some 2^o amines to the corresponding imines ($R_2CHNH_2 \rightarrow R_2C{=}NH$), and we agree that this is most likely the case for biogenic amines. However, there is also other compelling evidence for single electron transfer, based mainly on the behavior of certain compounds with *N*-cyclopropyl or *N*-cyclobutyl groups as electron transfer probes. These observations are not irreconcilable. Based upon these (and earlier results with flavin biomimetics), we suggest that the electron transfer pathway may always be available as an unfavorable equilibrium and is accessible to certain activated substrates which a) cannot react via the polar mechanism and, b) possess structural features that lower the pK_a of the corresponding radical cation. In the context of Le Chatelier's principle: an unfavorable

equilibrium (electron transfer) is driven towards products by of an extremely favorable follow up step (deprotonation).

2.6 References

[1] a) P. F. Fitzpatrick, *Arch. Biochem. Biophys.* **2010**, *493*, 13 - 25; b) R. R. Ramsay, A. Albreht, *J. Neural Transm.* **2018**, *125*, 1659 - 1683; c) N. S. Scrutton, *Nat. Prod. Rep.* **2004**, *21*, 722 - 730.

[2] J. R. Miller, D. E. Edmondson, *Biochemistry* **1999**, *38*, 13670 - 13683.

[3] a) R. Orru, M. Aldeco, D. E. Edmondson, *J. Neural Transm.* **2013**, *120*, 847 - 851; b) R. Vianello, M. Repič, J. Mavri, *Eur. J. Org. Chem.* **2012**, 7057 - 7065.

[4] a) R. B. Silverman, *Acc. Chem. Res.* **1995**, *28*, 335 - 342; b) R. B. Silverman, S. J. Hoffman, I. Catus, W. B., *J. Am. Chem. Soc.* **1980**, *102*, 7126 - 7128; c) J. T. Simpson, A. Krantz, F. D. Lewis, B. Kokel, *J. Am. Chem. Soc.* **1982**, *104*, 7155 - 7161.

[5] a) N. Castagnoli, Jr., K. Chiba, A. J. Trevor, *Life Sci.* **1985**, *36*, 225 - 230; b) K. Chiba, A. Trevor, N. Castagnoli, Jr., *Biochem. Bioph. Res. Co.* **1984**, *120*, 574 - 578.

[6] a) L. Hall, S. Murray, K. Castagnoli, N. Castagnoli Jr., *Chem. Res. Toxicol.* **1992**, *5*, 625 - 633; b) D. E. Edmondson, A. K. Bhattacharyya, M. C. Walker, *Biochemistry* **1993**, *32*, 5196 - 5202.

[7] H. Gaweska, P. F. Fitzpatrick, *BioMol Concepts* **2011**, *2*, 365 - 377.

[8] a) E. Abad, R. K. Zenn, J. Kästner, *J. Phys. Chem. B* **2013**, *117*, 14238 - 14246; b) K. Cakir, S. S. Erdem, V. E. Atalay, *Org. Biomol. Chem.* **2016**, *14*, 9239 - 9252.

[9] C. Franot, S. Mabic, N. Castagnoli Jr., *Bioorg. Med. Chem.* **1998**, *6*, 283 - 291.

[10] a) R. V. Dunn, A. W. Munro, N. J. Turner, S. E. J. Rigby, N. S. Scrutton, *ChemBioChem* **2010**, *11*, 1228 - 1231; b) A. T. Murray, M. J. H. Dowley, F. Pradaux-Caggiano, A. Baldansuren, A. J. Fielding, F. Tuna, C. H. Hendon, A. Walsh, G. C. Lloyd-Jones, M. P. John,

D. R. Carbery, *Angew. Chem. Int. Ed.* **2015**, *54*, 8997 - 9000; c) S. E. J. Rigby, R. M. G. H. Hynson, R. R. Ramsay, A. W. Munro, N. S. Scrutton, *J. Biol. Chem.* **2005**, *280*, 4627 - 4631.

[11] K. Yelekci, X. Lu, R. B. Silverman, *J. Am. Chem. Soc.* **1989**, *111*, 1138 - 1140.

[12] J.-M. Kim, M. A. Bogdan, P. S. Mariano, *J. Am. Chem. Soc.* **1991**, *113*, 9251 - 9257.

[13] a) S. S. Erdem, B. Büyükmenekşe, *J. Neural Transm.* **2011**, *118*, 1021 - 1029; b) G. Zapata-Torres, A. Fierro, G. Barriga-González, J. C. Salgado, C. Celis-Barros, *J. Chem. Inf. Model.* **2015**, *55*, 1349 - 1360.

[14] a) A. Nakamura, M. Abdel Latif, P. A. Deck, N. Castagnoli Jr., J. M. Tanko, *Chem. Eur. J.* **2020**, *26*, 823 - 829. b) A Nakamura, Ph.D. Thesis, Virginia Tech, 2013.

[15] H. Fischer, *Chem. Rev.* **2001**, *101*, 3581 - 3610.

[16] J. S. González, J. M. Tanko, *Chem. Thermodyn. Therm. Anal.* **2023**, *12*, 100119.

[17] V. Sichula, P. Kucheryavy, R. Khatmullin, Y. Hu, E. Mirzakulova, S. Vyas, S. F. Manzer, C. M. Hadad, K. D. Glusac, *J. Phys. Chem. A* **2010**, *114*, 12138 - 12147.

[18] a) A. Ehrenberg, F. Müller, P. Hemmerich, *Eur. J. Biochem.* **1967**, *2*, 286 - 293; b) R. Arpad, C. Einholz, B. Illarionov, L. Heidinger, T. Al Said, A. Bauss, M. Fischer, A. Bacher, S. Weber, E. Schleicher, *J. Am. Chem. Soc.* **2018**, *140*, 16521 - 16527.

[19] Spartan ’20, Wavefunction, Inc., Irvine, CA.

[20] X.-L. Li, Y. Fu, *J. Molec. Struct. Theochem* **2008**, *856*, 112 - 118.

[21] J. Lalevée, B. Graff, X. Allonas, J. P. Fouassier, *J. PHys. Chem. A* **2007**, *111*, 6991 - 6998.

[22] D. R. Weinberg, C. J. Gagliardi, J. F. Hull, C. F. Murphy, C. A. Kent, B. C. Westlake, A. Paul, D. H. Ess, D. G. McCafferty, T. J. Meyer, *Chem. Rev.* **2012**, *112*, 4016 - 4093.

[23] A. C. Tripathi, S. Upadhyay, S. Paliwal, S. K. Saraf, *Eur. J. Med. Chem.* **2018**, *145*, 445 - 497.

[24] C. K. Hiebert, R. B. Silverman, *J. Med. Chem* **1988**, *31*, 1566 - 1570.

[25] J.-M. Kim, M. A. Bogdan, P. S. Mariano, *J. Am. Chem. Soc.* **1993**, *115*, 10591 - 10595.

[26] a) S. K. Nimkar, A. H. Anderson, J. M. Rimoldi, M. Stanton, K. P. Castagnoli, S. Mabic, Y.-X. Wang, N. Castagnoli Jr., *Chem. Res. Toxicol.* **1996**, *9*, 1013 - 1022; b) S. Ghisla, U. Hartmann, P. Hemmerich, F. Mueller, *Justus Liebigs Ann. Chem.* **1973**, *8*, 1388 - 1415.

Chapter 3. Using Cyclopropyl Spin Traps as Radical Probes for the Oxidation of MPTP

3.1 Abstract

The use of cyclopropyl spin traps in MAO B biomimetic reactions would provide substantial evidence for the presence of radical substrate intermediates. The reaction of 3-methyllumiflavin (3MLF) and *N*-cyclopropyl MPTP was performed both aerobically and anaerobically. Both ^{1}H NMR and LC/MS spectra suggested the presence of several ring-opened intermediates and products derived from the *N*-cyclopropyl MPTP. One of these, propionaldehyde, is believed to be formed as the result of an unforeseen hydrolysis reaction. The presence of ring-opened products provided substantial evidence for an initial single electron transfer (SET) reaction between 3MLF and the substrate. The kinetics of this oxidation were subsequently probed using a kinetic isotope effect study, revealing that the SET step is coupled to but not concerted with a subsequent proton transfer step.

3.2 Introduction

Some tetrahydropyridines (THPs) are able to undergo oxidation by monoamine oxidase B (MAO B), an enzyme responsible for the metabolism of neurotransmitters.[1,2] Usually, substrates for MAO B are primary or secondary amines, however some THPs are notably tertiary, usually an exclusionary factor for the metabolic process.[3-11] Previously, we have argued that β-unsaturation from the tertiary amine center of those THPs such as MPTP allow for an alternative oxidative pathway by which they can react with MAO B, Figure 3.1.[12]

a) Anaerobic oxidation of MMTP by 3MLF

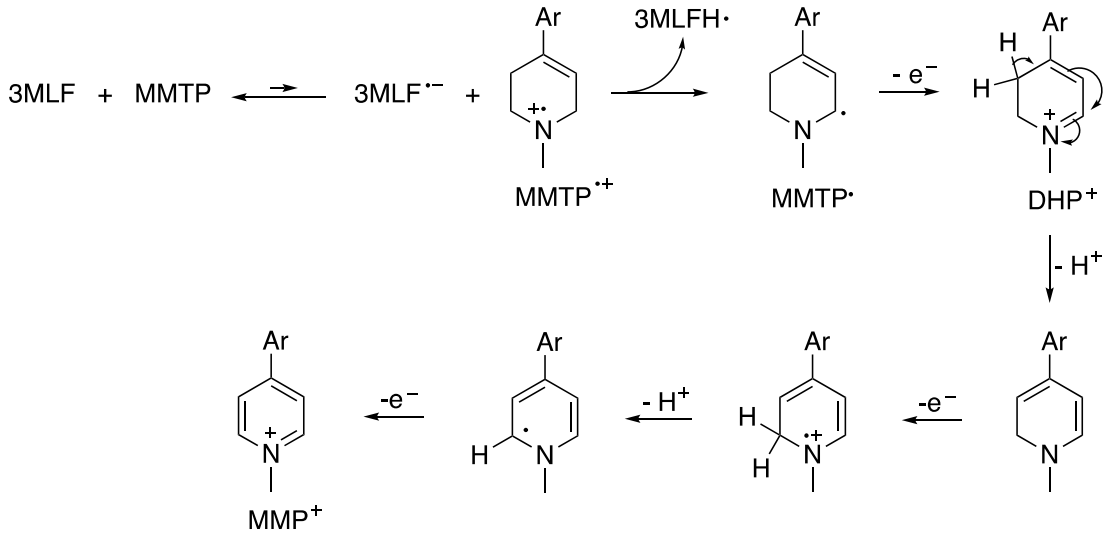

b) When oxygen is present, 3MLF is regenerated and the reaction is catalytic

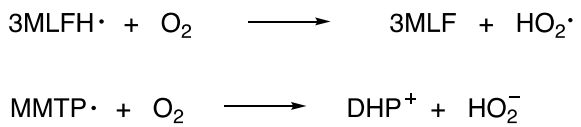

Figure 3.1: Proposed mechanism for the reaction of 3MLF with MMTP. Under anaerobic conditions (a) the reaction is stoichiometric and $3MLFH_2$ is a by-product. (b) In the presence of O_2, the reaction is catalytic; O_2 can also oxidize MMTP• to DHP^+.

The single-electron transfer (SET) hypothesis presented in Figure 3.1, first suggested by Silverman, has been contentious when considering primary and secondary amines. However, it is the only reasonable explanation for the oxidation of tertiary amines by MAO B. Much of the foundational work done by both Silverman and Castagnoli centered around the use of internal substrate spin traps in order to provide direct evidence for SET.[1, 2, 9-11] The most common of these spin traps is the cyclopropylcarbinyl radical rearrangement. A substrate containing a cyclopropyl moiety is able to undergo a ring-opening process if a radical is introduced to the alpha position, Figure 3.2. This is a thermodynamically possible process due primarily to the large amount of ring strain inherent to the cyclopropyl moiety. Applying this to the system of interest, a ring-opening is only able to occur if SET has converted the substrate from its neutral form to a radical cation,

Figure 3.2. These reactions have long been a standard for the characterization of radical processes.[1, 2, 9-11]

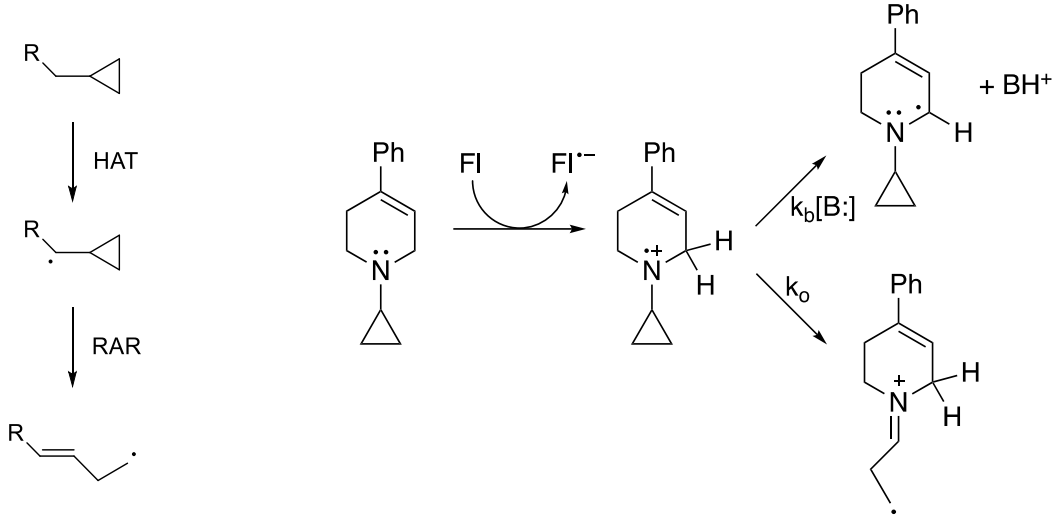

Figure 3.2: Left: Classical cyclopropylcarbinyl rearrangement probe. Introduction of a radical to the position alpha to the cyclopropyl ring allows for a rearrangement wherein the ring opens to form a primary radical. Right: Use of a single electron transfer probe to examine the mechanism of MAO-catalyzed oxidations. The *N*-cyclopropyl group diverts the initially produced radical cation forming a 1^{o} radical that disrupts the active site thereby deactivating the enzyme. Fl represents the flavin cofactor in MAO.

A principal method for investigation MAO B reactivity has been the use of biomimetics which feature the key flavin moiety responsible for the redox chemistry associated with neurotransmitter metabolism. Work done by Nakamura et al. was the first to show that the usefulness of these biomimetic probes extends beyond analysis of primary and secondary amine reactivity, and that the oxidation of THPs can be monitored using the same techniques.[13] In those studies, 5-ethyl-3-methyllumiflavinium perchlorate was used as the biomimetic to demonstrate that the oxidation of THPs involved the formation of radical flavin intermediates, providing substantial evidence that the reaction proceeds via an initial single-electron transfer (SET) event.

Later, Price et al. demonstrated that the same reactivity for THPs was observed using the neutral biomimetic, 3-methyllumiflavin (3MLF).[12] The neutral flavin has redox properties closer to those of MAO than the charged flavinium species used by Nakamura, making it a more accurate

mimic for the system of interest. While the study by Price et al. was promising in its premise, that work is mostly foundational. Our goal with the work presented below is to more fully characterize the oxidation of MPTP analogs with 3MLF by using several classic physical organic approaches.

Here, we aim to further demonstrate that the reaction of MPTP and MMTP, two β-unsaturated THPs, involves a SET via the use of a classic cyclopropyl spin trap. Further, we aim to characterize the relative reactivities of the cyclopropyl compounds and their methyl counterparts. Lastly, an analysis of the relative rates of reaction will be performed to determine whether or not the initial SET is concerted with, or simply coupled to, a proton transfer.

3.3 Anaerobic Reactions of Cyc-MPTP (1) with 3MLF

Reactions described below were prepared from stock solutions and carried out in NMR tubes at the mM scale. For anaerobic reactions, samples were freeze-pump thaw degassed and subsequently the NMR tubes were flame-sealed under vacuum to ensure minimal introduction of molecular oxygen into the reaction vessel. All reactions were stored in the dark at ambient temperature to avoid light-mediated reaction of 3MLF.

In our previous work with MMTP, anaerobic reaction conditions proved invaluable as they demonstrated unique, NMR-silent behavior with respect to the flavin, providing preliminary evidence for SET. It was demonstrated that after the transfer of one equivalent of electrons from the flavin to the substrate, the flavin signals broadened into the baseline of the ^{1}H NMR spectrum due to the self-exchange reaction outlined in Scheme 3.1. We hypothesize that the flavin should be NMR-silent when reacting with cyclopropyl substrates as well. To probe this, an anaerobic 1:1 (5.00 mM 3MLF, 5.00 mM cyc-MPTP) reaction of 3MLF and cyclopropyl-MPTP (cyc-MPTP) was performed and monitored as a function of time, Figure 3.3.

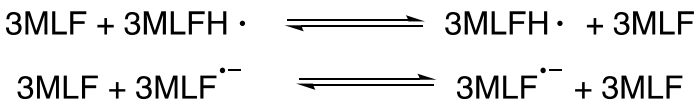

Scheme 3.1: Proposed anaerobic radical equilibrium of 3MLF from Price et al.[12]

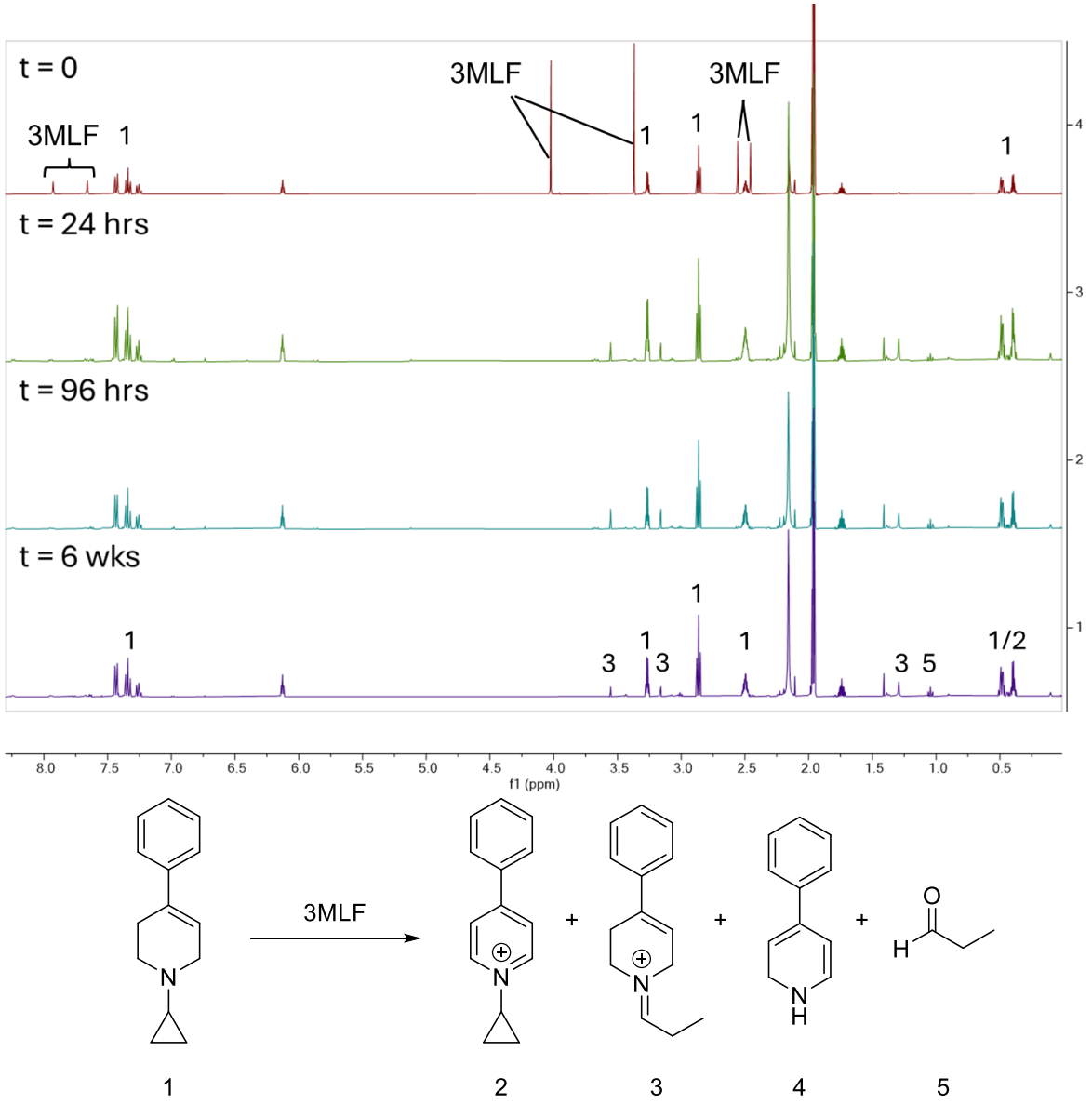

Figure 3.3: The [1]H NMR spectra for a 1:1 anaerobic reaction of cyc-MPTP (1) and 3MLF are shown (5.00 mM each). Within the first 24 hours, all signals belonging to 3MLF (Figure B.1) have broadened out of the spectrum, suggesting possible radical formation. This behavior is consistent with previous work with 3MLF. Full characterization of other species in solution were verified by [1]H NMR and LC/MS analysis (Section B.3).

After several hours, the signals associated with 3MLF disappeared from the [1]H NMR spectrum, suggesting the transfer of one equivalent of electrons was complete. The disappearance

of the flavin signal was accompanied by the appearance of several other signals suggesting that the reaction was able to proceed under anaerobic conditions. Signals at 3.6, 3.2, and 1.3 ppm suggest the formation of a ring-opened intermediate (3). Similarly, the presence of an aldehydic triplet at 9.40 ppm and a triplet at 1.05 ppm suggests the formation of an aldehydic product (Figure 3.5). The only reasonable progenitor of a triplet signal in the aliphatic region is a terminal methyl group of the ring-opened substrate. We hypothesize that excess water in the reaction vessel was able to induce hydrolysis of this iminium to form propionaldehyde as shown in Scheme 3.2. Isolation and characterization of the propionaldehyde product is discussed at length below.

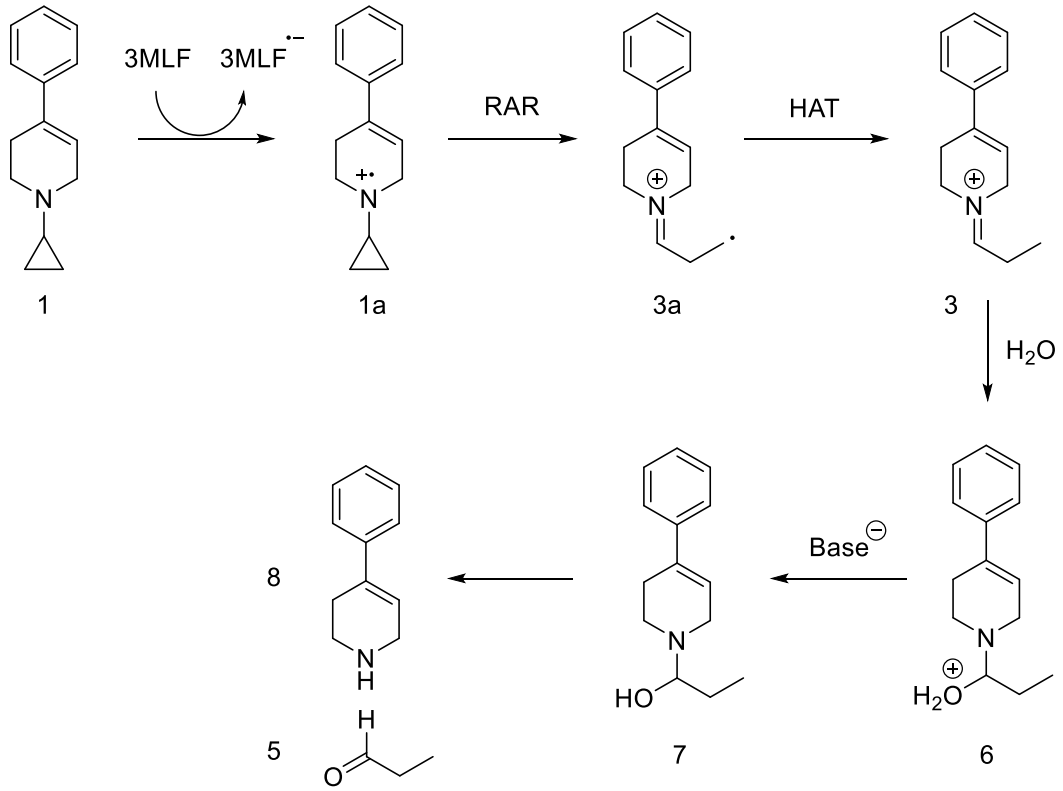

Scheme 3.2: The proposed hydrolysis of iminium intermediate resulting from ring opening to form propionaldehyde and secondary amine is shown. The base in solution is most likely a reduced form of 3MLF. The resultant secondary amine is hypothesized to be quickly oxidized by 3MLF.

After allowing the reaction to continue for 4 days, an orange precipitate was noted in the bottom of the reaction vessel. This behavior is consistent with our previous work and is indicative

of the complete reduction of 3MLF to $3MLH_2$. The introduction of air into this sample allowed for the reoxidation of the flavin ($3MLFH_2$ → 3MLF), again consistent with observations from previous studies.

While quantitation of anaerobic reactions by ^{1}H NMR would be exceedingly helpful in the complete characterization of the reaction, dynamic nuclear polarization (DNP) effects render this process ineffectual. In short, the integrations from these signals are affected by the presence of paramagnetic species in solution, and the exact measurement of these effects is beyond the scope of this study. As such, the anaerobic behavior of this reaction, while interesting, primarily serves to qualitatively demonstrate that the reactivity of the flavin is consistent when reacting with "normal" tetrahydropyridines (THPs) and their cyclopropyl derivatives.

3.4 Aerobic Reactions of Cyc-MPTP with 3MLF

Aerobic reactions were prepared from stock solutions in NMR tubes at the mM scale. Reaction vessels were subjected to constant mixing when not being actively analyzed. In contrast to previous work, the aerobic reactions provided much necessary information to understand the reaction of interest. Consistent with previous results, we believe that O_2 present in the aerobic reaction vessels quickly reoxidizes 3MLF from a partially reduced form back into its active form. As such, the complete oxidation of substrate is possible due to the catalytic nature of 3MLF. Further, the absence of radical flavin intermediates allows for robust quantitation of substrate intermediates using ^{1}H NMR. This is particularly useful when dealing with cyclopropyl probes as it allows for direct observation of the hypothesized competition between ring-opening and oxidation, Figure 3.2

Spectra obtained from the 1:1 aerobic reaction of cyc-MPTP and 3MLF (5.00 mM each) are shown in Figure 3.4. Based on the time-resolved spectra shown there, several critical

observations were made. First, we identified that the starting material was being consumed at a reasonable rate, consistent with previous results, indicating that reactions were able to proceed as hypothesized. Further, the appearance of several distinct signals as a function of time led us to the conclusion that multiple products were being formed, suggesting a partitioning between ring-open and ring-closed oxidation; complete analysis of these signals can be found in Section B.2. Again, this was consistent with our initial hypothesis. Finally, the appearance of an aldehydic triplet at 9.74 ppm coinciding with the formation of a triplet at 1.05 ppm, attributable to propionaldehyde, was consistent with anaerobic results and warranted further investigation.

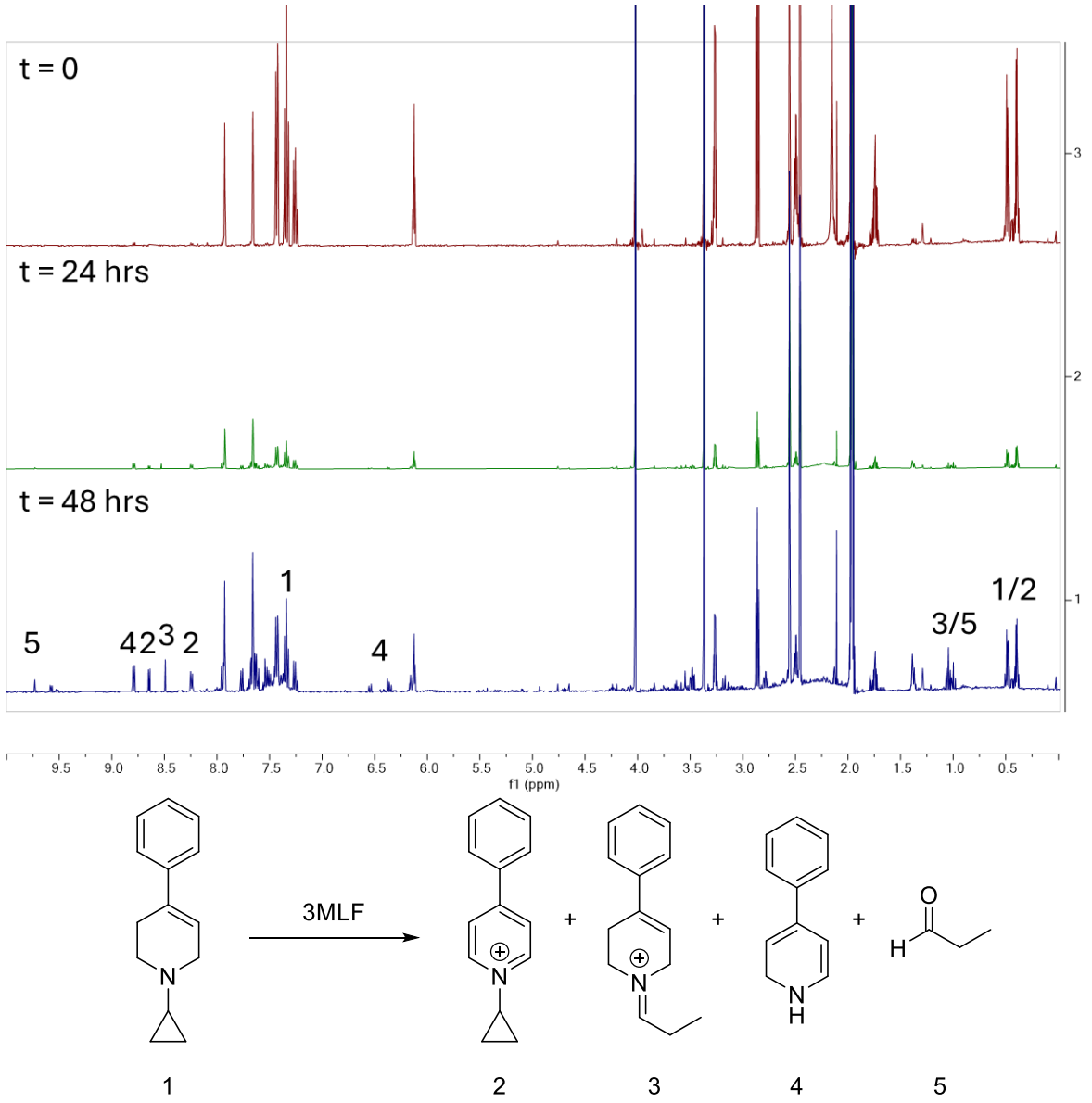

Figure 3.4: The 1:1 aerobic reaction of 3MLF and cyc-MPTP (5.00 mM each) was monitored as a function of time by ^{1}H NMR. At t=48 hrs, several important signals have formed. Full characterization of these species in solution were verified by ^{1}H NMR and LC/MS analysis (Section B.3). The presence of each of these compounds suggests that the hypothesized competition reaction is proceeding as expected, leading to the production of a mix of ring-opened and ring-closed products.

A 1:1 reaction of cyc-MPTP and 3MLF (5.00 mM each) was allowed to react for two weeks to ensure maximum conversion of the starting material to the product. After that two week period, isolation of volatile species was completed using trap-to-trap vacuum distillation at room temperature. The NMR spectrum of the volatile compounds was compared to that of

propionaldehyde, Figure 3.5. There was a direct match of the volatile compounds from the reaction mixture to a propionaldehyde standard. This indicates that propionaldehyde must be formed as a byproduct of this reaction.

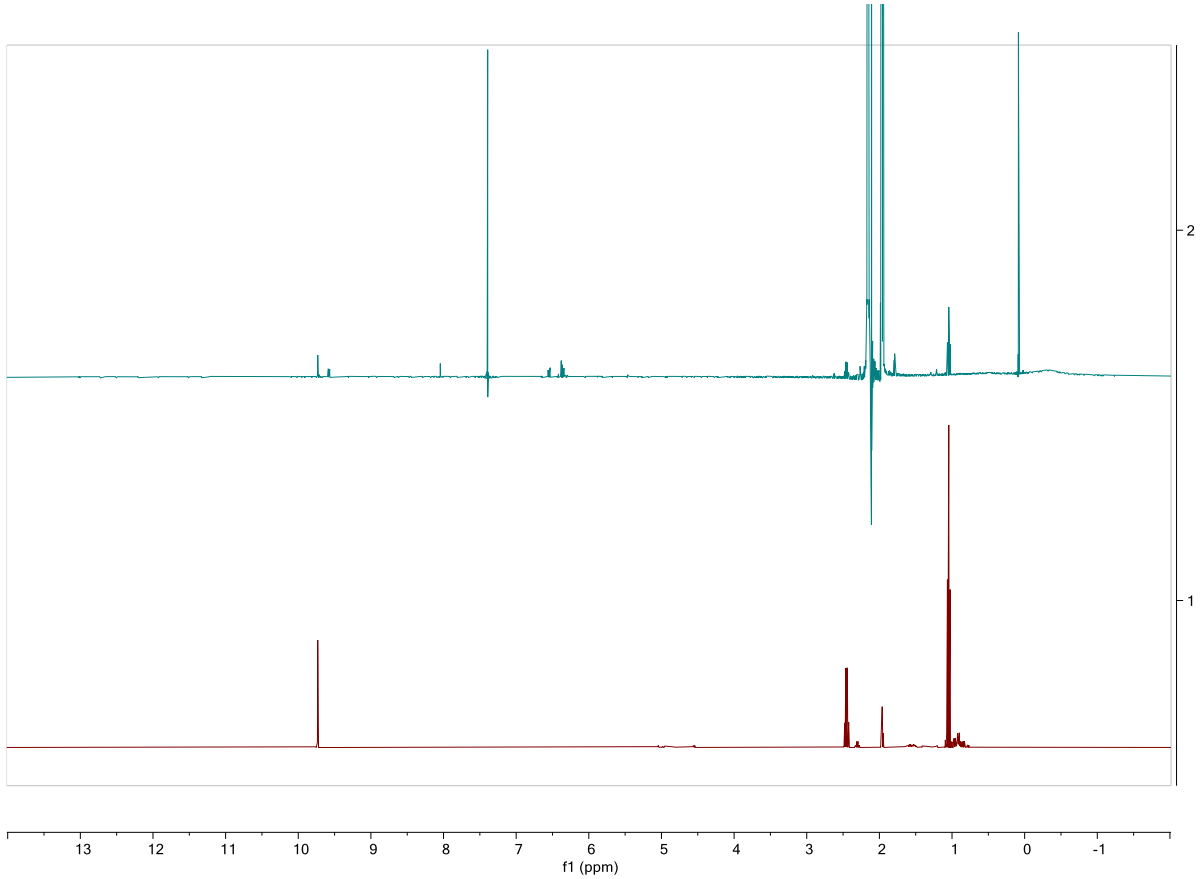

Figure 3.5: The reaction distillate (top) is compared directly with pure propionaldehyde (bottom). The aliphatic triplet and aldehydic NMR signals that are formed during the oxidation of cyc-MPTP are direct spectral matches for propionaldehyde in CD_3CN.

The most likely cause of this is hydrolysis of the hypothesized ring-opened intermediate. Small amounts of water in solution (most likely from the hygroscopic NMR solvent) allowed for the hydrolytic process shown in Scheme 3.3. An interesting byproduct of this coincidence arises when considering the stoichiometries of different species present in solution as a function of time. Another aerobic 1:1 reaction of 3MLF and cyc-MPTP (5.00 mM 3MLF and 6.20 mM cyc-MPTP) was prepared with a benzene internal standard for quantitation; results for this reaction are reported

in Table 3.1 while the spectra can be found in Figure B.8. As is apparent in Table 3.1, the formation of aldehyde coincides with the formation of ring-opened oxidation product (4) while the ring-closed oxidation product (2) seems to form independent of the others. The former assessment is unsurprising as it is expected that the aldehyde is formed as a result of the degradation of (4) However, the latter led us to question the nature of the competition between ring opening and oxidation.

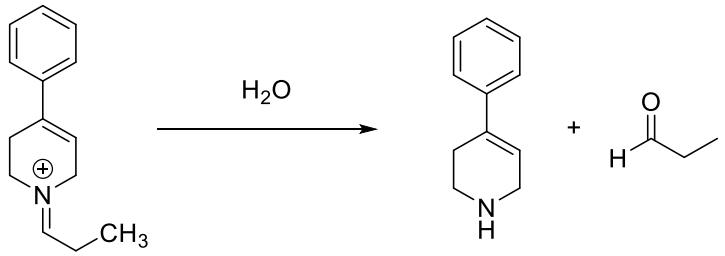

3 8 5

Scheme 3.3: Proposed hydrolysis step. The interaction of water in solution with a ring-opened iminium intermediate induces the favorable hydrolysis to form a secondary amine and the observed propionaldehyde.

Table 3.1: Concentrations of Reactants and Products for the Aerobic Reaction of 3MLF and cyc-MPTP

1:1 3MLF:cyc-MPTP	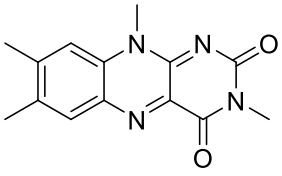 3MLF	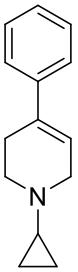 1	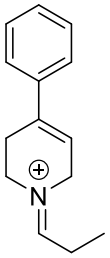 3	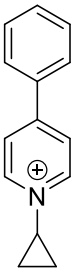 2	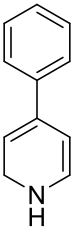 4	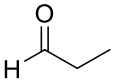 5
$[X]_0$	5.00	6.22	0.051	0.167	0.081	0.009
$[X]_{24}$	5.00	1.98	0.240	0.564	0.415	0.099
$[X]_{48}$	5.00	2.72	0.469	0.881	0.955	0.240

The formation of propionaldehyde (5) during this reaction necessitated a reevaluation of the reaction mechanism. As previously discussed, the formation of propionaldehyde was most likely the result of a hydrolytic process. However, the ability for the substrate to undergo

hydrolysis similarly necessitates a hydrogen atom transfer (HAT). This process could happen either inter- or intramolecularly, Scheme 3.4. To probe this behavior, an H/D isotope study was conducted.

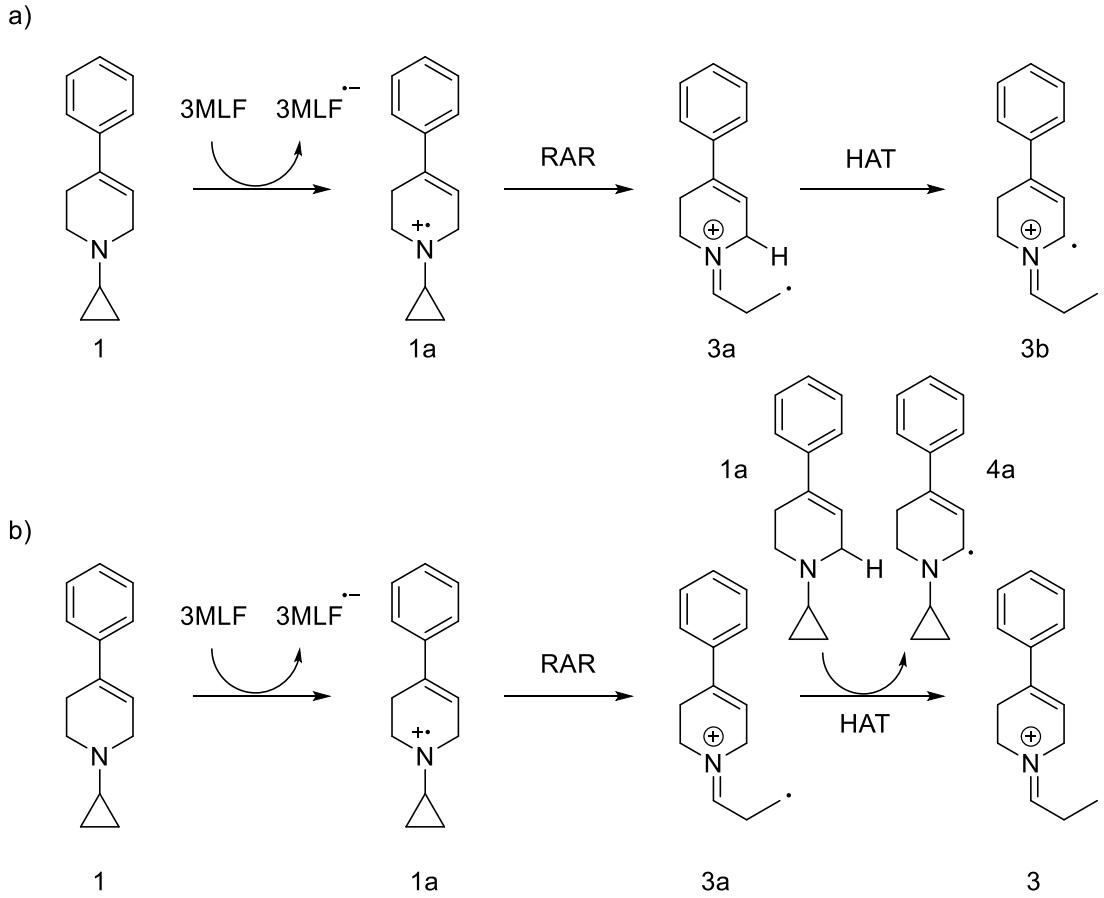

Scheme 3.4: Hypothesized HAT processes to form the ring-opened intermediate (3). The intramolecular pathway (a) involves the abstraction of a hydrogen atom from the alpha position of the ring-opened substrate. The intermolecular pathway (b) involves the abstraction of a hydrogen atom from a second equivalent of substrate to form the partially oxidized ring-closed intermediate and the observed ring-opened intermediate (3).

The 1:1:1 reaction of cyc-MPTP-d4 (13) and MPTP (9) with 3MLF was performed (2.50 mM each). The goal was to exploit the formation of aldehyde in order to probe the molecularity of the HAT reaction, Scheme 3.5. If the reaction was intramolecular, the expectation would be that only deuterated aldehyde is formed. If it was intermolecular, a mix of deuterated and normal propionaldehyde would form. Based on calculations, it is expected that MPTP and its cyclopropyl

derivative have a similar thermodynamic barrier to HAT (calculated C-H BDE for each is 73 kcal/mol), so there was little concern that the experiment was predisposed to one result or the other.

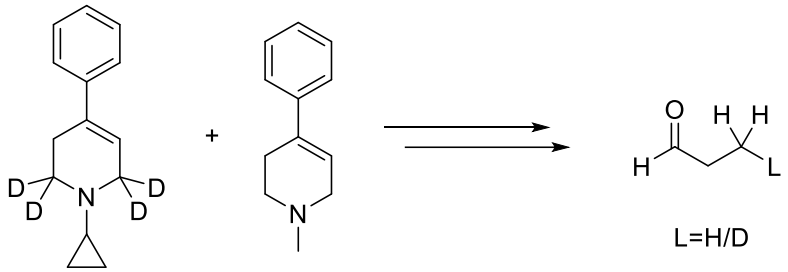

Scheme 3.5: The reaction of cyc-MPTP-d4, MPTP, and 3MLF is hypothesized to have two possible aldehydic product distributions. In the case of intramolecular HAT after ring-opening, only the deuterated aldehyde would form. However, intermolecular HAT would lead to a mix of deuterated and non-deuterated aldehyde.

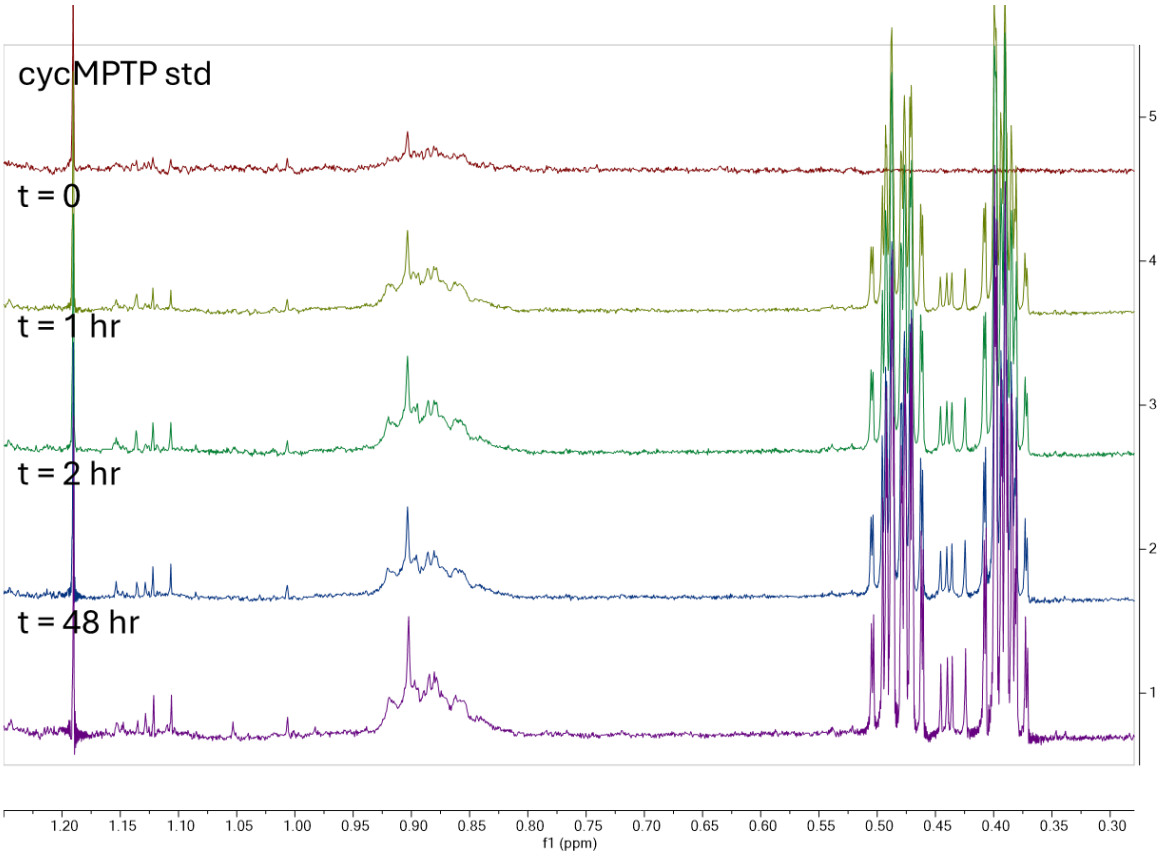

Figure 3.6: The aerobic 1:1:1 reaction of cyc-MPTP-d4, MPTP, and 3MLF is shown here as a function of time. By 48 hrs, there is no evidence for the production of propionaldehyde, suggesting a lack of reaction by cyc-MPTP-d4.

Surprisingly, the ^{1}H NMR in Figure 3.6 demonstrates that there is no propionaldehyde formed during this reaction due to the lack of a triplet signal at 1.05 ppm. This led us to test the reaction again in the absence of MPTP. Performing the reaction of cyc-MPTP-d4 and 3MLF aerobically yielded the same results as described above, even when allowing the reaction to proceed for several days (Figure B.9). Even though the propionaldehyde did not form, the ring-closed oxidation seemed to be progressing, albeit much slower than expected, leading us to reevaluate our hypothesis surrounding the ring-opening process.

Deuterium substitution at the alpha position of cyc-MPTP seemingly halted the ring-opening process. This suggests that the HAT necessitated by the presence of propionaldehyde in non-D-substituted cyc-MPTP reactions must use the hydrogen atom at the alpha position of cyc-MPTP as the hydrogen atom source. This result mirrors conclusions made by Castagnoli et al. wherein a metal-mediated reaction initiated an intermolecular HAT from (1) to an equivalent of *t*-BuO·, suggesting that the substrate itself is a good source of hydrogen atoms.[14] They further suggested that in the presence of $Fe(Phen)_3^{+3}$, (1) is able to undergo an intramolecular HAT to form (3). We speculate that the unfavorable ring-opening reaction must have a kinetic barrier to deuterium atom transfer (DAT) when the H/D substitution is made, inhibiting the reaction altogether (Scheme 3.6). Ultimately, this leads us to the conclusion that the HAT reaction occurs between substrate equivalents. No definitive speculation can be made herein, however, about whether the reaction is inter- or intramolecular. For simplicity, the proposed mechanism in Figure 3.7 depicts the HAT as being intermolecular.

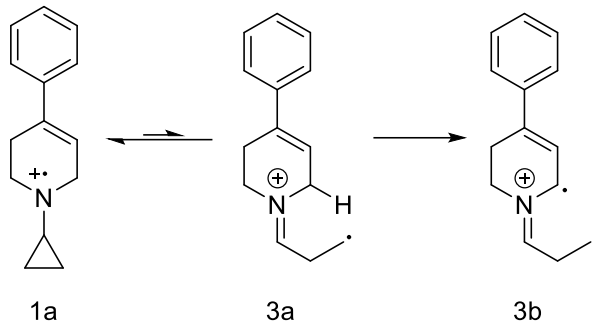

Scheme 3.6: Fate of ring-opened intermediate. Unpublished results from a series of single-point calculations with geometries optimized using M062X/pVDZ performed in Spartan 20 suggest an endothermic rearrangement (ΔG = 3.16 kcal/mol), leading to the conclusion that the ring opening is unfavorable.[15] However, the relatively low C-H BDE at the alpha position (73 kcal/mol) thermodynamically drives the reaction forward.[16] The presence of a deuterium atom at the alpha position of the substrate is hypothesized to pose too high of a kinetic barrier to react, effectively "turning off" ring-opening by deactivating the second step shown here.

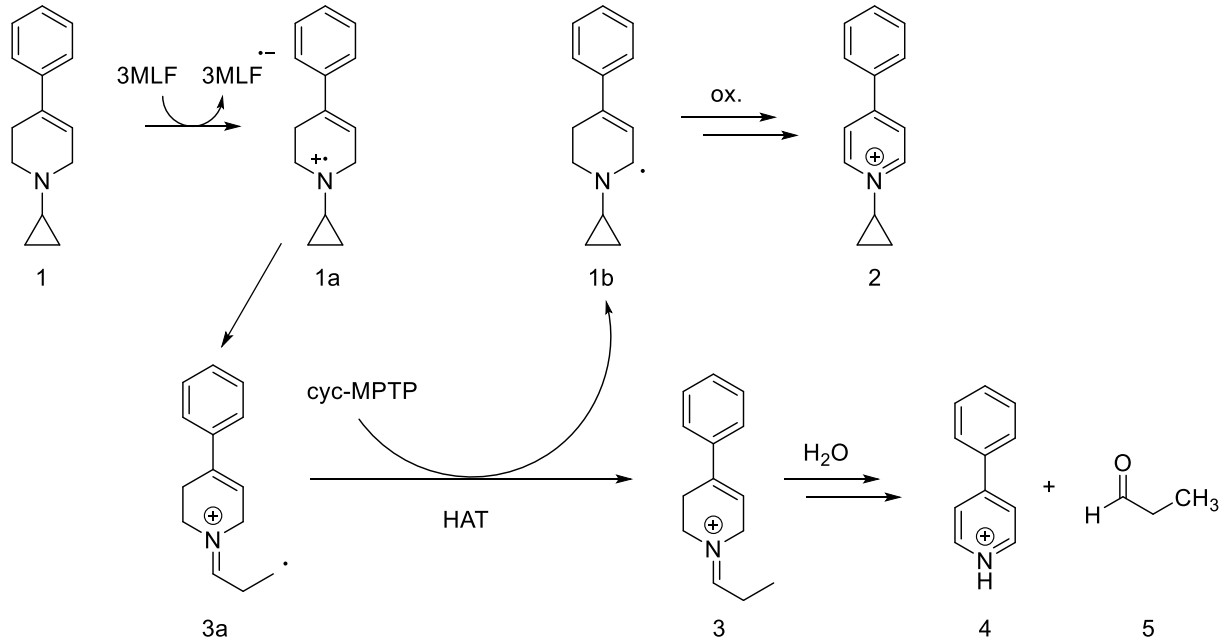

Figure 3.7: A mechanistic hypothesis for the oxidation of cyc-MPTP by 3MLF is provided here. After initial SET, a ring opening occurs, resulting in the formation of a primary iminium radical. A fast, intermolecular HAT with another equivalent of substrate leads to the simultaneous formation of the iminium and the neutral substrate radical. The iminium is then able to undergo hydrolysis while the neutral substrate radical is able to be oxidized.

3.5 Physical Organic Studies of MMTP and MPTP Reactivities

To more fully characterize the oxidation of MMTP and MPTP, there was interest in determining the exact rate-determining step. Specifically, we were interested in whether or not the initial SET was rate determining as has been long-hypothesized. To probe the RDS, a kinetic isotope effect (KIE) study was performed. The H/D effect was probed at the critical alpha position of both MMTP and MPTP. As previously discussed, the alpha hydrogens are hypothesized to be lost in a proton-coupled electron transfer event, allowing the reaction to be thermodynamically favorable. Following this hypothesis, the observance of an isotope effect would suggest that the steps are concerted while the absence of an isotope effect would suggest they are stepwise (Figure 3.8) and that the SET event is rate determining.

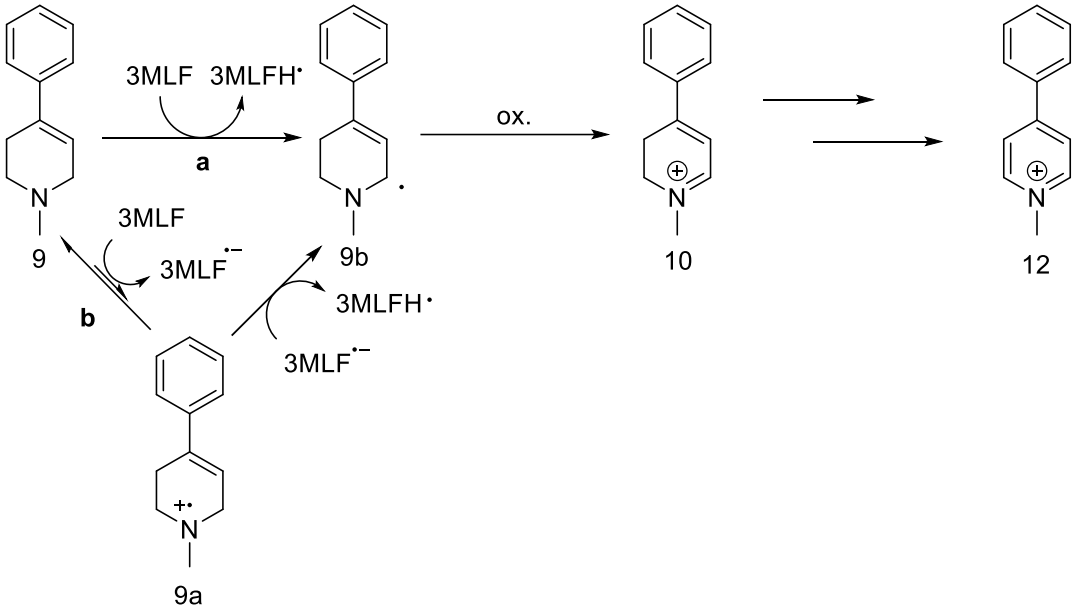

Figure 3.8: Two pathways of initial oxidation of MPTP are shown here. Pathway a depicts the concerted proton and electron transfer to arrive at the hypothesized substrate radical intermediate. Pathway b depicts a stepwise reaction where the unfavorable electron transfer is coupled with a highly favorable proton transfer.

The 2:1 (substrate:flavin) reactions of MMTP and MPTP with 3MLF were probed independently from one another, and the kinetics of each were determined using ^{1}H NMR with a benzene internal standard as the spectral probe. These reactions were carried out aerobically over the course of

several weeks in order to ensure complete consumption of the starting material. The concentration of benzene in solution is constant, allowing for a quantitative analysis of the exact concentrations of 3MLF, substrate, and oxidized product as a function of time.

$$rate = k[substrate][3MLF] \quad (1)$$

$$\frac{d[substrate]}{dt} = k[substrate][3MLF] \quad (2)$$

$$when\ [3MLF]\ is\ constant\ \ldots \quad \frac{d[substrate]}{dt} = k_o[substrate] \quad (3)$$

$$where\ \ldots\ k_o = k[3MLF]$$

$$Taking\ the\ integral\ with\ respect\ to\ t\ \ldots \quad [substrate] = [substrate]_0 e^{-k_o t} \quad (4)$$

$$Thus\ \ldots \quad ln[substrate] = \ln\,[substrate]_0 - k_o t \quad (5)$$

Performing these reactions under aerobic conditions allows for a pseudo-first order kinetic treatment with respect to [substrate]. The catalytic nature of 3MLF holds its concentration effectively constant. As such, [3MLF] is intrinsically factored into the observed rate constant (k_o), and pseudo-first order conditions are met. Thus, a plot of ln[substrate] vs. time provides the observed rate constants for the oxidations of MMTP and MPTP by 3MLF as shown in eqs. 1-5. After factoring out [3MLF] from each (again, found from the average integration value by NMR relative to benzene), we are left with several rate constants which can be directly compared in search of an H/D isotope effect, shown in Table 3.2. All spectra and plotted data are available in Section B.6-7.

Table 3.2: Average rate constants for the oxidation of H/D substituted MMTP and MPTP				
	MMTP	MMTP-d4	MPTP	MPTP-d4
First-Order Rate Constant (k) (s^{-1})	$2.19\pm0.77 \times 10^{-3}$	$2.05\pm0.75 \times 10^{-3}$	$9.40\pm8.00 \times 10^{-4}$	$2.62\pm1.08 \times 10^{-3}$

In addition to the direct measurement of rate constants through time-resolved kinetics, competition experiments were performed. A 1:1:1 reaction of MPTP, MPTP-d4, and 3MLF (2.50 mM each) was conducted as a confirmation of the results of the previous study. The signal at 6.14 ppm was selected for analysis due to the partial overlap of MPTP and MPTP-d4 signals at that position. To deconvolute these signals from one another, the nature of symmetrical NMR signals was exploited, Figure 3.9. Since the integrations for both halves of a symmetric NMR signal should be identical, this signal was integrated in two halves. The left half of the signal represents half of the MPTP integral value at that position while the right half of the signal represents half of the MPTP and all of the MPTP-d4. After an arithmetic treatment, these values were converted to concentrations and subsequently plotted according to the integrated first order rate law, Figure 3.10. From these plots, k_H/k_D values of 1.06 +/- 0.80 for MMTP and 0.36 +/- 0.28 for MPTP were calculated. While these values represent crude measurements of k_H/k_D, they are clear enough to suggest there is no KIE and that SET alone is the RDS for each. This conclusion stems from the fact that a primary isotope effect would be expected if the two steps were concerted. The consistent observation of little to no isotope effect clearly rules out a primary isotope effect as a possibility.

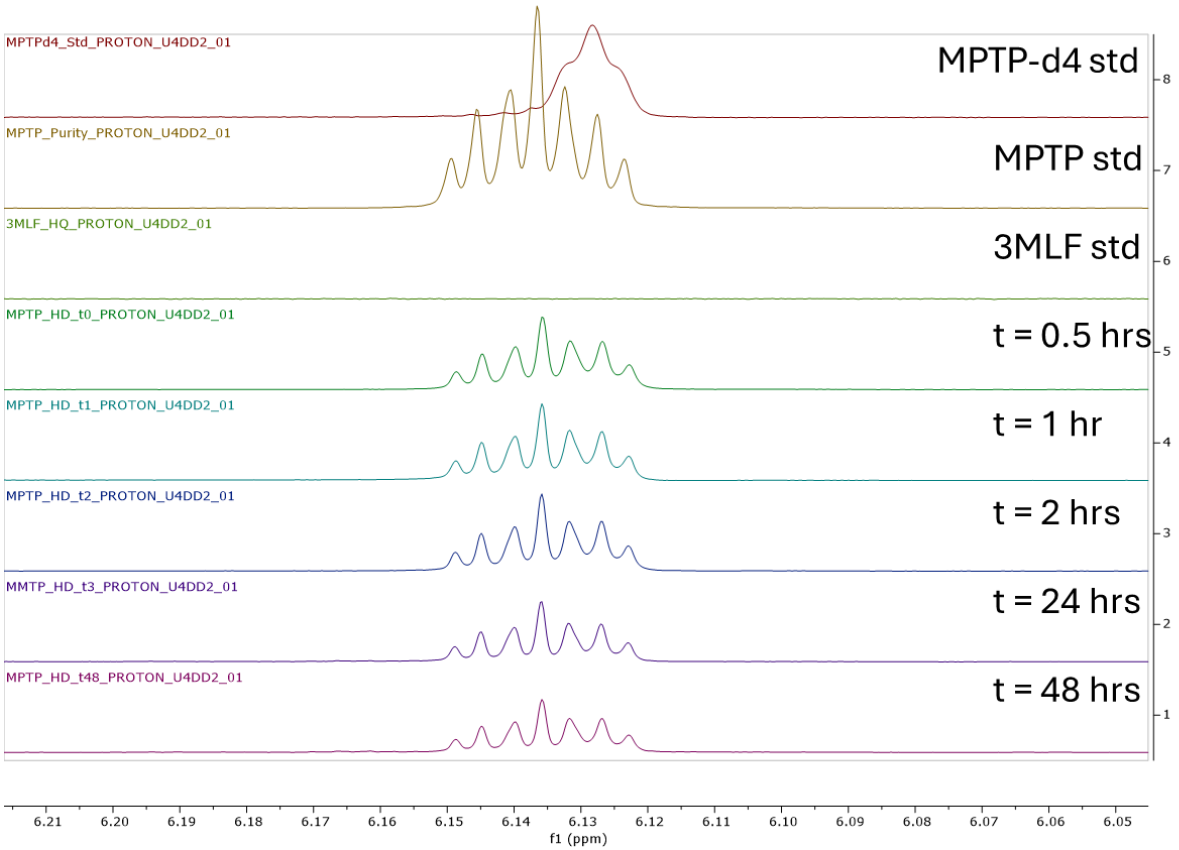

Figure 3.9: Spectra demonstrating the overlap of MPTP and MPTP-d4 ^{1}H NMR signals in the 1:1:1 reaction of MPTP, MPTP-d4, and 3MLF: MPTP-d4 (8), MPTP (7), and 3MLF (6) standards are stacked on time-resolved reaction signals (5-1). While there is significant overlap, a deconvolution process allows for the isolation of the signal contribution from both MPTP and MPTP-d4.

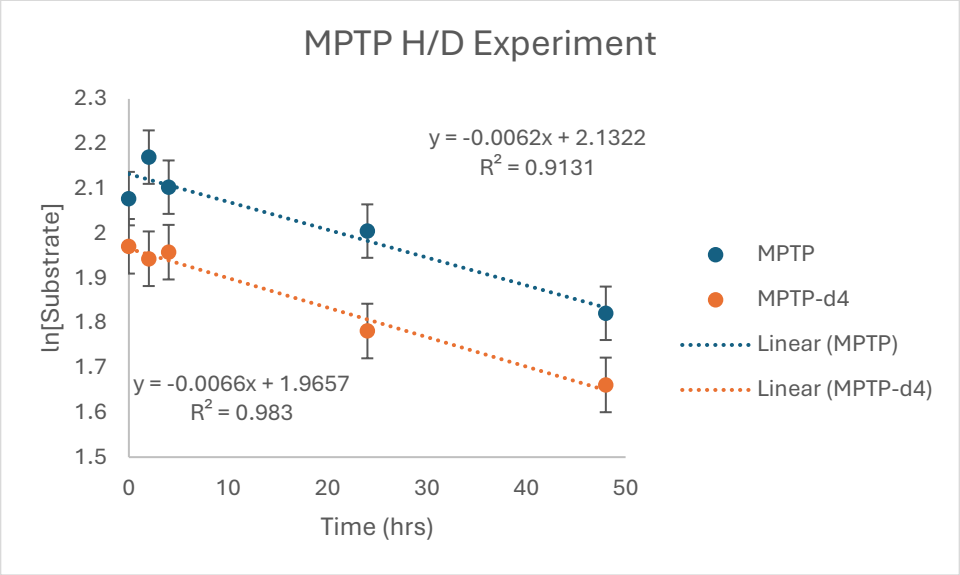

Figure 3.10: The plot of ln[substrate] vs time for the oxidation of MPTP and MPTP-d4 with 3MLF reveals that there is no KIE for these reactions (k_H/k_D = 0.940).

From these reactions, there is no observable KIE for the oxidation of MMTP or MPTP by 3MLF. Practically, this suggests that the proton-coupled electron transfer hypothesized to allow this reaction to occur is not concerted. As such, we propose that the reaction mechanism is that shown in Figure 3.11. Similarly, this result rules out a previous hypothesis presented by Castagnoli et al. which suggested that the initial step of this reaction could be a hydrogen atom transfer from the substrate to the flavin. Since the proposed HAT directly involves the hydrogen atoms at the critical alpha site, it would be expected that the H/D isotope effect was ~7. Since this study suggested no isotope effect, that hypothesis is effectively ruled out for this system.

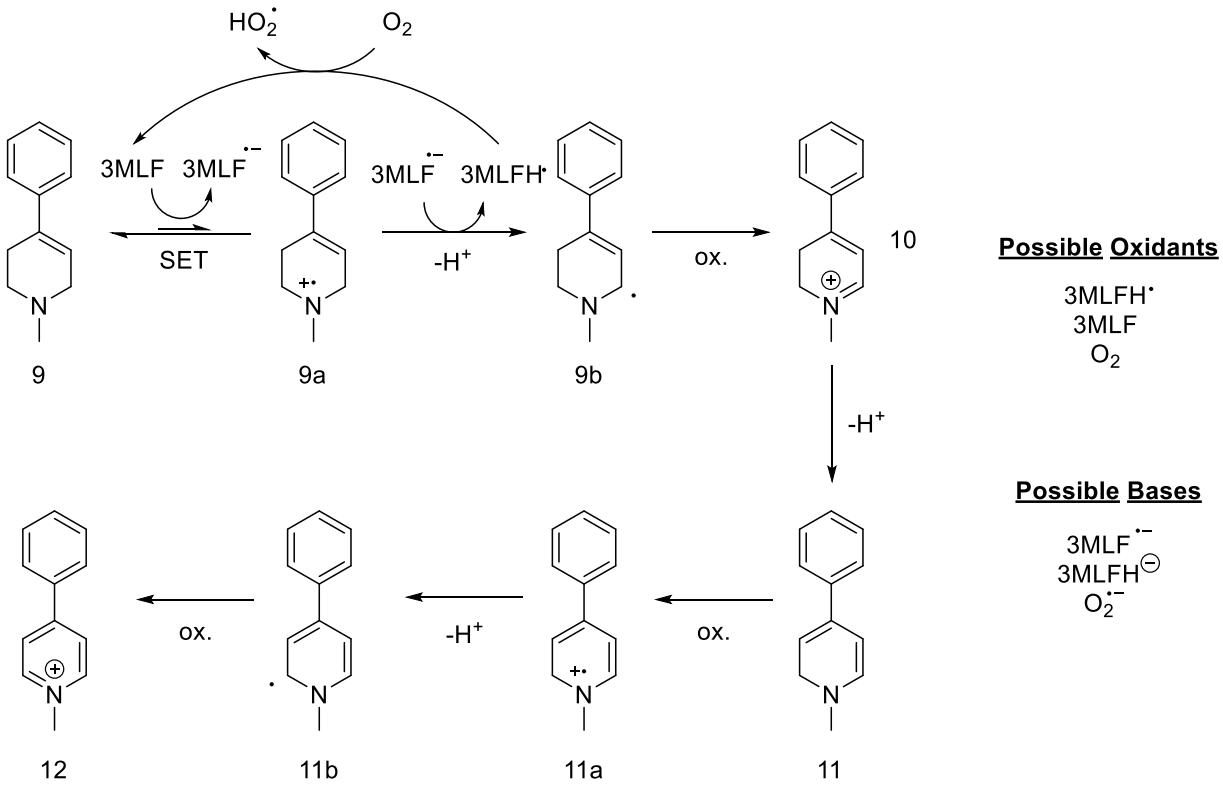

Figure 3.11: Proposed mechanism for the oxidation of MMTP and MPTP by 3MLF. The fate of 3MLF is not described here; only the stepwise nature of the oxidation of substrate (MPTP shown, but broadly applicable to structurally similar compounds).

3.6 Conclusions

Where our previous work using 3MLF paved the way for the SET mechanism, the above work drove it home. The employment of cyclopropyl tetrahydropyridine probes allowed for a much more nuanced look into the extent to which 3MLF is a faithful biomimetic for MAO B. Paralleling work done by Silverman and Castagnoli at the outset of investigation into this system, oxidation by an SET mechanism is the only reasonable explanation for the behavior described above. The presence of ring-opened intermediates and products in this work provide irrefutable evidence that the SET mechanism has a place in the modern conversation surrounding MAO B.

For β-unsaturated tertiary amines, the SET mechanism is undoubtedly the most realistic mechanistic picture with regards to their oxidation by MAO B. As has been characterized here and in our previous work, neutral flavin biomimetics are able to undergo one-electron reductions

followed by proton transfer to begin the oxidative process for these amines. Here, we demonstrated two critical points in support of this: 1) the initial, coupled steps occur stepwise and 2) this behavior is consistent for cyclopropyl-containing derivatives, leading to ring-opened intermediates and products. We believe that this is consistent with and in support of work done primarily by Castagnoli et al. with respect to the enzyme.

Of course, while this work is consistent with expectations for reactivity, these cyclopropyl tetrahydropyridine probes also reveal a potential shortcoming of this approach. The necessitation of a second substrate equivalent for the critical HAT reaction suggests that the latter part of the proposed oxidative process does not necessarily mimic biological conditions. We believe the fate of the cyclopropyl carbinyl radical is different under the experimental conditions described above than under biological conditions due to the availability and proximity of secondary substrate molecules.

Work done by Castagnoli et al. suggests that in the absence of a second substrate equivalent, the cyclopropyl carbinyl radical would instead covalently bind to the flavin active site of the enzyme, leading to inactivation. Here, that same radical was able to undergo intermolecular HAT in order to produce a stable ring-opened intermediate which was then hydrolyzed. However, the discoveries made with respect to the overall reactivities, particularly in the early stages of the proposed mechanism, mimic the expected biological behavior of the substrate.

Having fully characterized this reaction in terms of substrate behavior, we anticipate focusing our attention on two distinct pathways. First is the repetition of these experiments using purified mammalian MAO B. Our expectation is that using the enzyme will fully clarify the extent to which these results were predictive of biological behavior, and, by extension, the extent to which 3MLF is a faithful biomimetic for MAO B. The second is a more classic physical organic approach

to flavin chemistry in general. By tuning the electronic properties of the flavin, we hope to alter the favorability of the initial SET, allowing for better control over the reaction mechanism. For reaction containing a cyclopropyl tetrahydropyridine derivative, if the SET is made more favorable, then the expectation is that the RDS would become the competition step. As such, there would be more of an emphasis placed on the rate of ring opening vs. oxidation, allowing us to better probe the behavior of the radical cation.

3.7 References

1) N. Castagnoli, Jr., K. Chiba, A. J. Trevor, *Life Sci.* **1985**, *36*, 225 – 230.

2) K. Chiba, A. Trevor, N. Castagnoli, Jr., *Biochem. Bioph. Res. Co.* **1984**, *120*, 574 - 578.

3) P. F. Fitzpatrick, *Arch. Biochem. Biophys.* **2010**, *493*, 13 - 25.

4) R. R. Ramsay, A. Albreht, *J. Neural Transm.* **2018**, *125*, 1659 - 1683

5) N. S. Scrutton, *Nat. Prod. Rep.* **2004**, *21*, 722 - 730.

6) J. R. Miller, D. E. Edmondson, *Biochemistry* **1999**, *38*, 13670 - 13683.

7) R. Orru, M. Aldeco, D. E. Edmondson, *J. Neural Transm.* **2013**, *120*, 847 – 851.

8) R. Vianello, M. Repič, J. Mavri, *Eur. J. Org. Chem.* **2012**, 7057 - 7065.

9) R. B. Silverman, *Acc. Chem. Res.* **1995**, *28*, 335 – 342.

10) R. B. Silverman, S. J. Hoffman, I. Catus, W. B., *J. Am. Chem. Soc.* **1980**, *102*, 7126 – 7128.

11) J. T. Simpson, A. Krantz, F. D. Lewis, B. Kokel, *J. Am. Chem. Soc.* **1982**, *104*, 7155 - 7161.

12) N. Price, A. Nakamura, N. Castagnoli Jr., J. M. Tanko, *ChemBioChem*, **2024**, *25*, 1-7.

13) A. Nakamura, M. A. Latif, P. A. Deck, N. Castagnoli Jr., J. M. Tanko, *Chem. Eur. J.*, **2020**, *26*, 823-829.

14) C. Franot, S. Mabic, N. Castagnoli Jr., *Bioorg. Med. Chem.* **1998**, *6*, 283-291.

15) J. M. Tanko, Virginia Tech, Blacksburg, VA. Unpublished work, 2024.

16) J. S. González, J. M. Tanko, *Chem. Thermodyn. Therm. Anal.* **2023**, *12*, 100119.

Chapter 4. Exploration of Alternative Flavins for Biomimetic Studies

4.1 Abstract

Further investigations into the reactivity of 3-methyllumiflavin (3MLF) sparked curiosity surrounding alternative flavins that may be of use for biomimetic studies. A commercially available flavin, 10-ethyl-3-methyllumiflavin (ETD), has a strikingly similar structure to 3MLF, leading to the hypothesis that the two may share reactivities. Further, there was interest in the creation of a more potently oxidizing flavin, so the reactivity of 5,10-diethyl-3-methyllumiflavinium perchlorate (5-Et-ETD$^+$) was also probed. The behavior of ETD matched that of 3MLF in terms of both NMR and EPR as a function of time, leading to the conclusion that they share reactivity with respect to the oxidation of β-unsaturated tertiary amines. 5-Et-ETD$^+$ showed unique reactivity in that the expected silent NMR effect did not take hold under anaerobic conditions; rather, the partially reduced forms of 5-Et-ETD$^+$ were diamagnetic in nature, allowing them to be tracked as a function of time using ^{1}H NMR. Both of the biomimetic systems studied herein pose their own unique advantages for the study of tertiary amine oxidation, and lead to the conclusion that further flavins may be of interest when approaching this chemistry.

4.2 Introduction

MAO B is responsible for the catalytic oxidation of biogenic amines such as the neurotransmitters dopamine and serotonin.[1] Additionally, much work has been done surrounding the interaction of MAO B with β-unsaturated tertiary amines such as MPTP.[2-3] Previously, we have shown that 3-methyllumifvain (3MLF) and 5-ethyl-3-methyllumiflavinium perchlorate (5-Et-3MLF$^+$) are suitable biomimetics for MAO B with respect to MPTP-like substrates.[4-5]

The application of flavins as biomimetics for MAO B has been discussed at length in the literature.[6-9] Yet to be considered, though, is a related system of flavins for more complete

characterization of substrate reactivity. The goal of the present work is to provide practical chemical insight into four related MAO B biomimetic flavins. Taking inspiration from the work done on the related 3MLF and 5-Et-3MLF$^+$, two new flavin biomimetics, 10-ethyl-3-methyllumiflavin (ETD) and 5,10-diethyl-3-methyllumiflavinium perchlorate (5-Et-ETD$^+$) are discussed below.

The work performed with 3MLF sparked curiosity surrounding alternative flavins that may be of use for biomimetic studies.[4] A commercially available flavin, 10-ethyl-3-methyllumiflavin (ETD), has a strikingly similar structure to 3MLF (Figure 4.1), leading to the hypothesis that the two may share reactivities. The obvious advantage to this comes in the form of accessibility. While ETD is commercially available, 3MLF requires a lengthy, somewhat temperamental, synthesis. To determine whether ETD is a suitable candidate for the continuation of biomimetic studies, it was subjected to the same examination as 3MLF.

As a continuation of the study of a variety of flavins, the question of flavinium reactivity piqued our interest. Work done by Nakamura et al. suggests that 5-Et-3MLF$^+$ is a more reactive form of 3MLF.[5] As such, the activated analog of ETD, 5,10-diethyl-3-methyllumiflavinium perchlorate (5-Et-ETD$^+$), is expected to exhibit a much more favorable reactivity toward MPTP-like substrates compared to ETD. Specifically, the large partial positive charge local to the N5 position of 5-Et-ETD$^+$ effectively lowers the energy barrier for the requisite initial SET. As such, its reactivity is expected to be substantially different from that of 3MLF and ETD. To test this hypothesis as well as uncover the most reasonable mechanism for its reaction with MMTP, several studies were conducted wherein the stoichiometries, radical behavior, and the fate of 5-Et-ETD$^+$ itself were probed in depth.

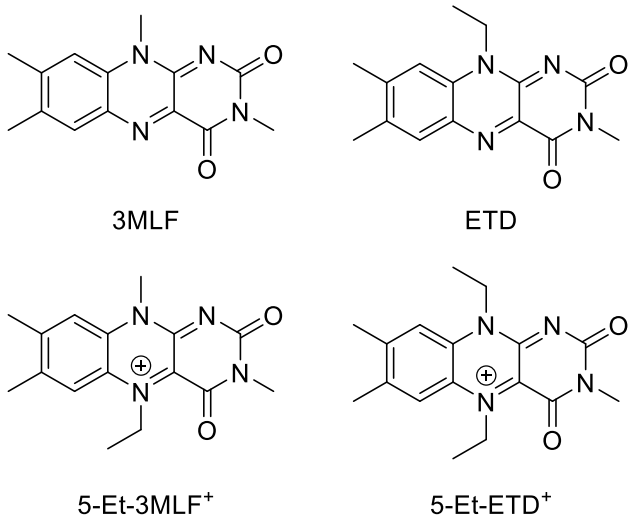

Figure 4.1: The structures of 3MLF, ETD, 5-Et-3MLF$^+$, and 5-Et-ETD$^+$ are shown here. Given the structural similarities between the 3MLF and ETD, their reactivities are expected to mirror each other. The same is true for 5-Et-ETD$^+$ and 5-Et-3MLF$^+$.

4.3 10-Ethyl-3-methyllumiflavin (ETD)

Both aerobic and anaerobic studies were performed using ETD. Anaerobic reactions were prepared in NMR tubes and immediately freeze-pump-thaw degassed. The NMR tubes were subsequently flame sealed to ensure that no ambient air was able to enter the vessel post preparation. The time required to mix the solutions before degassing did not lead to excess reaction. Aerobic studies were also conducted in NMR tubes. While not being actively analyzed by NMR, these samples were continually mixed using a stirring table. In both cases, reactions were kept out of ambient light to avoid any unwanted photochemical reactions.

The question of catalysis was the first to be addressed for ETD. Since 3MLF proved to be robust and capable of multiple turnovers during its aerobic reaction with MMTP, ETD would be held to the same standard. An 8:1 (MMTP:ETD) reaction mixture was prepared with a benzene internal standard (7.0 mM) and allowed to react for 24 hours, Scheme 4.1. Integrating with respect to the internal standard revealed that the apparent concentration of the flavin did not change over

that period while the MMTP experienced one complete turnover to produce an equivalent (0.26 mM) of MMP^+, Figure 4.2. This result suggests that ETD is a suitable catalyst for the oxidation of MMTP and other similar compounds given that it does not readily degrade.

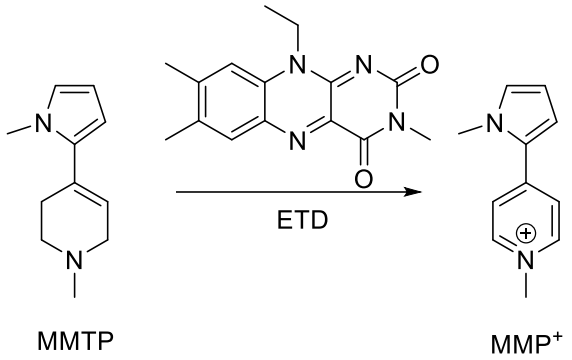

Scheme 4.1: The reaction of MMTP and ETD is expected to produce the oxidized form of the substrate, MMP^+.

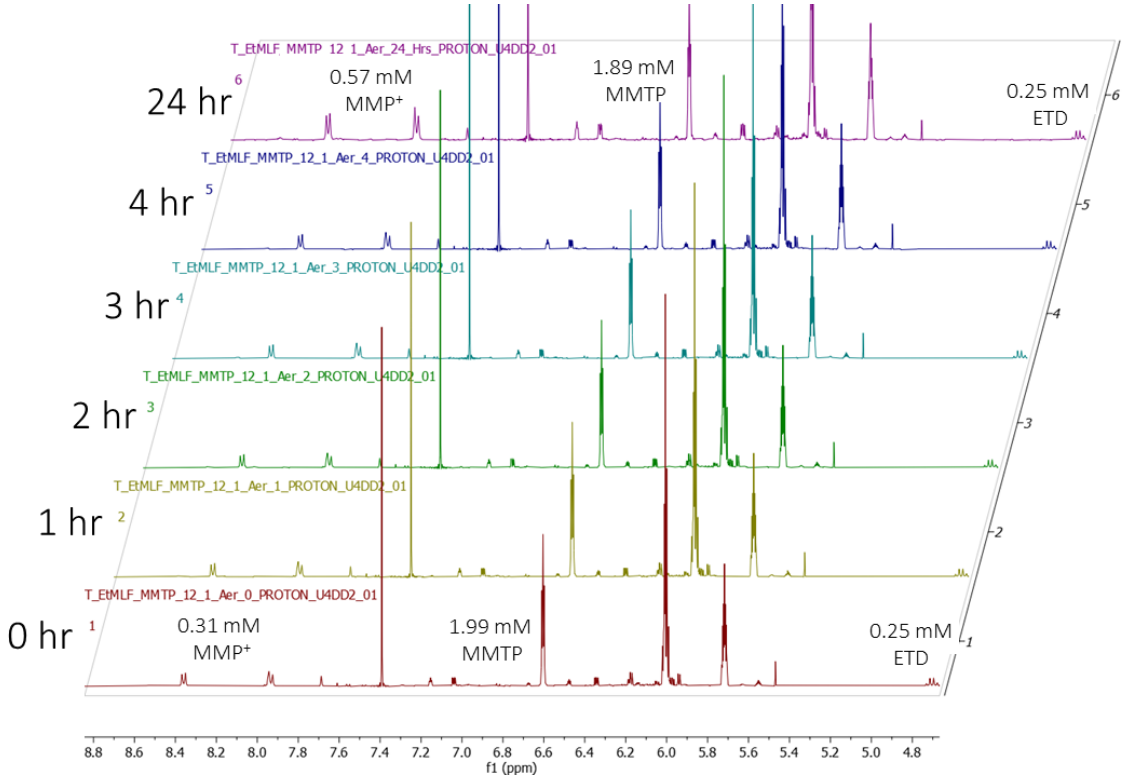

Figure 4.2: The time resolved ^1H NMR spectra for the 8:1 (MMTP:ETD) aerobic reaction of MMTP and ETD with a benzene internal standard are shown. Over the course of 24 hours, the MMTP oxidation is able to begin taking place, converting from MMTP to MMP^+, as expected. During the same period, the concentration of ETD is constant, indicating catalytic behavior.

Complementary anaerobic studies were conducted to determine whether the radical behavior of ETD matched that of 3MLF. The expectation for these reactions was that if the behavior mimicked that of 3MLF, then the line broadening associated with silent NMR would be visible during the early portion of the reaction, and the signals attributable to ETD would eventually broaden into the baseline of the spectrum. While this was tested at several relative concentrations of MMTP:ETD (1:1, 1:2, 2:1, and 1:4), the 1:4 reaction is shown in Figure 4.3. This particular set of spectra was chosen for this demonstration simply because the excess ETD best emphasizes the line-broadening behavior. The phenomenon was present in all anaerobic samples.

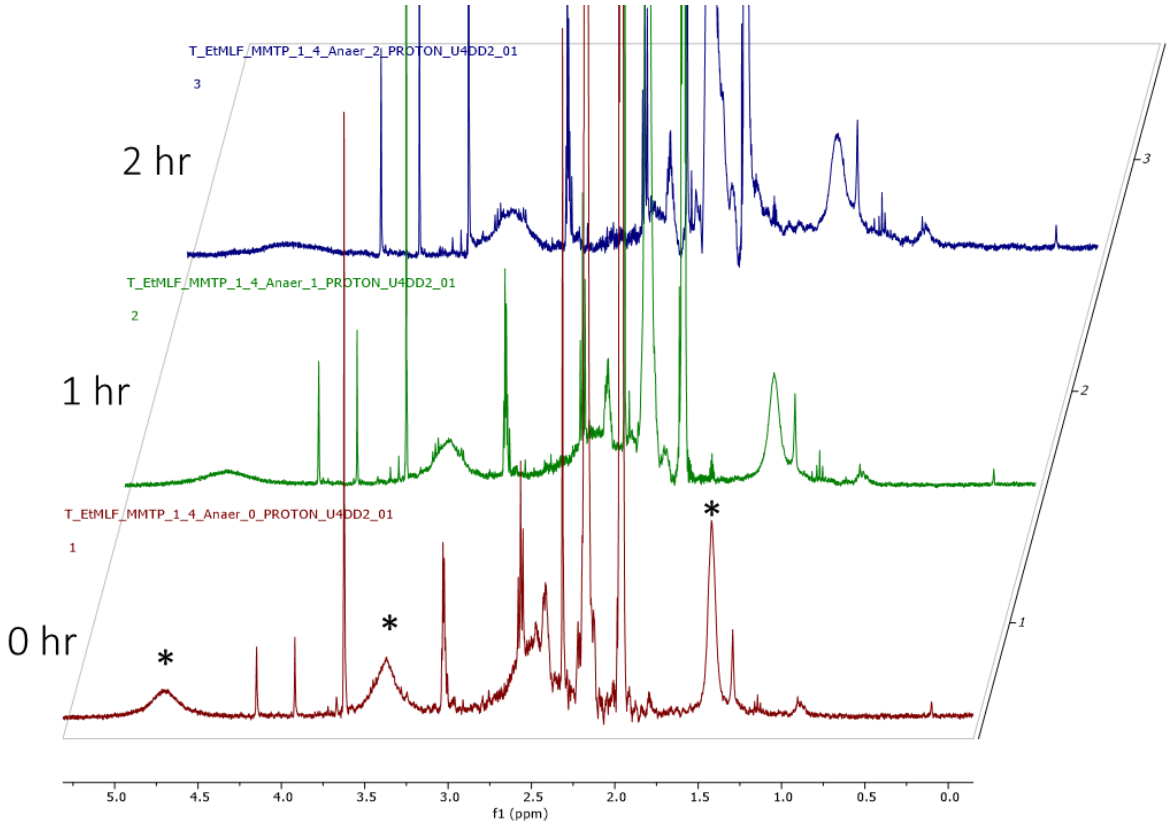

Figure 4.3: Time-resolved ^{1}H NMR spectra for the 1:4 (MMTP:ETD) anaerobic reaction of ETD and MMTP are shown here. Signals denoted with "*" belong to ETD. As a function of time, these signals broaden significantly, indicating paramagnetic behavior from the flavin. Notably, the signal at 1.49 ppm, attributable to the terminal methyl group at the N10 position of ETD is the slowest to broaden.

As was the case with 3MLF, the aromatic signals attributed to ETD disappeared from the spectrum at t=0. More interesting, however, is that the expected behavior in terms of the aliphatic signals were even more exaggerated in ETD spectra than in 3MLF. That is to say that the presence of an ethyl group at the N10 position (ETD) instead of a methyl group (3MLF) was even slower to broaden and disappear from the ^{1}H NMR spectrum. As such, the terminal methyl of the N10 ethyl group was the last to disappear from the spectrum. Again, this is likely due to the localization of radical spin density to the ring system of the flavin, meaning that the "pendant" ethyl group experiences less of the paramagnetism associated with the unpaired electron, see Figure 2.11.

Since it has the least paramagnetic character in the molecule, its ^{1}H NMR signal is the most robust in the system.

To confirm that this result was indicative of radical behavior, an EPR study was conducted as a function of time. As was the case with 3MLF, the EPR results suggested that a flavin radical (Figure 4.4) grew in as a function of time. This growth mirrored the inverse behavior with respect to the silent NMR phenomenon. That is to say, as the signals attributable to ETD disappeared from the ^{1}H NMR, the strength of the EPR signal increased. We then conclude by suggesting that this radical has the same characteristics as 3MLF. As such, we reason that since the two flavins share the same characteristics at all points in time and under all tested conditions, that the two reasonably share a mechanism for the oxidation of MMTP, Scheme 4.2.

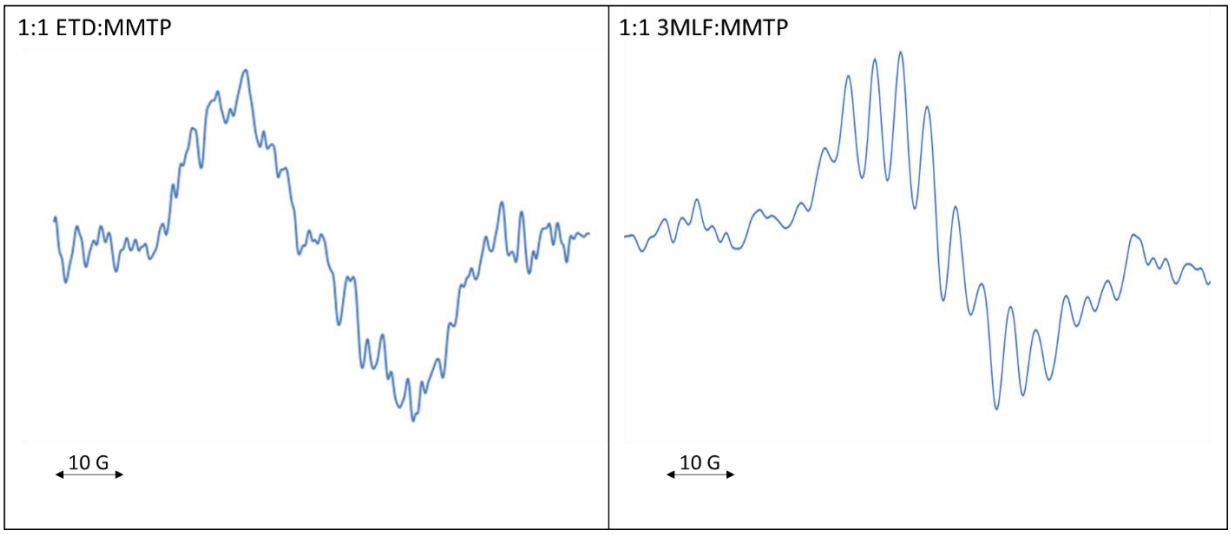

Figure 4.4: The EPR spectra for the anaerobic 1:1 reactions of ETD and MMTP (left) and the 1:1 reaction of 3MLF and MMTP (right) after 4 hours of reaction are shown.

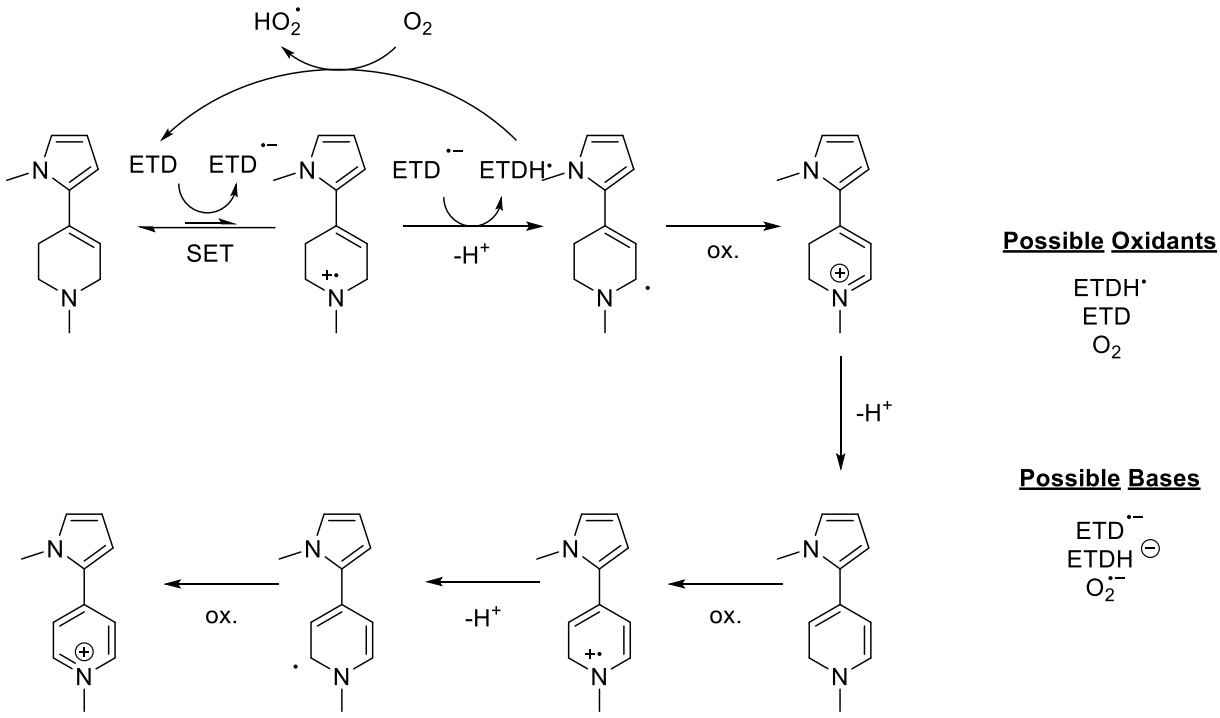

Scheme 4.2: The hypothesized reaction mechanism for the oxidation of MMTP by ETD. The initial step is hypothesized to be an unfavorable SET. This is coupled to, but not concerted with, an extremely favorable proton transfer to produce the partially reduced neutral flavin radical as well as a delocalized substrate radical. Under aerobic conditions, it is hypothesized that O_2 is able to instigate a reoxidation of the partially reduced ETD before complete reduction to reform starting material and produce an oxygen-centered radical to complete the catalytic cycle for ETD. The neutral substrate radical intermediate undergoes several subsequent oxidations and proton transfer steps. Potential oxidants for these reaction have been left purposely vague as several species (O_2, ETD, ETDH·) have the oxidative power to accomplish these transformations. Similarly, several bases in solution have the capacity to cause the listed deprotonation steps.

While the stated goal of this work was to determine whether or not ETD was a suitable flavin for the biomimetic study of MAO B, which it is, it became clear during the pursuit of an answer that its purpose was two-fold. The second is a confirmation of the results that were obtained during our initial probe into this system using 3MLF. Having approached this system with multiple flavins and substrates and obtained consistent mechanistic conclusions underlines a key feature of this chemistry: it is not unique to the selected system. We hypothesize that the underlying reactivities of flavins with β-unsaturated tertiary amines are consistent regardless of the identities

of the flavin and the amine. As such, further variation in the selected compounds would serve primarily to reinforce the hypotheses laid out herein.

4.4 5,10-Diethyl-3-methyllumiflavinium perchlorate (5-Et-ETD$^+$)

The reaction of 5-Et-ETD$^+$ and MMTP was carried out both aerobically and anaerobically. For both sets of experiments, reactions were prepared from stock solutions and carried out in NMR tubes. The stock solutions were prepared in a completely anhydrous environment (See C.2 for stock preparation) as it was found that even slight amounts of water in solution led to a hydroxyl addition to the flavinium, preventing substrate oxidation (See Figure C.1-2 for characterization of -OH adduct). Aerobic experiments were kept under constant stirring when not being actively analyzed. Anaerobic reactions were freeze-pump-thaw degassed, and their NMR tubes were subsequently flame sealed to ensure that no atmospheric O_2 interfered with the reaction. In both cases, the reactions were stored in the dark to ensure that no unwanted light-mediated reactions occurred.

Unlike previous reactions discussed here, both the aerobic and anaerobic reactions of 5-Et-ETD$^+$ and MMTP demonstrated similar reactivity. The expected silent-NMR behavior typically associated with flavins was not observed for 5-Et-ETD$^+$. As shown in Figure 4.5, the 5-Et-ETD$^+$ starting material has entirely disappeared from the ^{1}H NMR spectrum early in the reaction. This is correlated with a change in reaction color from dark purple to transparent green. Critically, this NMR behavior is not the same as was noted with 3MLF and ETD. Instead, the disappearance of 5-Et-ETD$^+$ corresponds to the formation of similar peaks which are attributable to a partially reduced form of the flavin, Fl$^-$. The partially reduced flavin is then extant in solution for several hours, after which those signals also disappear, giving way to the formation of a final, fully reduced

flavin, FlH. The complete reduction of this flavin is thus able to be tracked as a function of time using NMR spectroscopy both aerobically and anaerobically.

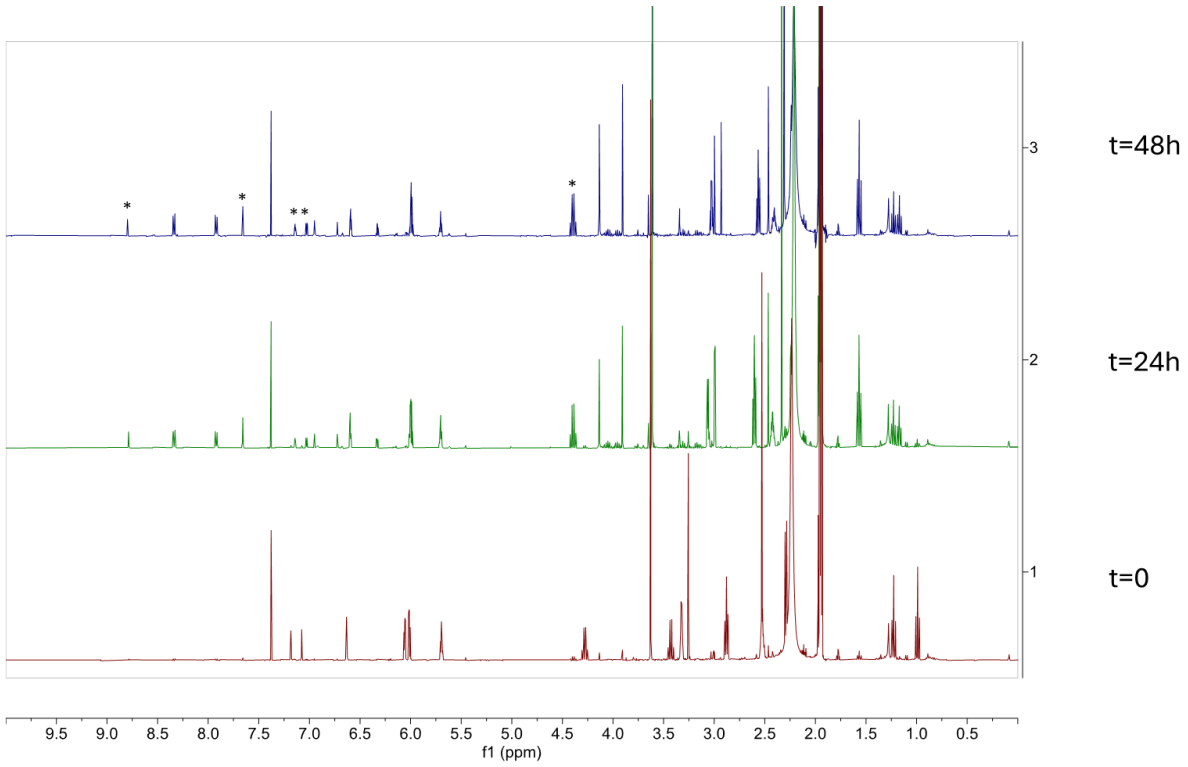

Figure 4.5: The time-resolved ^{1}H NMR spectra for the 1:3 (5-Et-ETD^{+}:MMTP) aerobic reaction of 5-Et-ETD^{+} and MMTP are shown. Signals denoted with "*" in the top spectrum (t = 48hrs) belong to a partially reduced flavin. This behavior is unique to the 5-Et-ETD^{+} system. It is a more robust flavin in that it does not simply degrade during the oxidative process. Rather, the formation of reduced flavins is able to be observed by ^{1}H NMR.

The NMR spectra of the aerobic and anaerobic reactions suggest that the MMTP behaves similarly in both cases as well, with the key difference being the speed at which the oxidation occurs. Curiously, the mechanism of MMTP oxidation seems to differ from the results observed in the ETD/3MLF reactions. Upon mixing, the immediate color change which suggests the reduction of flavinium coincides with the formation of MMTPH^{+} (Figure 4.6). As the reaction progresses, the peaks attributable to MMTPH^{+} seem to reconverge to MMTP (Figure 4.7). This

indicates that as a function of time the $MMTPH^+$ is being consumed. The mechanistic consequence of this behavior is a hypothesized proton transfer from $MMTPH^+$ to Fl^- resulting in the simultaneous formation of MMTP and FlH (Figure 4.9). Aerobic reactions tend to proceed slightly faster than their anaerobic counterparts, likely due to the presence of atmospheric O_2 which can behave as an additional substrate/intermediate oxidant. In both cases, the oxidation of MMTP results in the direct formation of MMP^+ with the hypothesized dihydropyridinium species seemingly transient in solution.

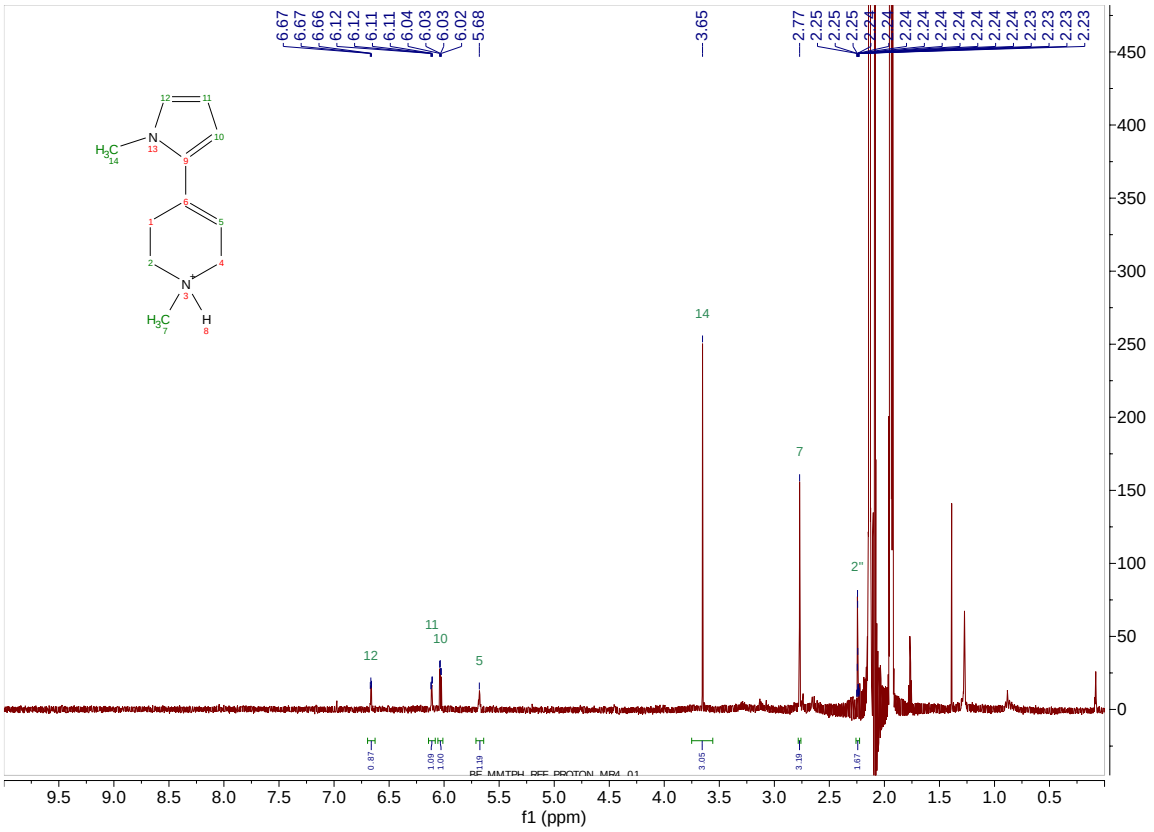

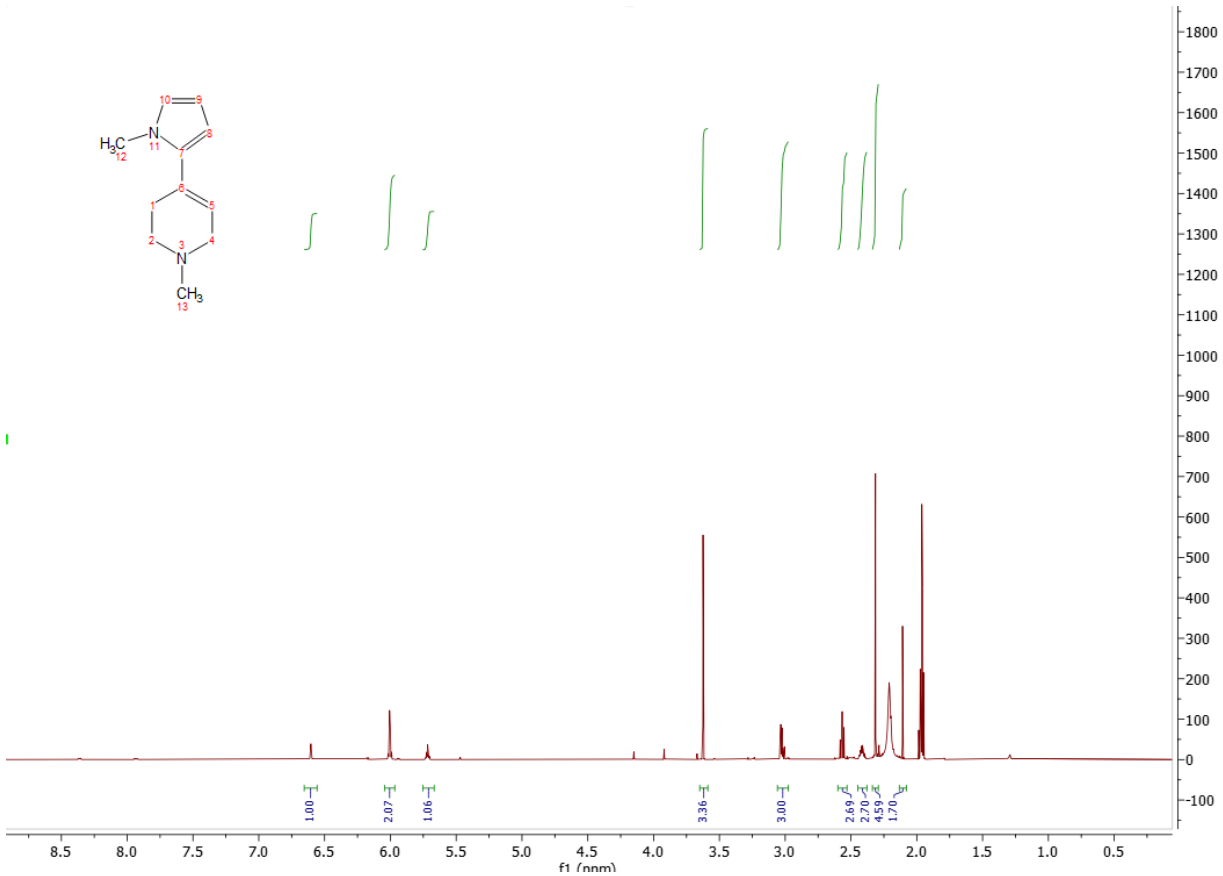

Figure 4.6: The reference ^{1}H NMR spectra for MMTPH^{+}•Cl^{-} (top) and MMTP (bottom) are shown here. These spectra differ primarily in the signal(s) around 6.00-6.15 ppm. While the spectrum shown here for MMTPH^{+}•Cl^{-} has two well-resolved peaks (each 1H eq.), the same signal for MMTP presents as a multiplet (2 H eq.).

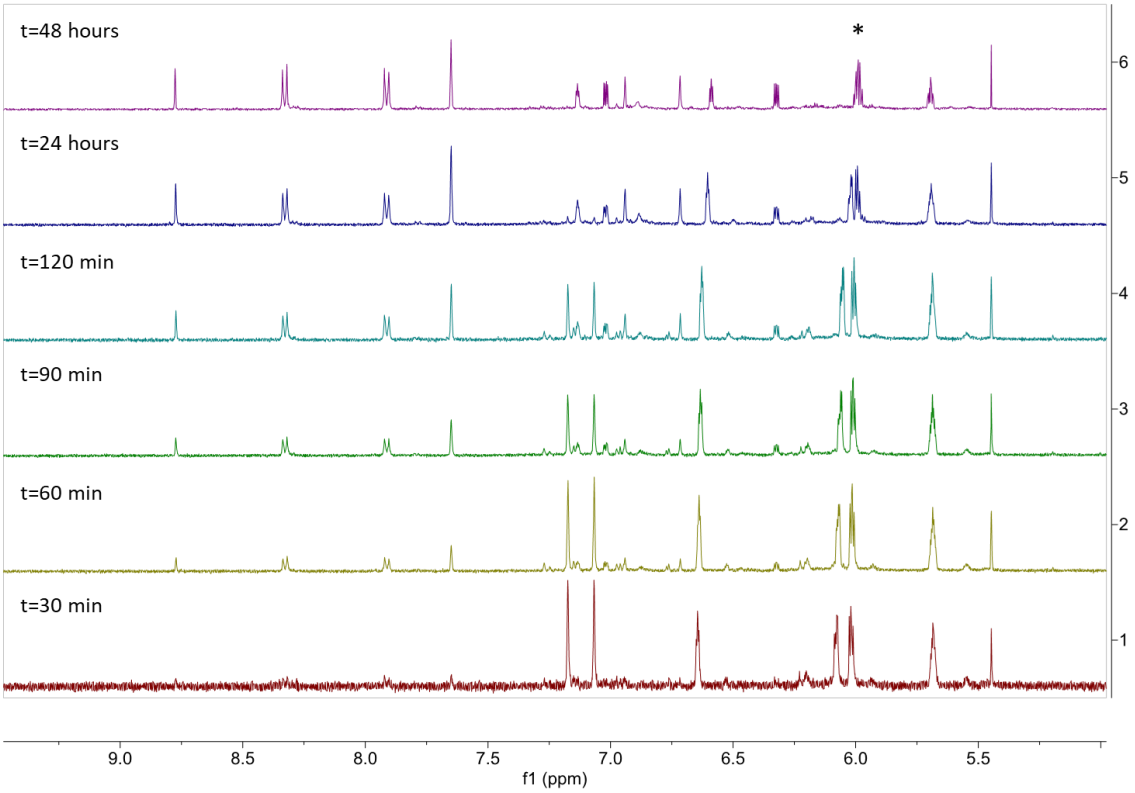

Figure 4.7: Time-resolved ^{1}H NMR spectra for the 1:2 (5-Et-ETD^{+}:MMTP) reaction of 5-Et-ETD^{+} and MMTP are shown. The signal associated with MMTP, denoted at t = 48 hours with an asterisk arises after a "reconvergence" from the MMTPH^{+} signals observed at t = 30 mins.

The tendency for the aerobic and anaerobic reactions to behave the same way is most likely attributable to the nature of 5-Et-ETD^{+}, particularly in that it is a more powerful oxidant than both ETD and 3MLF. While the latter flavins demonstrate catalytic behavior in solution, FlH degrades as the reaction progresses. Nakamura et al. noted similar behavior when working with the methylated variant of 5-Et-ETD^{+}, 10-ethyl-3-methyllumiflavinium perchlorate (10-Et-3MLF^{+}ClO$_4^{-}$). The degradation product, 1,3-diethyl-5,6-dimethyl-1*H*-benzo[*d*]imidazole-3-ium, forms gradually in solution as evidenced by LC-MS (Figure 4.8). Since 5-Et-ETD^{+} is not catalytic, the presence of O_2 does not affect a catalytic cycle with the flavin, hence the aerobic and anaerobic reactions proceed the same way.

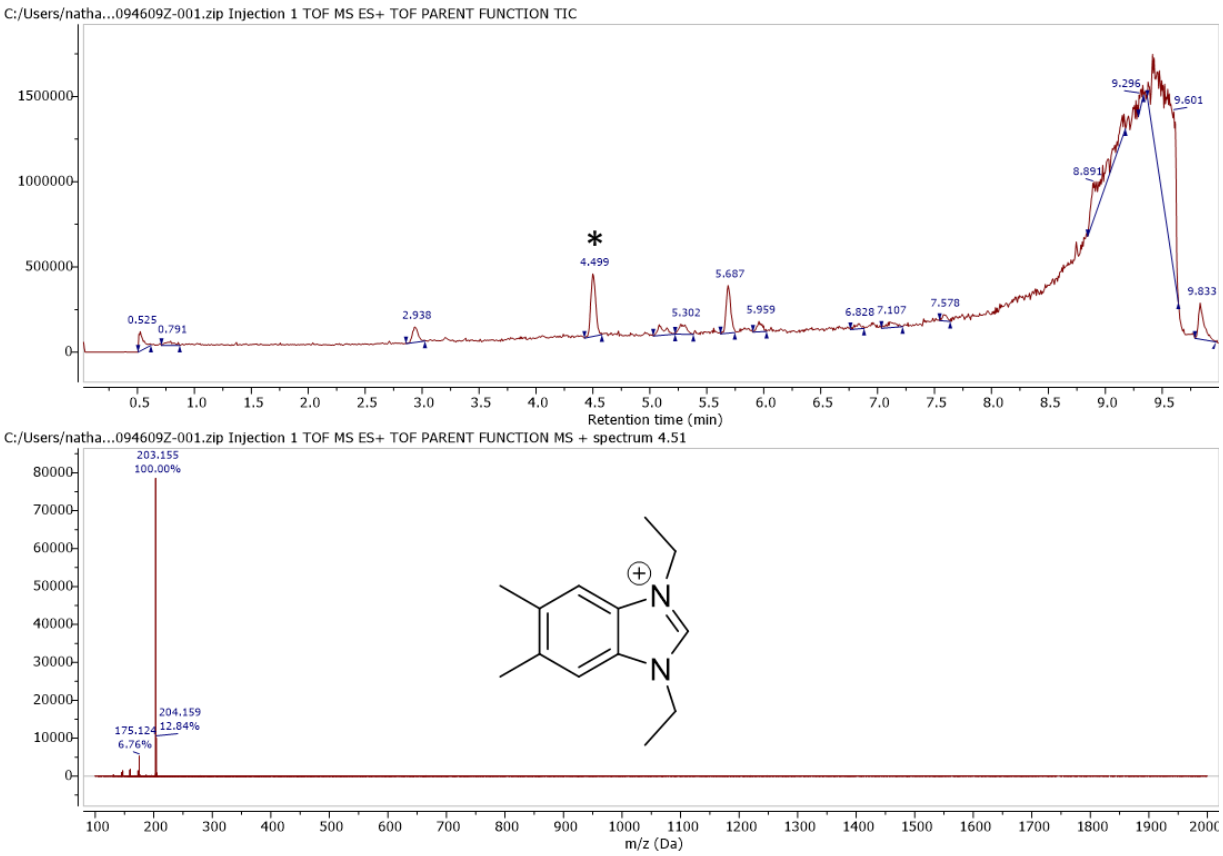

Figure 4.8: The liquid chromatogram (top) associated with the 1:2 (5-Et-ETD$^+$:MMTP) reaction of 5-Et-ETD$^+$ and MMTP is shown. The signal denoted by "*" has its mass spectrum shown (bottom). The base peak in the mass spectrum has a mass of 203.155 m/z, an exact match for the hypothesized benzimidazolium intermediate resultant from the degradation of 5-Et-ETD$^+$.

Based on the experimental results outlined above, we propose a (relatively) straightforward reaction mechanism for the oxidation of MMTP by 5-Et-ETD$^+$, shown in Figure 4.9. The initial SET is a relatively fast reaction, happening immediately upon mixing. The resultant aminyl radical cation (MMTP•$^+$) then undergoes a proton transfer with an equivalent of MMTP, likely the most basic species in solution, to form MMTPH$^+$ and MMTP•. The neutral MMTP radical is then hypothesized to be oxidized by either 5-Et-ETD$^+$ or Fl• (O_2 is also capable of completing this oxidation but has been excluded for simplicity). The resultant DHP$^+$ intermediate is believed to be transient; the final steps of the oxidation are believed to be fast, resulting in the formation of

MMP^+. In a side reaction, $MMTPH^+$ undergoes a proton transfer with partially reduced flavin to produce MMTP and FlH. The fully reduced flavin is eventually degraded into its corresponding benzimidazolium in a process likely similar to that speculated by Nakamura et al.

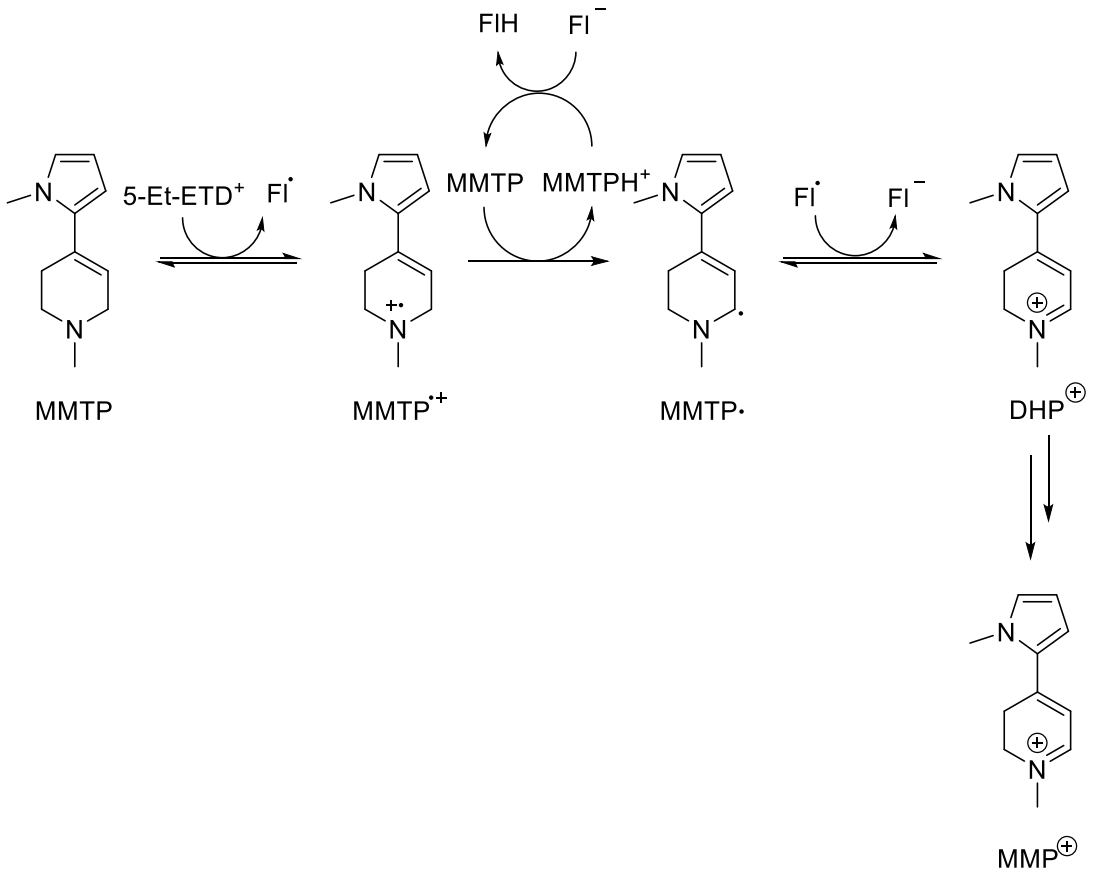

Figure 4.9: The hypothesized reaction mechanism for the oxidation of MMTP by 5-Et-ETD^+ is shown. Beginning with a promoted SET from MMTP to 5-Et-ETD^+ to form the expected aminyl radical cation alongside a partially reduced, neutral flavin radical. From there, it is hypothesized that a second equivalent of substrate starting material behaves as a base to cause deprotonation of the aminyl radical cation. It is then hypothesized that the neutral flavin radical promotes a second SET to form the DHP^+ intermediate from the neutral substrate radical. Additionally, a diamagnetic flavin anion is formed in this step. This flavin anion is expected to behave as a base, reacting with the protonated starting material, $MMTPH^+$, to form MMTP and the fully reduced flavin.

4.5 Future Work

The nature of 5-Et-ETD$^+$ predisposes it to a more favorable SET when reacting with MMTP compared to the neutral flavins 3MLF and ETD. We hypothesize that the favorability of that elementary step is enough to alter the fundamental reactivity. Specifically, the SET no longer serves as the rate-determining step. Instead, the intermolecular proton transfer following the SET would serve as the RDS in this reaction. Practically, this has useful applications in the realm of mechanism discovery. Changing the RDS allows for a more meaningful probe into the nature of the proton transfer and, by extension, the oxidation of MMTP. Taking advantage of this characteristic of flavinium-mediated oxidations, we hypothesized that the rate of proton transfer may be sufficiently slow to incur a competition reaction between oxidation and ring-opening when dealing with cyclopropyl-substituted MMTP (Figure 4.10).

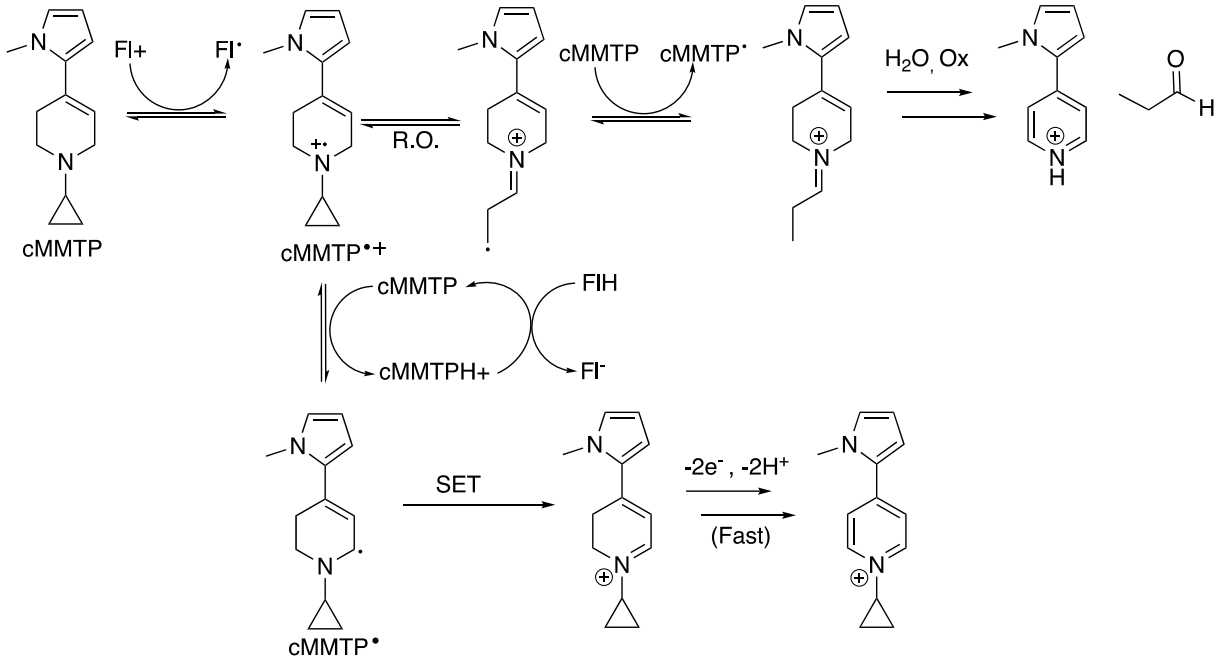

Figure 4.10: The hypothesized mechanism for the reaction of cyclopropyl MMTP and 5-Et-ETD$^+$ is shown here. The initial SET step produces an aminyl radical cation as well as a neutral flavin radical. The bottom pathway describes the proton transfer between the aminyl radical cation and a second equivalent of substrate. From there, the oxidation is expected to proceed as described previously. The top pathway describes a potential ring-opening step. After ring opening, an intermolecular HAT is shown as a potential pathway by which an iminium intermediate is produced. It is hypothesized that the iminium can then undergo subsequent hydrolysis as was described for the previously studied 3MLF system.

Classically, cyclopropyl ring openings have been used as radical probes because they happen at a consistent, relatively high, rate. A competition reaction, then, allows for the direct determination of the rate of the reaction competing with ring-opening by simple measurement of the relative concentrations of the two resultant products. However, when this was attempted with 3MLF, an intermolecular proton transfer appeared to interfere with the competition reaction (Chapter 3.4). In that case, the RDS was determined to be the initial SET, meaning the coupled proton transfer was sufficiently fast to avoid the desired competition. By changing the RDS with the use of 5-Et-ETD$^+$, we hypothesize that the competition may reemerge as a viable path of exploration.

4.6 Conclusions

Here, we have discussed two new biomimetics for the study of MAO B reactions. Both ETD and its activated counterpart, 5-Et-ETD$^+$, demonstrate robust reactivity with β-unsaturated tetrahydropyridines. Similarly, their reactivities mirror those of similar, previously studied systems, 3MLF and 5-Et-3MLF$^+$. The contributions discussed herein serve to reinforce the conclusions drawn previously with the similar 3MLF/5-Et-3MLF$^+$ systems. That said, there is much work to be done within the realm of biomimetic chemistry.

Specifically, there are two major directions which this work can lead. The first is further repetition of work previously done by the authors: reactions with cyclopropyl-containing derivatives of β-unsaturated tertiary amines. Further probing into this work using these novel compounds would allow for a more meaningful delineation of the reaction mechanisms speculated for the oxidations of those compounds. As has been previously noted, the employment of activated flavins for the oxidation of cyclopropyl-containing derivatives could provide further insight into the competition between ring-opening and oxidation, allowing for a more complete picture of how exactly these reactions proceed.

Second, further expansion of the flavin catalog could provide further insight into the mechanism of oxidation. Small perturbations of the chemical composition of flavins could tweak their reactivities with respect to substrate oxidation, allowing for the optimization of the oxidative process *in vitro*. While the flavin variants discussed here are focused primarily on the N5 and N10 positions of the flavin, the N1 and N3 positions are also able to be altered. Further, the aromatic methyl groups are rife with potential for substitution.

4.7 References

1) D. E. Edmondson, C. Binda in *Membrane protein complexes: Structure and function* (Eds.: J. R. Harris, E. J. Boekama), Springer, Singapore **2018**, pp. 117-139.

2) N. Castagnoli, Jr., K. Chiba, A. J. Trevor, *Life Sci.* **1985**, *36*, 225 – 230.

3) K. Chiba, A. Trevor, N. Castagnoli, Jr., *Biochem. Bioph. Res. Co.* **1984**, *120*, 574 - 578.

4) N. Price, A. Nakamura, N. Castagnoli Jr., J. M. Tanko, *ChemBioChem*, **2024**, *25*, 1-7.

5) A. Nakamura, M. A. Latif, P. A. Deck, N. Castagnoli Jr., J. M. Tanko, *Chem. Eur. J.*, **2020**, *26*, 823-829.

6) J. M. Kim, M. A. Bogdan, P. S. Mariano, *J. Am. Chem. Soc.* **1993**, *115*, 10591-10595.

7) S. E. Rigby, J. Basran, J. P. Combe, A. W. Mohsen, A. van Thiel, H. Toogood, M. J. Sutcliffe, D. Leys, A. W. Munro, N. S. Scrutton, *Biochem. Soc. Trans.* **2005**, *33*, 754-757.

8) J. M. Kim, M. A. Bogdan, P. S. Mariano *J. Am Chem. Soc.* **1991**, *113*, 9251-9257.

9) J. M. Kim, M. A. Bogdan, P. S. Mariano *J. Am Chem. Soc.* **1995**, *117*, 100-105.

Appendix A: Supporting Information for Reactions that shouldn't happen. Why does monoamine oxidase (MAO) catalyze the oxidation of some tetrahydropyridines?

Nathan J. Price, Akiko Nakamura, Neal Castagnoli, Jr., and James M. Tanko
Department of Chemistry
Virginia Tech
Blacksburg, VA 24060, USA

A.1 Experimental

NMR spectra were recorded using an Agilent U4-DD2 (400 MHz) or Bruker Avance II (500 MHz). Data analyses were performed using MestreNova. EPR spectra were recorded using a Bruker EMXplus EPR spectrometer with Bruker Xenon software.

All reactions were prepared using degassed CD_3CN stock solutions. Stocks were kept refrigerated unless being actively used. This was done primarily to maintain consistency in sample preparation. Aerobic reactions were prepared directly in NMR tubes with a total reaction volume of 0.6 mL. To ensure proper and consistent aeration of the sample, the tubes were placed on a mixing table when not being analyzed. Anaerobic reactions were also prepared directly in NMR tubes, but were immediately freeze-pump-thaw degassed (the process started <1 minute after mixing). After degassing, the NMR tubes were flame-sealed. Although control experiments did not suggest that light plays a role in this reaction, tubes were stored in the dark to minimize the risk of photochemical side reactions.

A.2 Synthesis of 1-methyl-4-(1-methyl-1H-pyrrol-2-yl)-1,2,3,6-tetrahydropyridine (MMTP)

MMTP was synthesized following a standard literature procedure,[1] and stored as an HCl salt to protect it from oxidation. The overall synthetic scheme is depicted below.

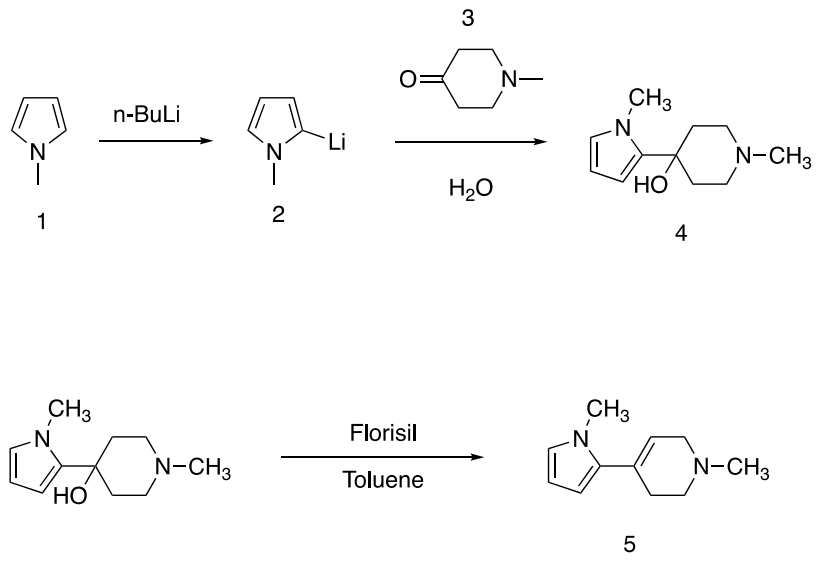

Scheme A.1: The synthetic pathway to form MMTP

A.2.1 Synthesis of 1-methyl-4-hydroxyl-4-(1-methylpyrrol-2-yl)-piperidine (MMPP) [1] (4)

Add a 1.6 M n-butyllithium in hexane (40 mL, 0.063 mol) dropwise a room temperature to a solution of N-methylpyrrole (1) (5.0 g, 5.5 mL, 0.06 mol) in 50 mL of anhydrous diethyl ether in a round bottom flask under argon. After addition, heat the mixture under reflux for 16 - 20 hours then cool to 0^{o}C. To that mixture, add 1-methyl-4-piperidone (B) (7 g, 0.063 mol) dropwise from an addition funnel. During the addition, cool the flask further with a dry-ice/acetone bath. After addition, stir the reaction mixture for 3 hours at room temperature. Quench the reaction in ice water. Recrystallize in heptane. The recrystallization should be performed on brownish/tan clumps; anything that is red can be discarded as it is over oxidized.

A.2.2 Synthesis of MMTP•HCl[1] (5•HCl)

Add an equal mass (3 g) of MMPP (**4**) and Florisil to 50 mL of toluene. Reflux for 7 - 8 hours then cool to room temperature. Use a syringe filter to separate the toluene from the Florisil, and perform flash/column chromotagraphy on the sample. Expect elution of the sample around 50% EtOAc/Hexanes – 80% Etoac/Hexanes. Sample is marked by a distinct UV-Vis trace as well

as a slight decoloration. Note: the sample is NOT necessarily the stark yellow band; latent N-methylpyrrole tends to discolor the solution to yellow, not MMTP. MMTP tends to elute first in a more polar solvent. Evaporate the product to leave a heavy oil. Dissolve this oil in 20 mL of diethyl ether. Slowly add ethereal HCl to this solution with heavy stirring, stopping when the sample has completely decolored. Quickly filter the solid using vacuum filtration and collect the solid in a scintillation vial. This vial should be placed in a desiccator for no fewer than 24 hours before the sample is weighed and moved to the freezer for long-term storage.

A.2.3 Generation of free base MMTP (5)

To a scintillation vial, add the desired amount of MMTP•HCl. Add enough distilled water to dissolve the salt completely. To that solution, add K_2CO_3 to produce a cloudy solution. Perform a liquid extraction using CH_2Cl_2. Isolate the organic layer using a syringe filter to leave a transparent organic solution. If the solution is a moderate to dark yellow, preparative TLC is necessary. Using a mobile phase of 75% ethyl acetate/25% hexanes and a silica TLC plate, the band with r.f. 0.4-0.6 is the desired free MMTP. Once isolated, release from silica using CH_2Cl_2. Evaporate the solvent under reduced pressure, leaving a pale yellow oil.

^{1}H-NMR (400 MHz, CD_3CN) δ: 2.314 (s, 3H), 2.416 (m, 2H), 2.568 (t, 2H, J = 6.02 Hz), 3.030 (q, 2H, J = 3.34 Hz), 3.625 (s, 3H), 5.718 (m, 1H), 6.001 (m, 2H), 6.603 (t, 1H, J = 2.35 Hz)

A.3 Synthesis of 3-methyllumiflavin (3MLF)

Details of the synthesis of 3-methyllumiflavin (3MLF) can be found in the work originally reported by Ghisla *et al*.[2] 3MLF was stored as a solid under ambient conditions.

^{1}H NMR (CD_3CN, 400 MHz): δ 2.453 (s, 3H), 2.554 (s, 3H), 3.368 (s, 3H), 4.021 (s, 3H), 7.660 (s, 1H), 7.925 (s, 1H)

A.4 Reference ^{1}HNMR spectra and assignments for 3MLF, MMTP, and MMP^{+}

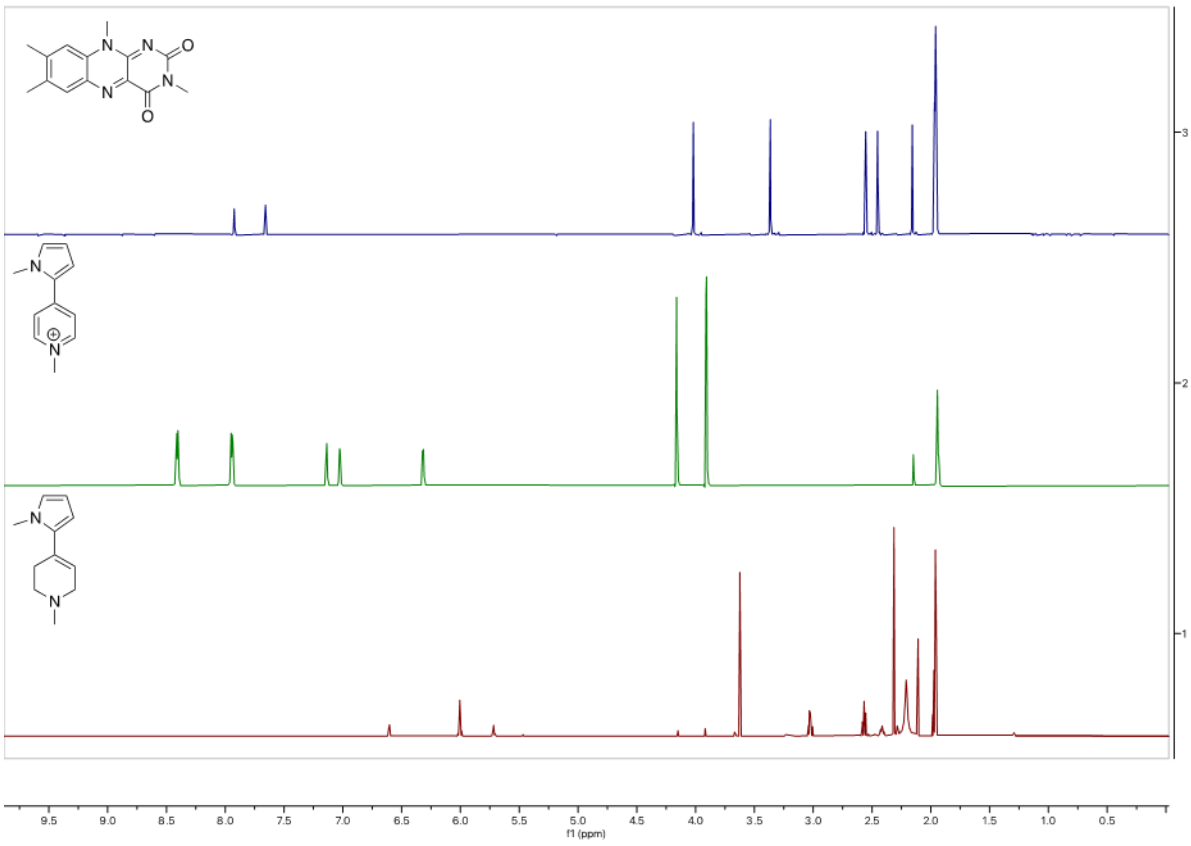

Figure A.1: Reference spectra for 3MLF (top), MMP^{+} (middle), and MMTP (bottom) are shown. 3MLF: ^{1}H NMR (CD_3CN, 400 MHz): δ 2.453 (s, 3H), 2.554 (s, 3H), 3.368 (s, 3H), 4.021 (s, 3H), 7.660 (s, 1H), 7.925 (s, 1H). MMP^{+}: ^{1}H NMR (CD_3CN, 400 MHz): δ 3.911 (s, 3H), 4.162 (s, 3H), 6.319 (quint, 1H, *J* = 2.15 Hz), 7.025 (m, 1H), 7.137 (d, 1H, *J* = 1.48 Hz), 7.946 (d, 2H *J* = 5.49 Hz), 8.400 (d, 2H, *J* = 5.49 Hz). MMTP: ^{1}H NMR (CD_3CN, 400 MHz): δ 2.314 (s, 3H), 2.416 (m, 2H), 2.568 (t, 2H, *J* = 6.02 Hz), 3.030 (q, 2H, *J* = 3.34 Hz), 3.625 (s, 3H), 5.718 (m, 1H), 6.001 (m, 2H), 6.603 (t, 1H, *J* = 2.35 Hz)

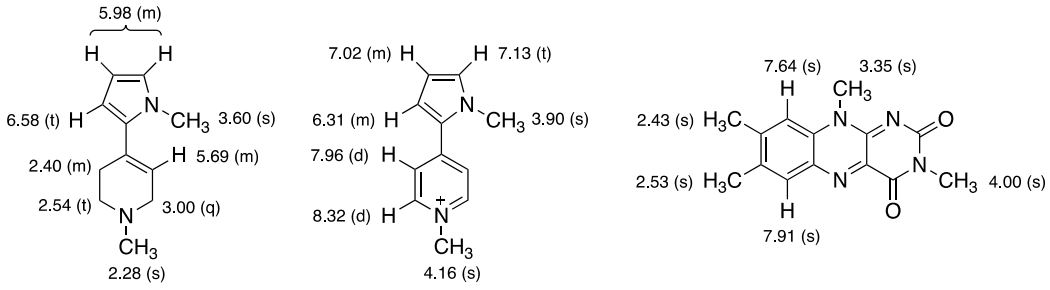

Figure A.2: ^{1}H NMR spectral assignments for MMTP, MMP^{+}, and 3MLF.

A.5 Aerobic reaction of MMTP and 3MLF (1:1 molar ratio)

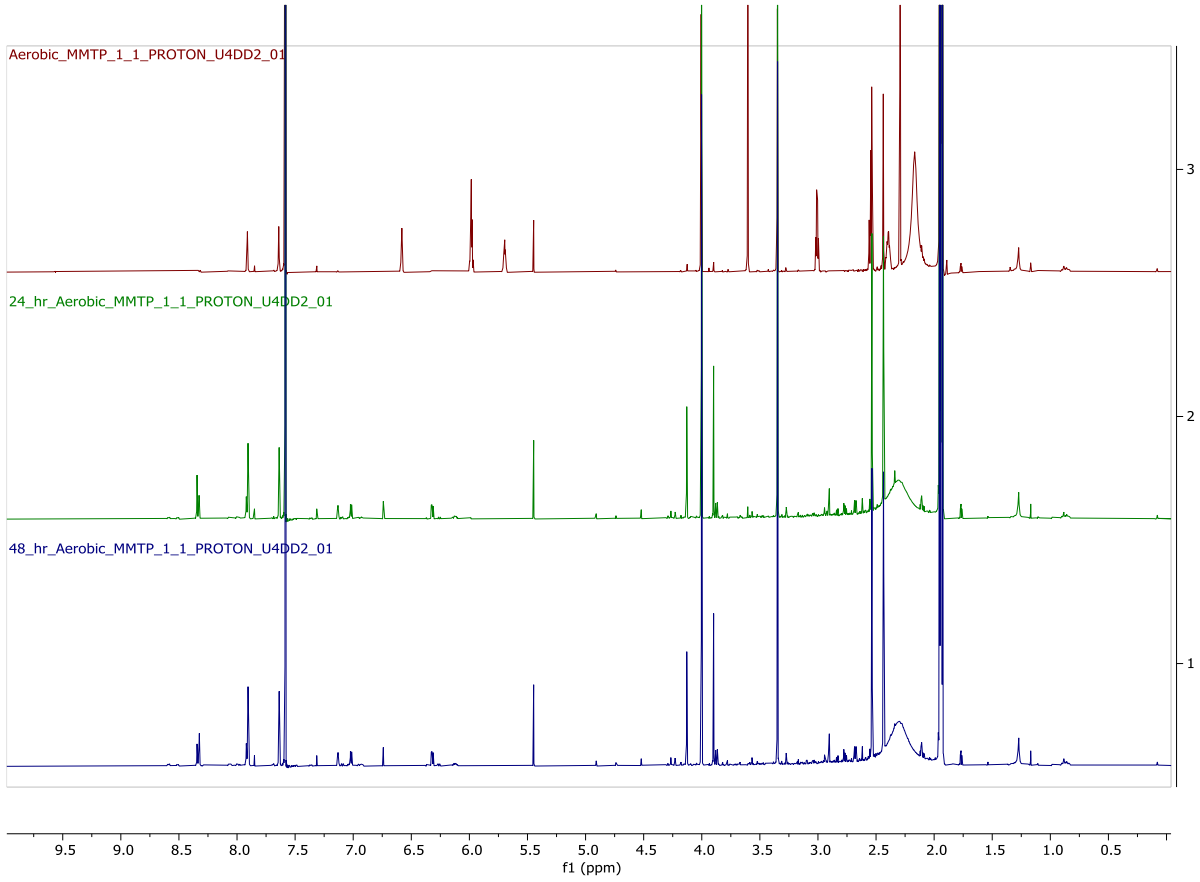

Figure A.3: The complete 1:1 aerobic reaction of MMTP and 3MLF occurs within the first 48 hours (t = 0, 24 hrs, 48 hrs; top to bottom). This reaction features an internal benzene standard at 7.60 ppm for quantitation.

A.6 Aerobic reaction of MMTP and 3MLF (8:1 molar ratio)

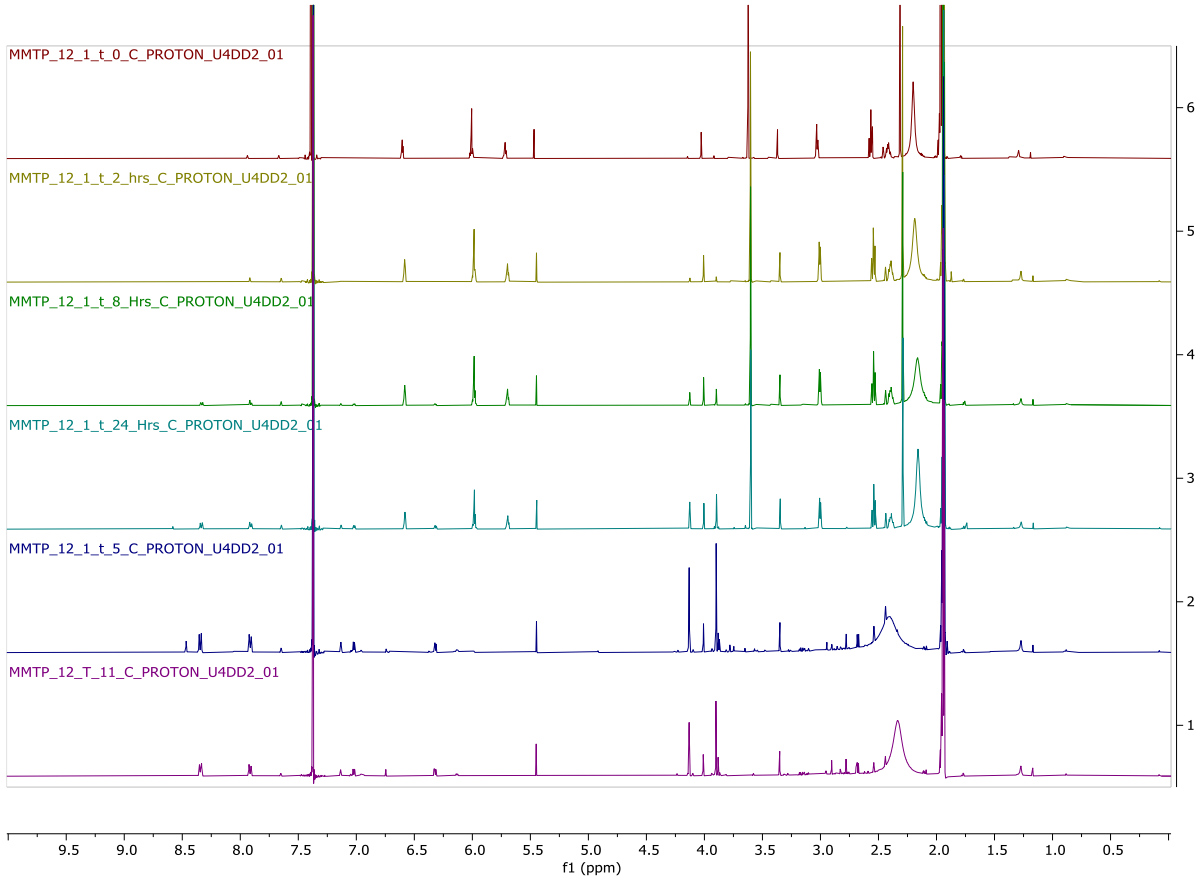

Figure A.4: An 8:1 aerobic reaction of MMTP and 3MLF was allowed to occur with sporadic monitoring for 11 days (t = 0, 2 hrs, 8 hrs, 24 hrs, 5 days, 11 days; top to bottom). This reaction features an internal benzene standard at 7.60 ppm for quantitation.

A.7 Long term aerobic reaction of MMTP and 3MLF (1:1 molar ratio)

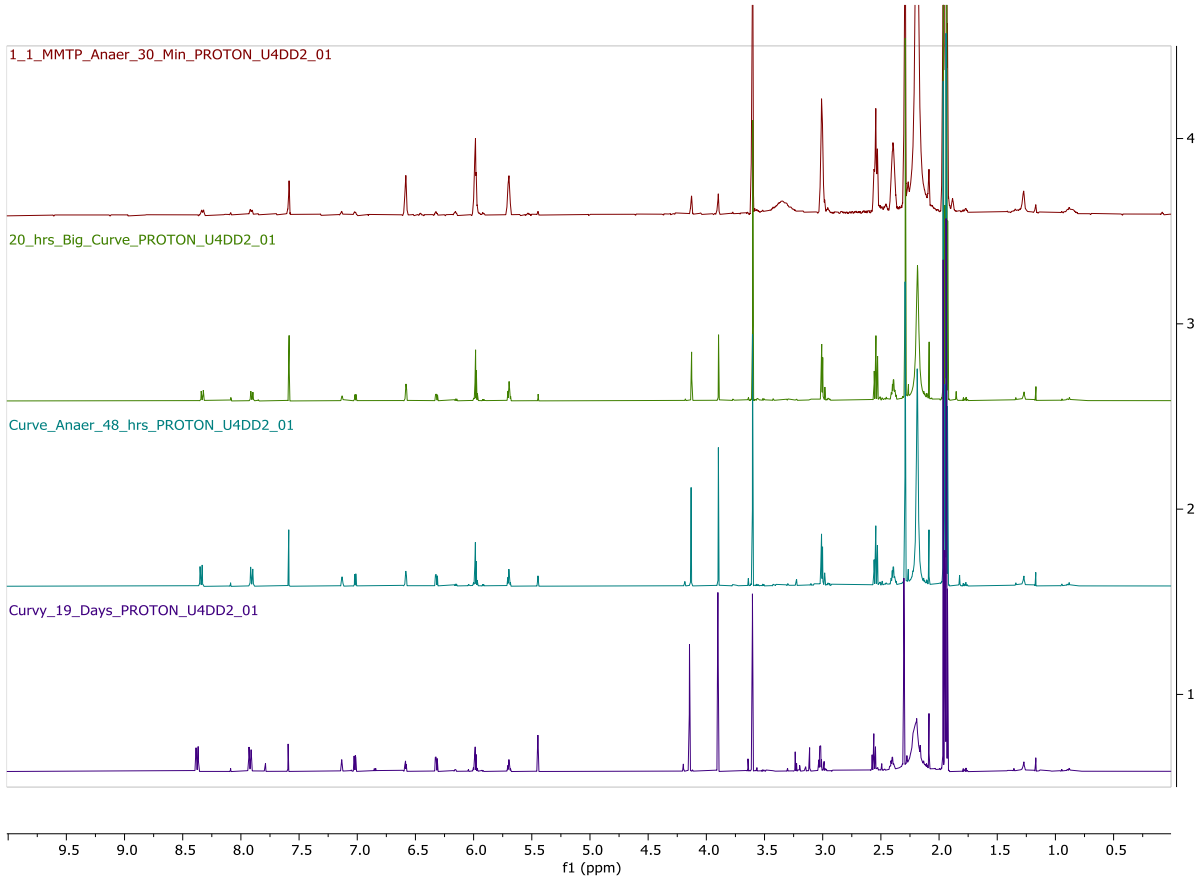

Figure A.5: The 1:1 anaerobic reaction of MMTP and 3MLF demonstrates little significant change after the first 48 hours (t = 0, 24 hrs, 48 hrs, 19 days; top to bottom). This reaction features an internal benzene standard at 7.60 ppm for quantitation.

A.8 Anaerobic reaction of MMTP and 3MLF (2:1) interrupted after one hour and exposed to air

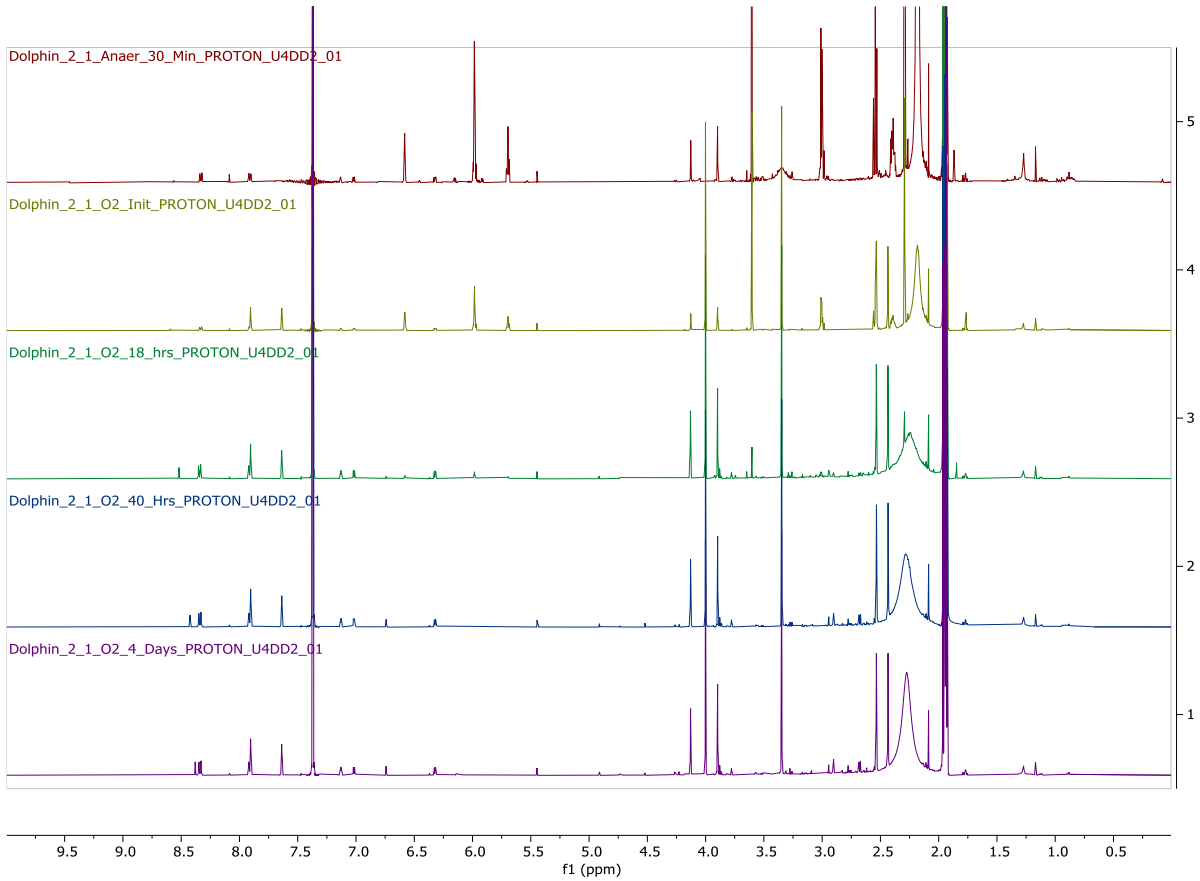

Figure A.6: This reaction, begun anaerobically and exposed to air after 1 hour, proceeded normally as an aerobic reaction (t = 0, air exposure coinciding with 1 hour, 18 hrs, 40 hrs, 4 days; top to bottom). This reaction features an internal benzene standard at 7.60 ppm for quantitation.

A.9 Anaerobic reaction of MMTP and 3MLF (1:1) monitored by EPR spectroscopy as a function of time

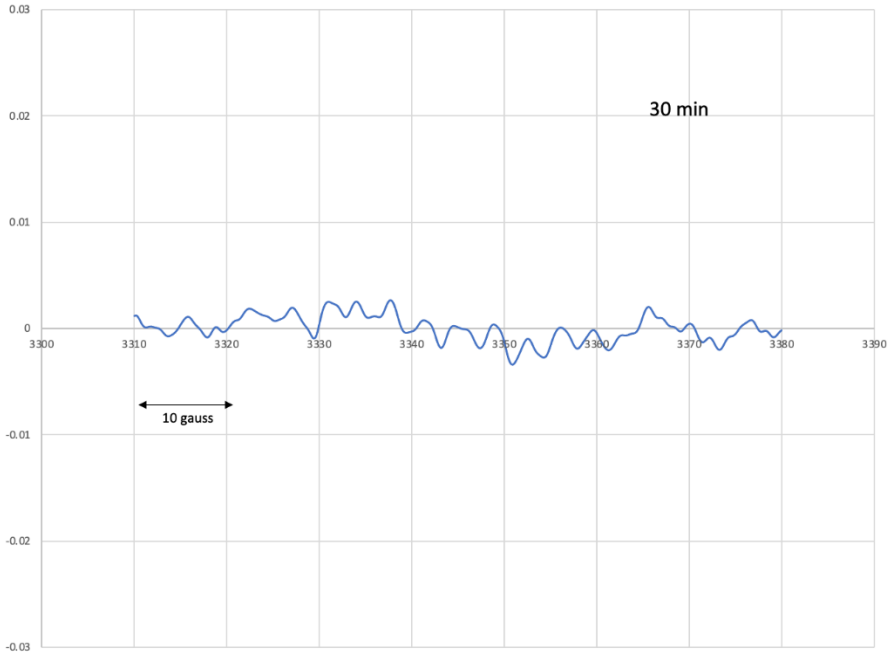

Figure A.7: The EPR spectrum of a 1:1 (MMTP:3MLF, 2.05 mM) reaction at t = 30 minutes.

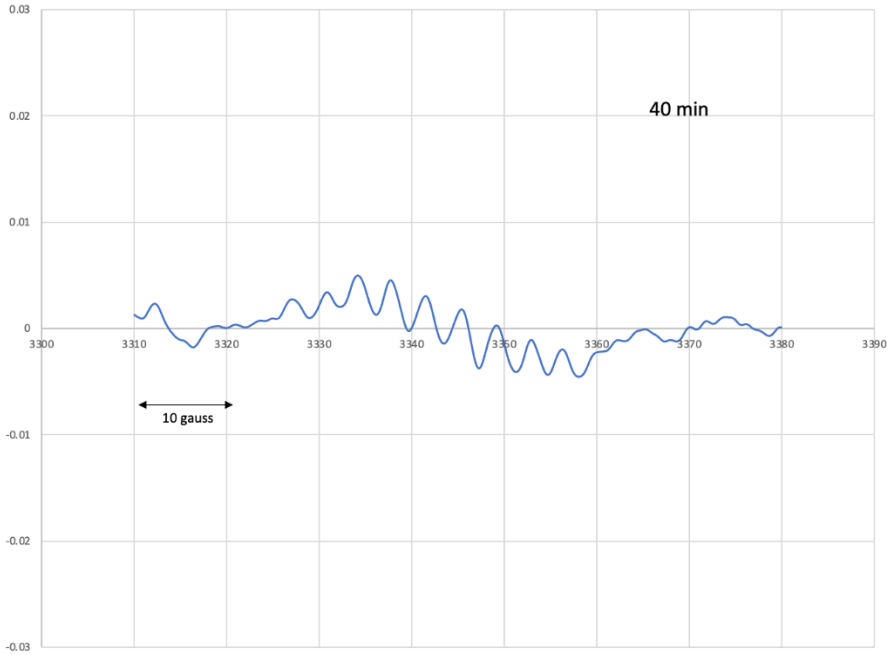

Figure A.8: The EPR spectrum of a 1:1 (MMTP:3MLF, 2.05 mM) reaction at t = 40 minutes.

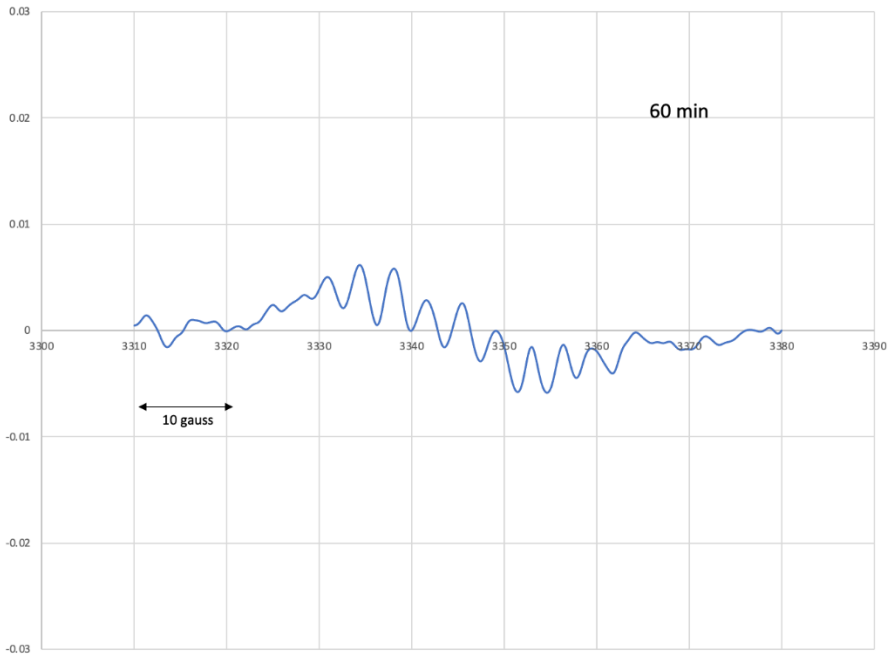

Figure A.9: The EPR spectrum of a 1:1 (MMTP:3MLF, 2.05 mM) reaction at t = 60 minutes.

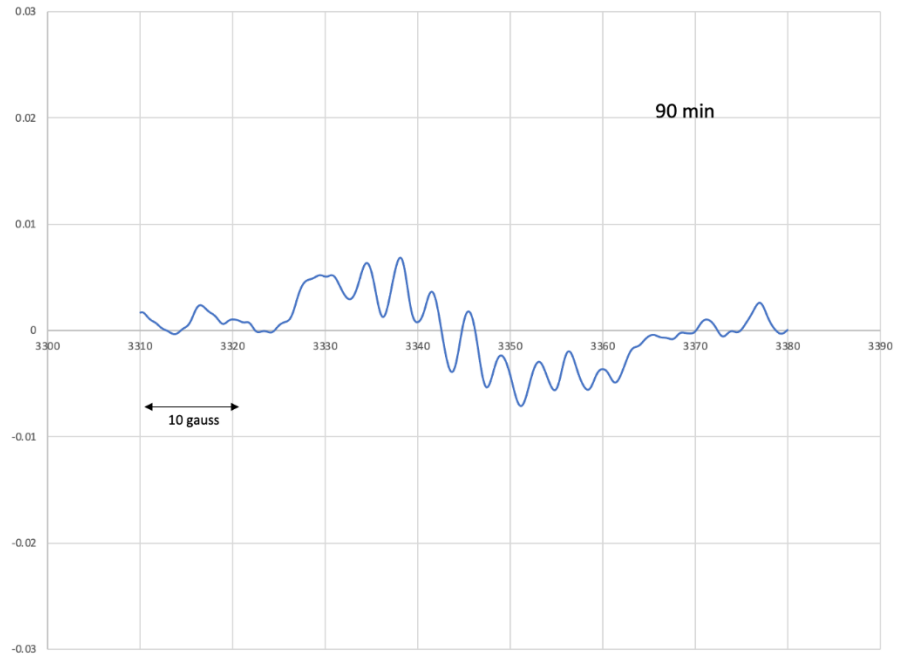

Figure A.10: The EPR spectrum of a 1:1 (MMTP:3MLF, 2.05 mM) reaction at t = 90 minutes.

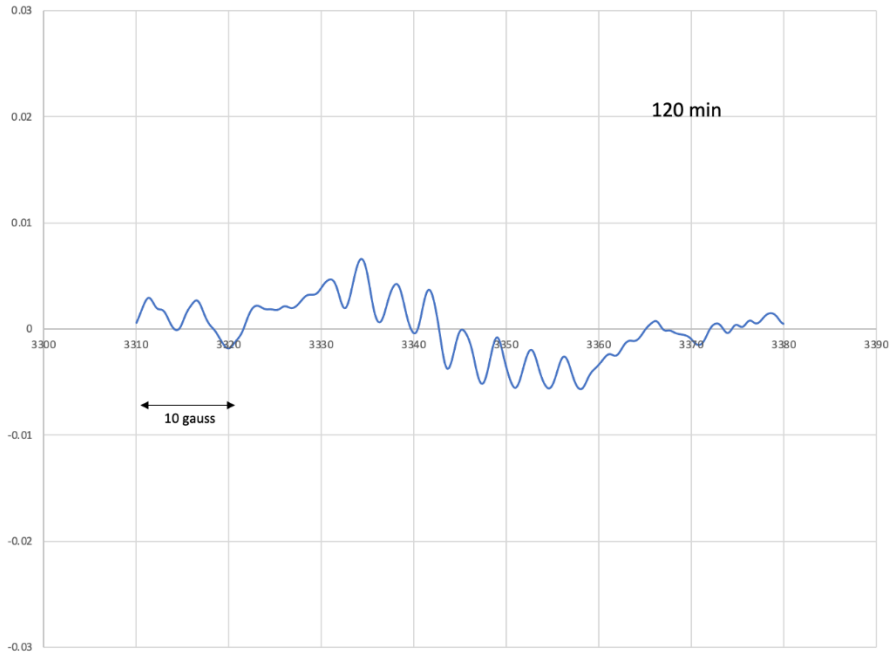

Figure A.11: The EPR spectrum of a 1:1 (MMTP:3MLF, 2.05 mM) reaction at t = 120 minutes.

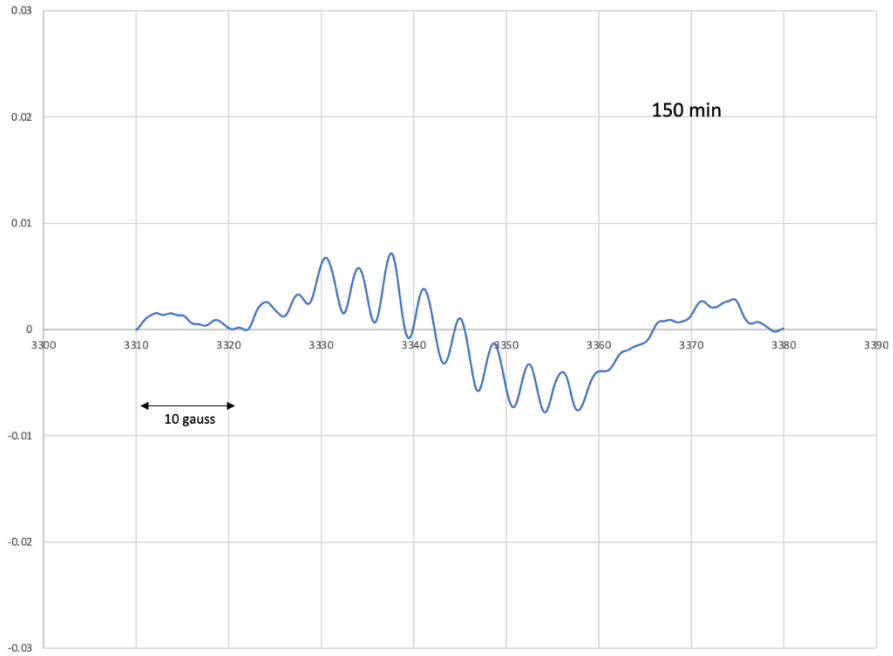

Figure A.12: The EPR spectrum of a 1:1 (MMTP:3MLF, 2.05 mM) reaction at t = 150 minutes.

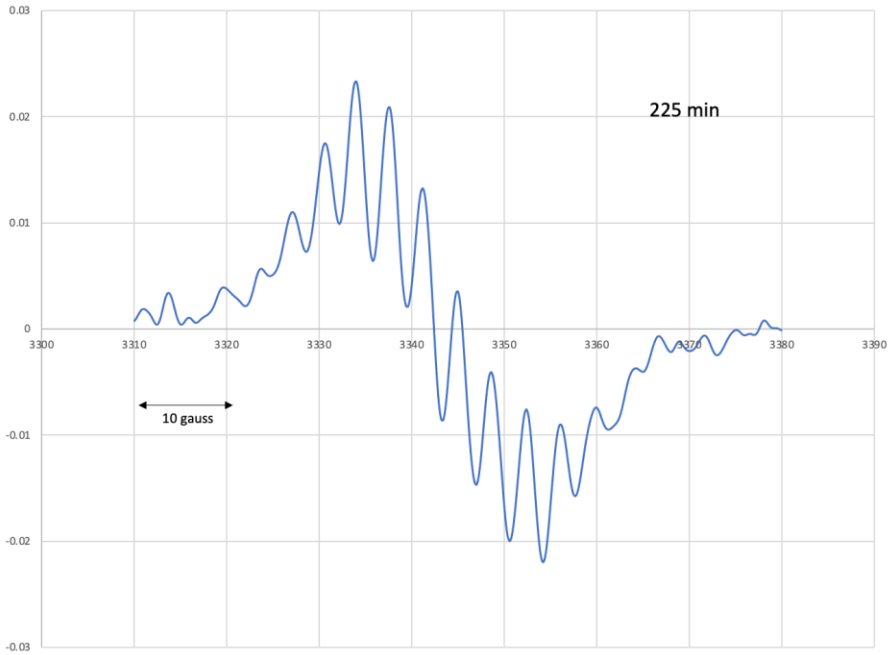

Figure A.13: The EPR spectrum of a 1:1 (MMTP:3MLF, 2.05 mM) reaction at t = 225 minutes.

A.10 References

1. Nimkar, S. K.; Anderson, A. H.; Rimoldi, J. R.; Stanton, M.; Castagnoli, K. P.; Mabic, S.; Wang, Y. X.; Castagnoli, N. Synthesis and Monoamine Oxidase B Catalyzed Oxidation of C-4 Heteroaromatic Substituted 1,2,3,6-Tetrahydropyridine Derivatives. *Chem. Res. Toxicol.* **1996**, *9*, 1013-1022.
2. Ghisla, S.; Hartmann, U.; Hemmerich, P.; Mueller, F., Flavine series. XVIII. Reductive alkylation of the flavine nucleus. Structure and reactivity of dihydroflavines. *Justus Liebigs Annalen der Chemie* **1973**, *8*, 1388-415.

Appendix B: Supporting Information for Using Cyclopropyl Spin Traps as Radical Probes for the Oxidation of MPTP

B.1 Experimental

NMR spectra were recorded using an Agilent U4-DD2 (400 MHz) or Bruker Avance II (500 MHz). Data analyses were performed using MestreNova. All reactions were prepared using degassed CD_3CN stock solutions. Stocks were kept refrigerated unless being actively used. This was done primarily to maintain consistency in sample preparation. Aerobic reactions were prepared directly in NMR tubes with a total reaction volume of 0.6 mL. To ensure proper and consistent aeration of the sample, the tubes were placed on a mixing table when not being analyzed. Anaerobic reactions were also prepared directly in NMR tubes, but were immediately freeze-pump-thaw degassed (the process started <1 minute after mixing). After degassing, the NMR tubes were flame-sealed. Although control experiments did not suggest that light plays a role in this reaction, tubes were stored in the dark to minimize the risk of photochemical side reactions.

B.2 Reference ^{1}H NMR Spectra

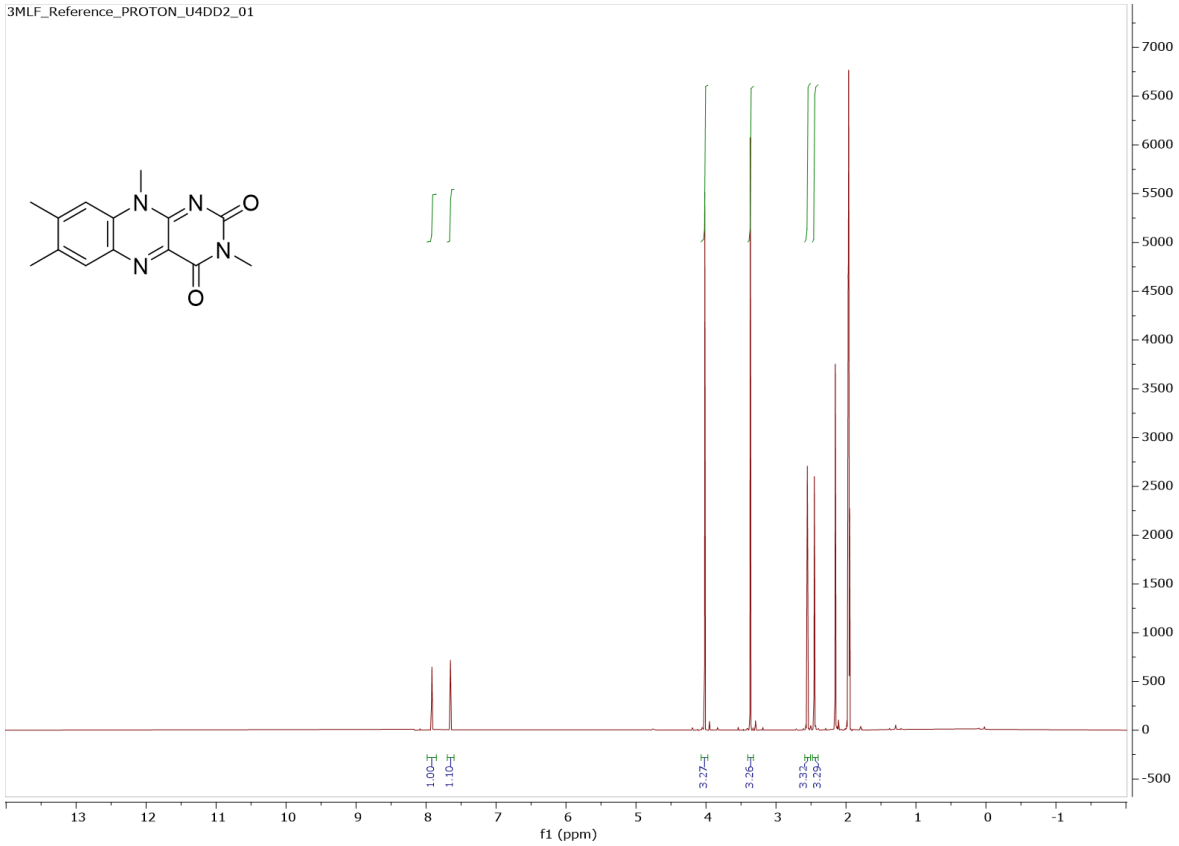

Figure B.1: The reference ^{1}H NMR spectrum for 3MLF

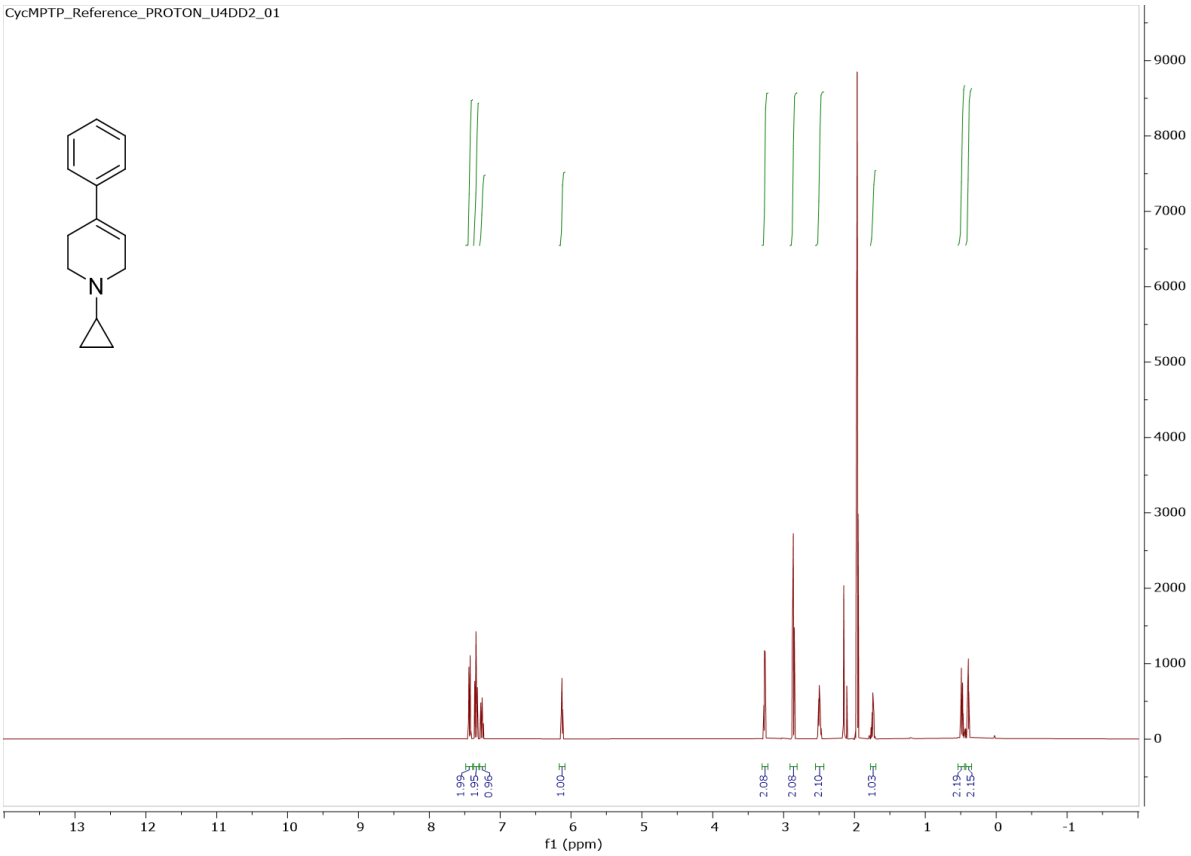

Figure B.2: The reference ^{1}H NMR spectrum for cyc-MPTP

B.3 Characterization of Intermediates Derived from Cyc-MPTP

B.3.1 ^{1}H NMR Spectral Assignments

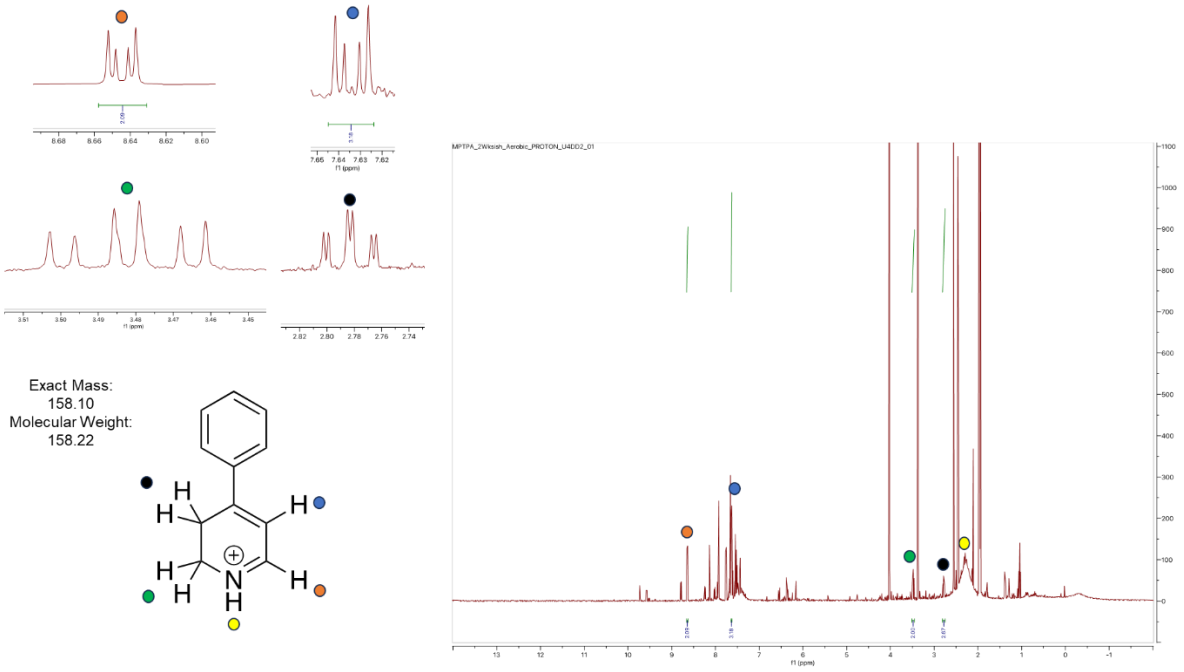

Figure B.3: ^{1}H NMR spectral assignments for the hypothesized dihydropyridinium intermediate. The ^{1}H NMR spectrum was recorded from an aerobic 1:1 reaction of cyc-MPTP and 3MLF at t = 48 hours.

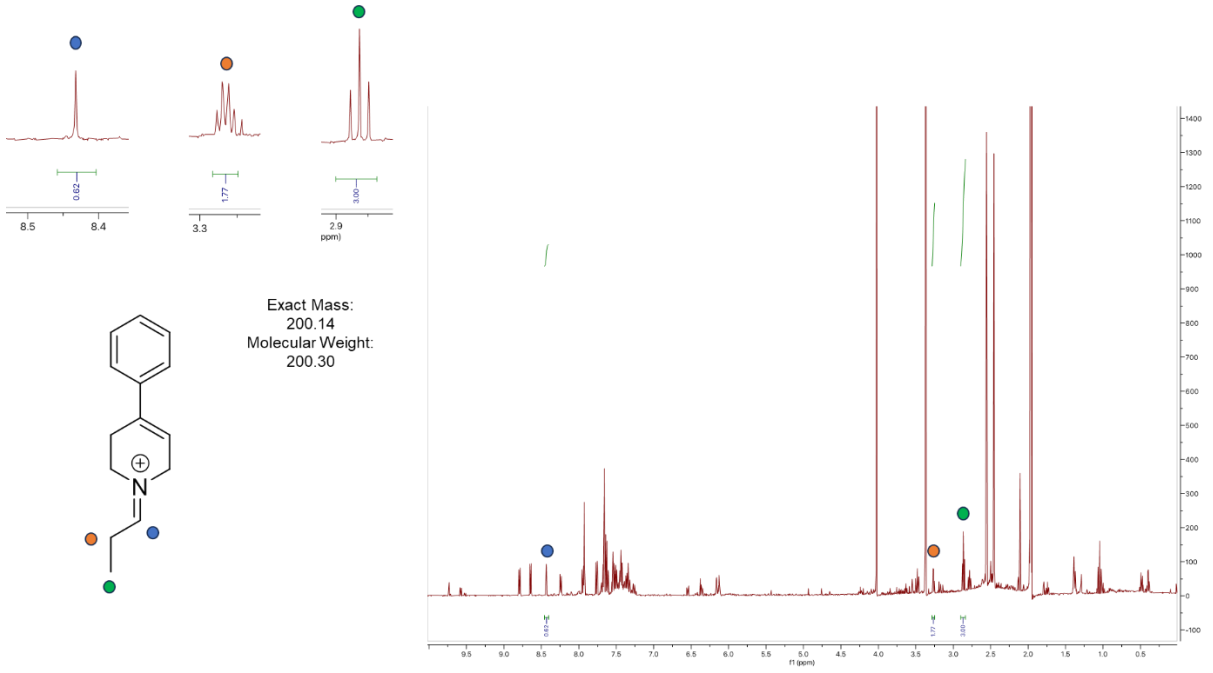

Figure B.4: ^{1}H NMR spectral assignments for the hypothesized iminium intermediate. The ^{1}H NMR spectrum was recorded from an aerobic 1:1 reaction of cyc-MPTP and 3MLF at t = 48 hours.

B.3.2 LC/MS Assignments

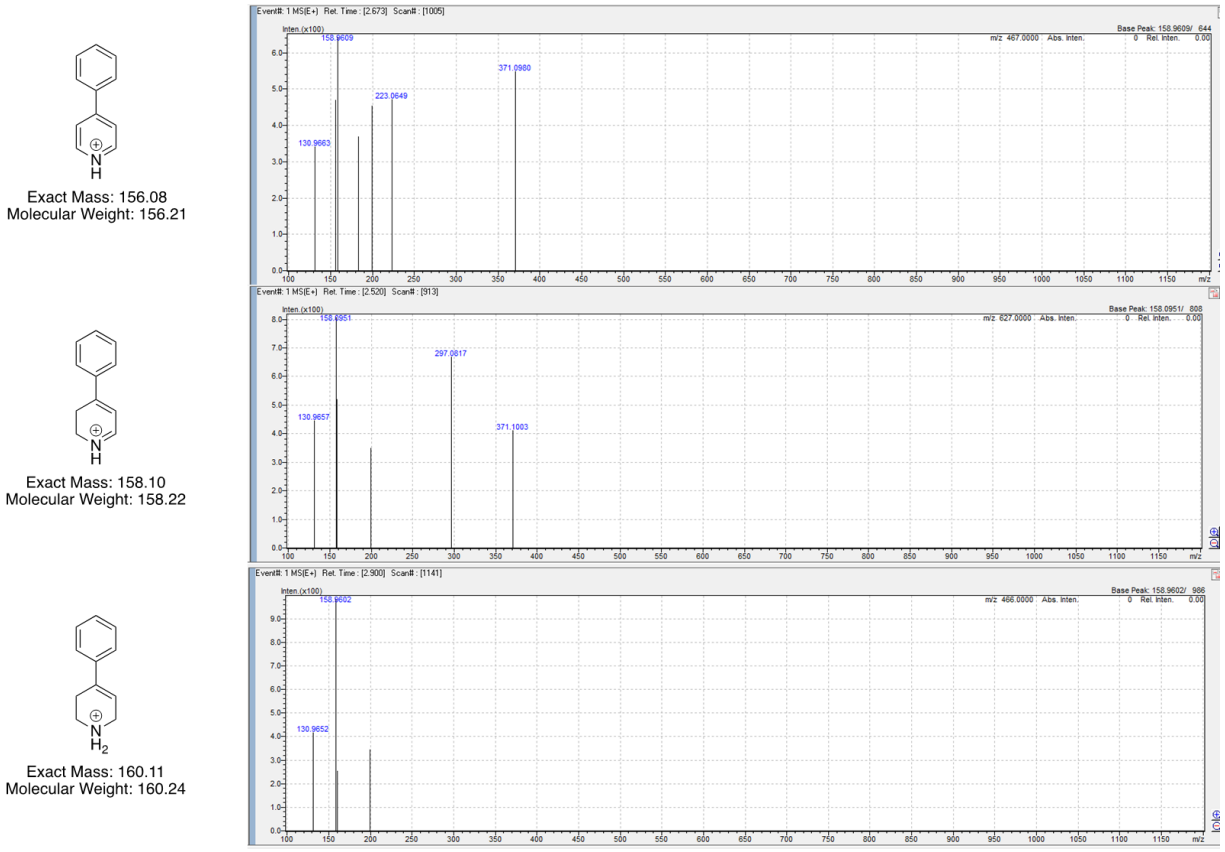

Figure B.5: Mass spectra for the hypothesized intermediates and products for the reaction of 3MLF with cyc-MPTP. Spectra were recorded from an aerobic 1:1 reaction of 3MLF and cyc-MPTP at t = 48 hrs.

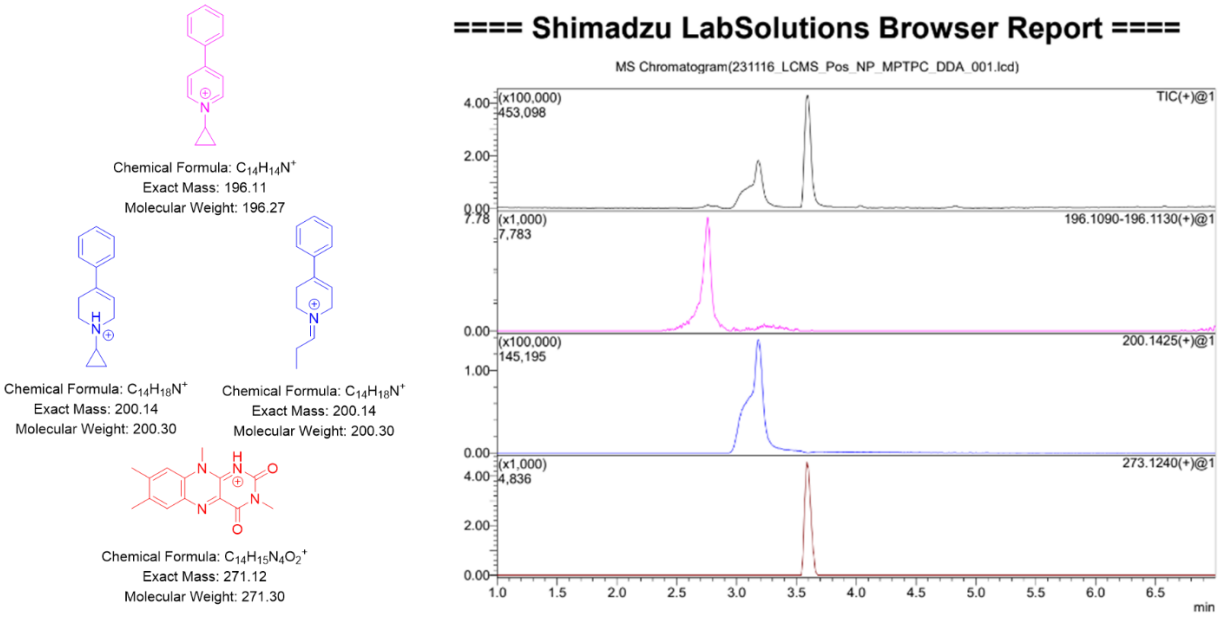

Figure B.6: Total ion (top) and selected ion chromatograms for the hypothesized intermediates and products for the reaction of 3MLF with cyc-MPTP. Spectra were recorded from an aerobic 1:1 reaction of 3MLF and cyc-MPTP at t = 48 hrs.

B.4 Air Exposure of an Anaerobic Sample

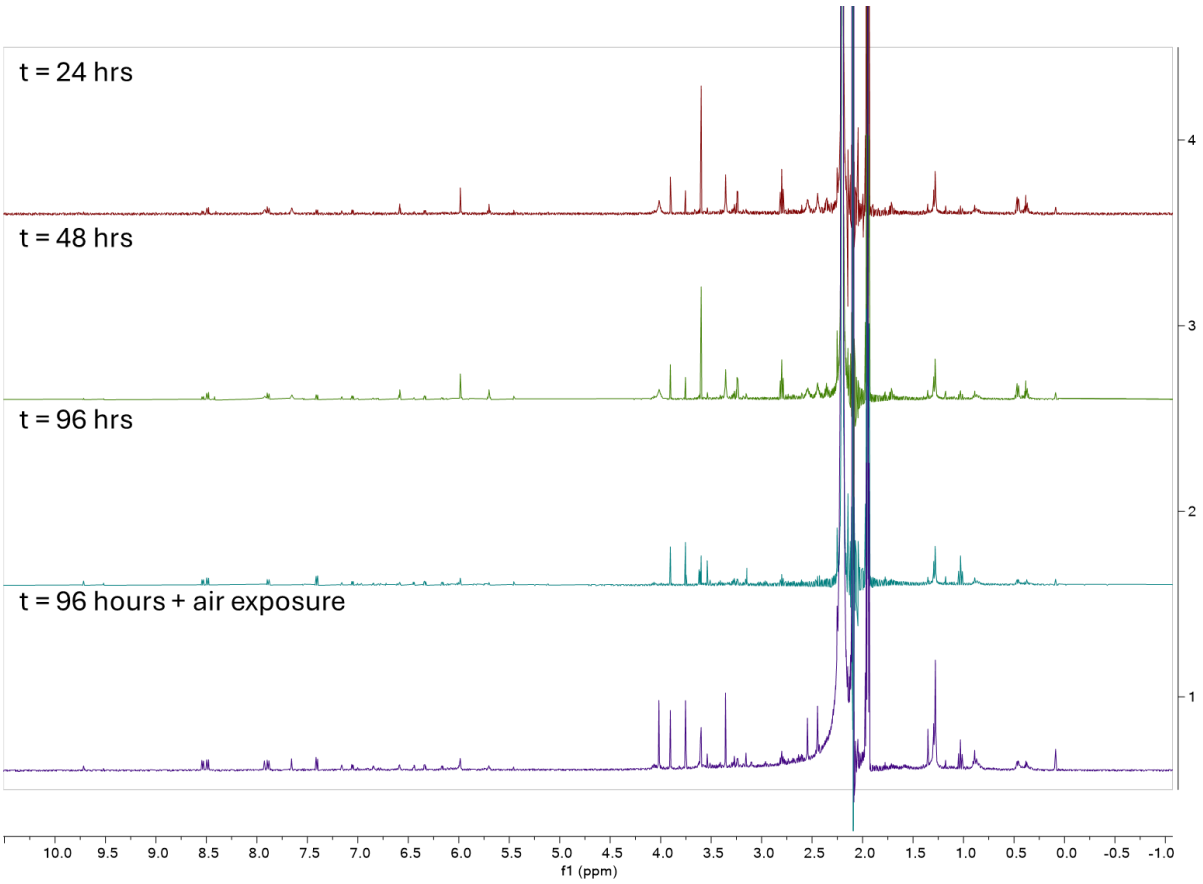

Figure B.7: Anaerobic 1:1 reaction of 3MLF and cyc-MPTP shown as a function of time. Peaks attributable to 3MLF reemerge after exposure to air.

B.5 Aerobic 1:1 Reaction of Cyc-MPTP and 3MLF for Quantitation

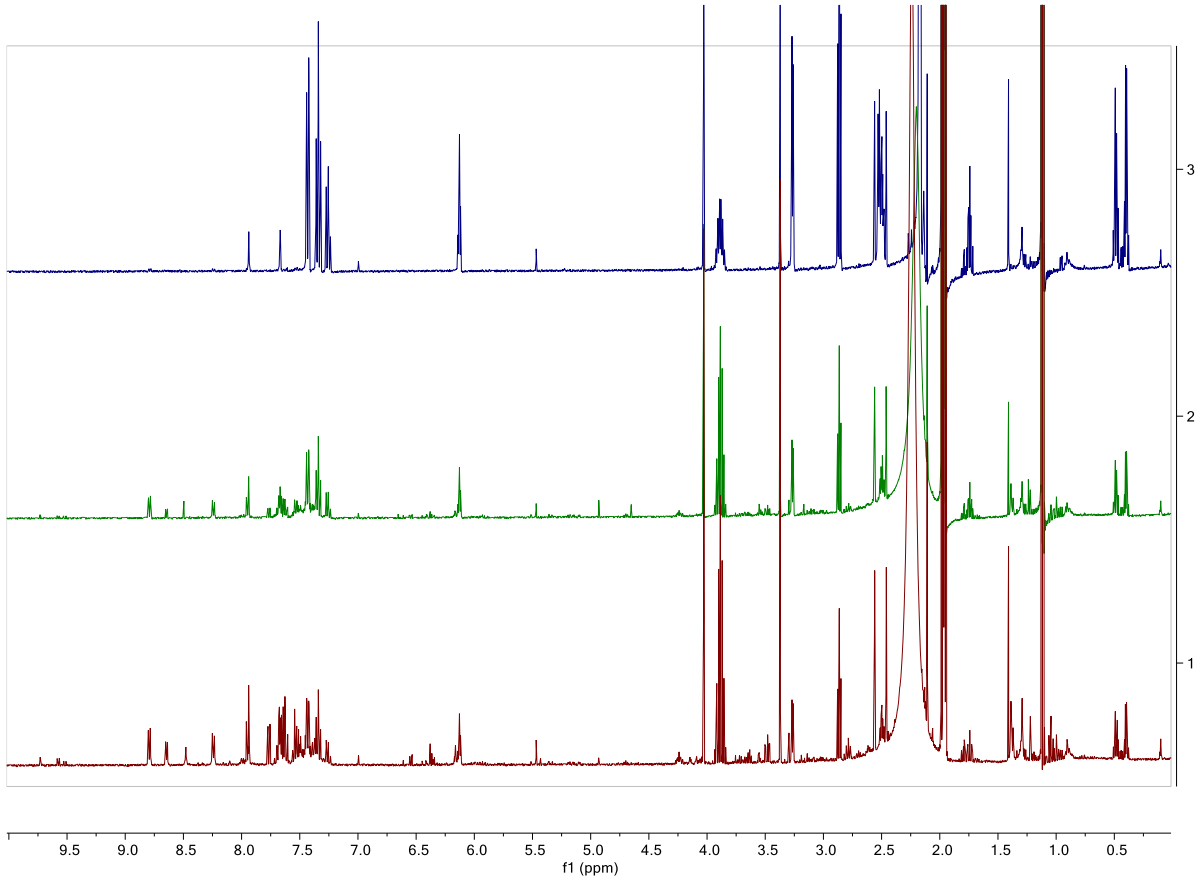

Figure B.8: Time-resolved ^{1}H NMR spectra from the aerobic 1:1 reaction of 3MLF and cyc-MPTP. The top spectrum was recorded at t = 0, the middle recorded at t = 24 hrs, and the bottom recorded at t = 48 hrs.

B.6 Aerobic 1:1 Reaction of Cyc-MPTP-d4 and 3MLF

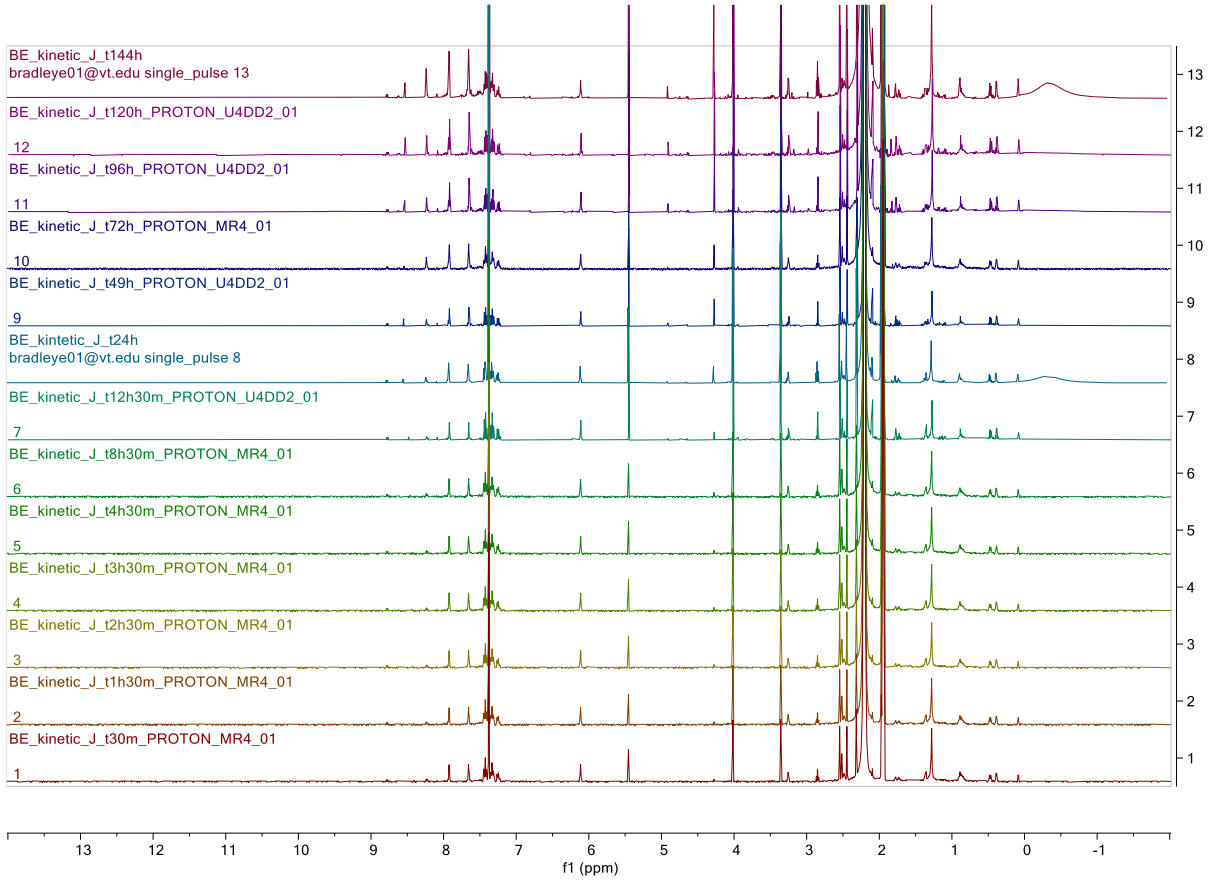

Figure B.9: The time-resolved ^{1}H NMR spectra from the aerobic 1:1 reaction of 3MLF and cyc-MPTP-d4 are shown. Notably, even after 144 hours, no aldehyde has formed.

B.7 Representative Reaction Spectra for the Study of H/D Kinetic Isotope Effect in the Reaction of 3MLF with MMTP/MPTP

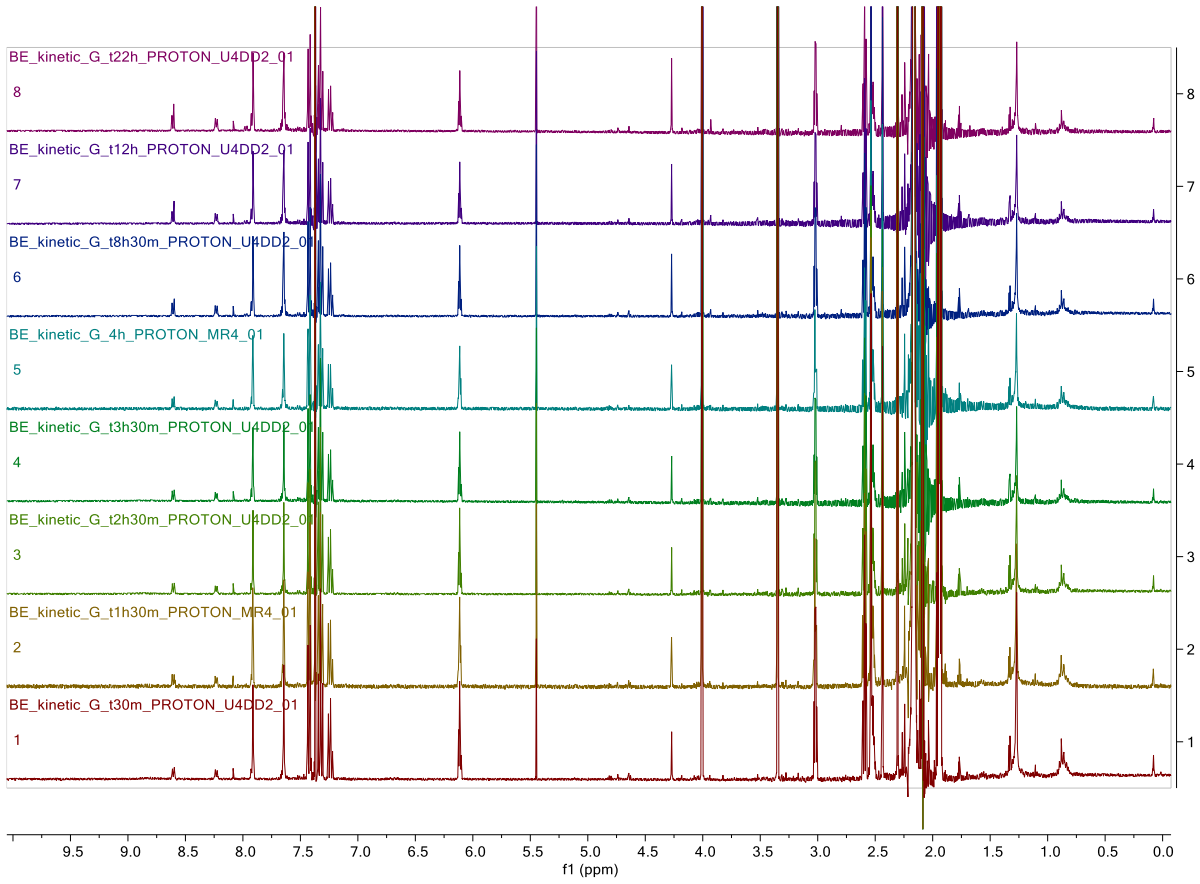

Figure B.10: Time resolved ^{1}H NMR spectra for the aerobic 1:2 (3MLF:MPTP) reaction of 3MLF and MPTP.

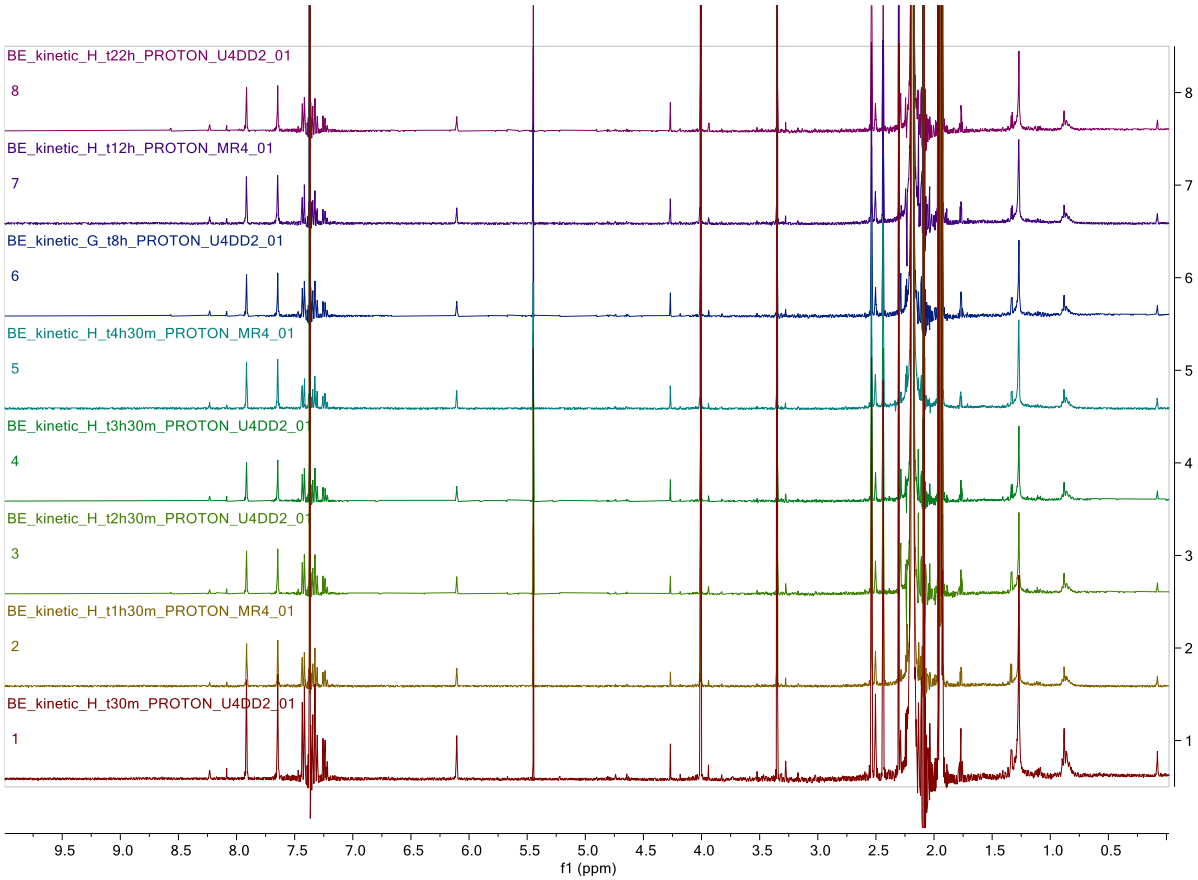

Figure B.11: Time resolved ^{1}H NMR spectra for the aerobic 1:2 (3MLF:MPTP-d4) reaction of 3MLF and MPTP-d4.

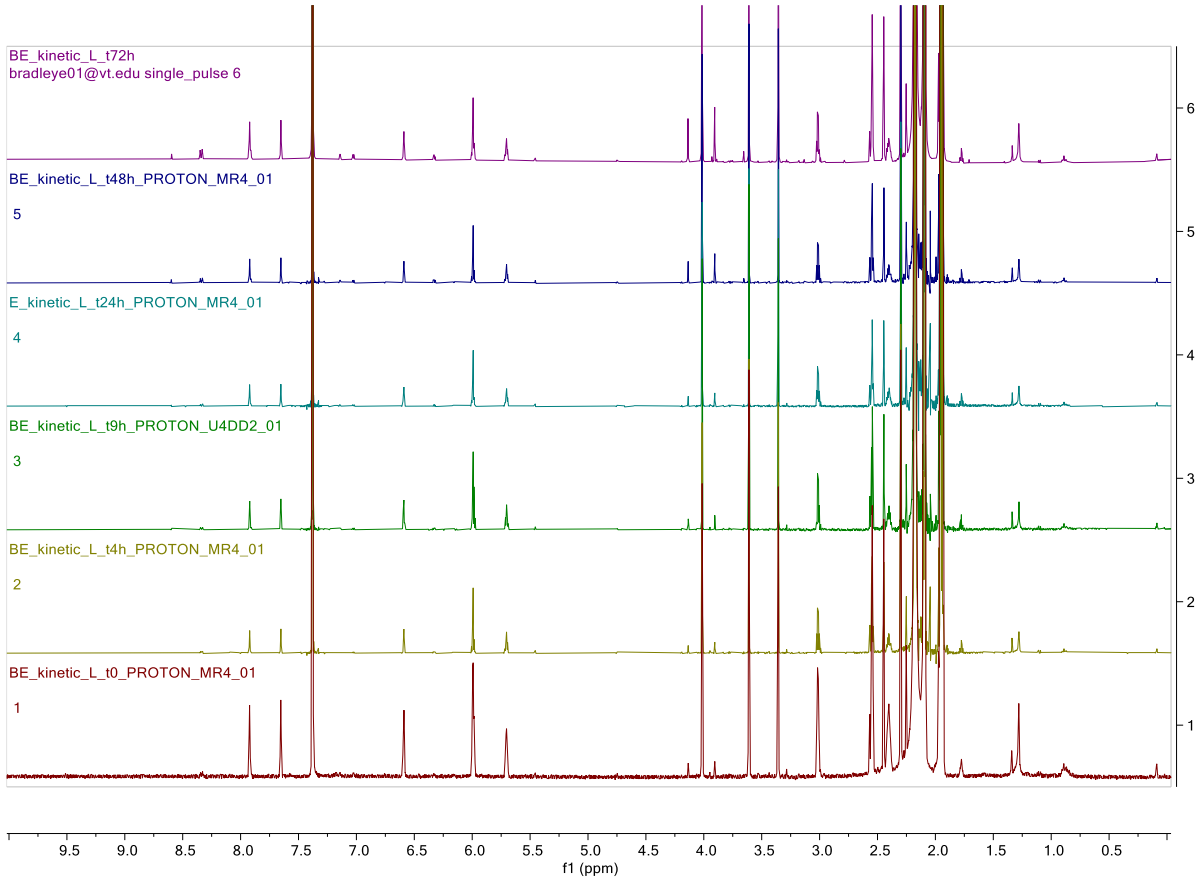

Figure B.12: Time resolved ^{1}H NMR spectra for the aerobic 1:2 (3MLF:MMTP) reaction of 3MLF and MMTP.

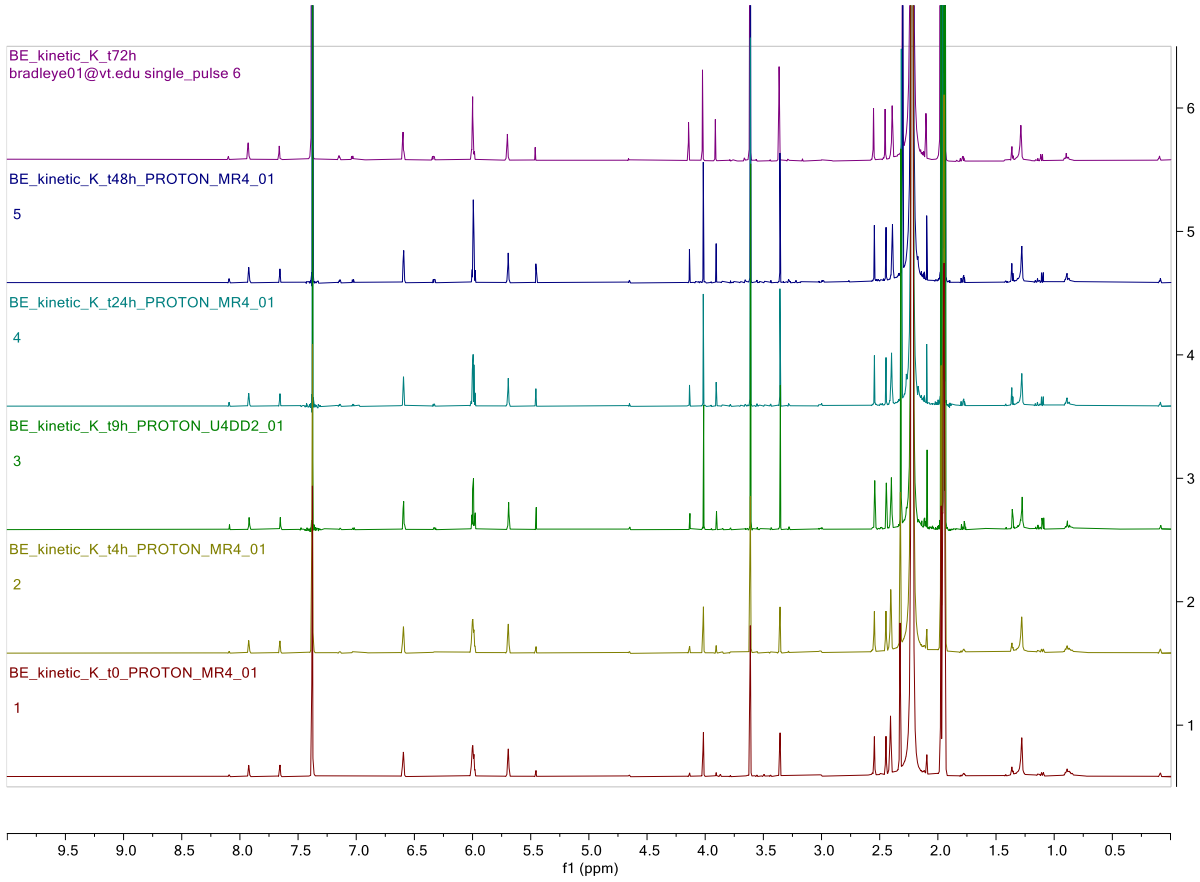

Figure B.13: Time resolved ^{1}H NMR spectra for the aerobic 1:2 (3MLF:MMTP-d4) reaction of 3MLF and MMTP-d4.

B.8 Kinetic Isotope Effect Plots

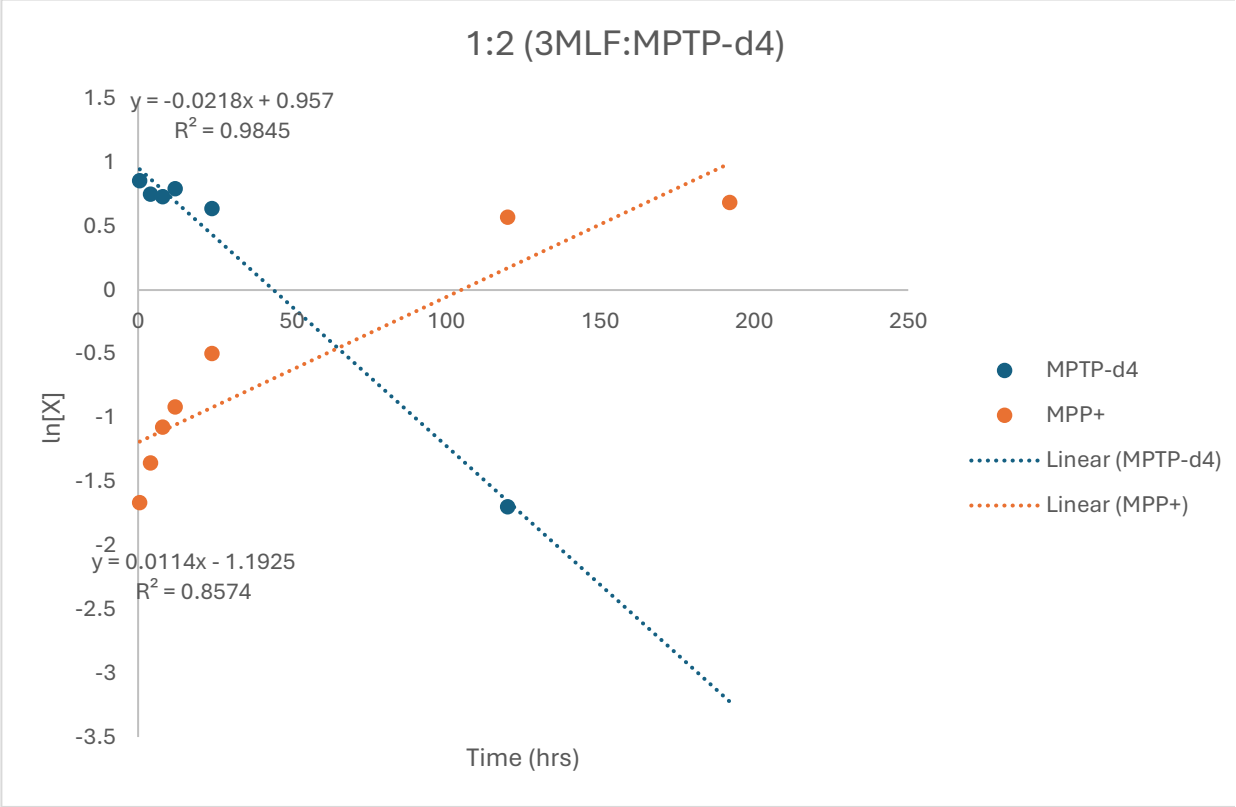

Figure B.14: Plot of ln[MPTP-d4] and ln[MPP^+] vs. time. Obtained from analysis of time-resolved ^1H NMR integrations with a benzene internal standard.

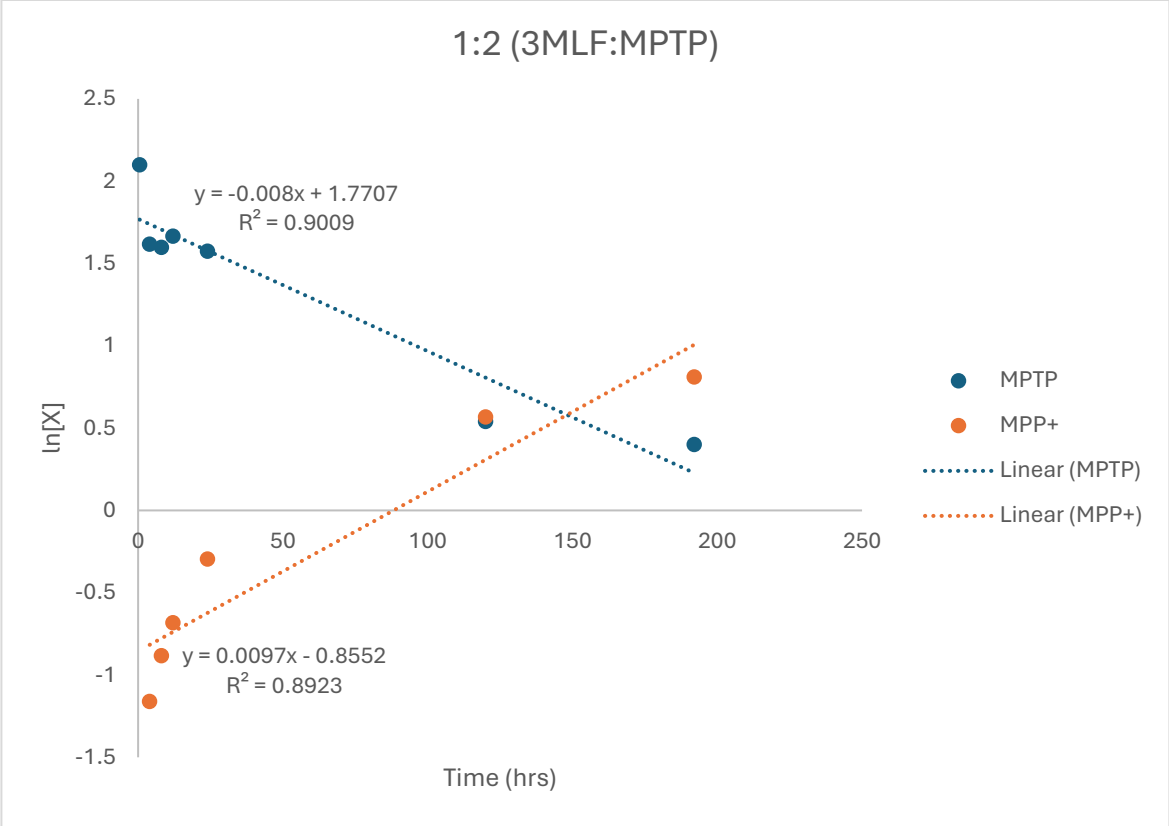

Figure B.15: Plot of ln[MPTP] and ln[MPP^+] vs. time. Obtained from analysis of time-resolved ^1H NMR integrations with a benzene internal standard.

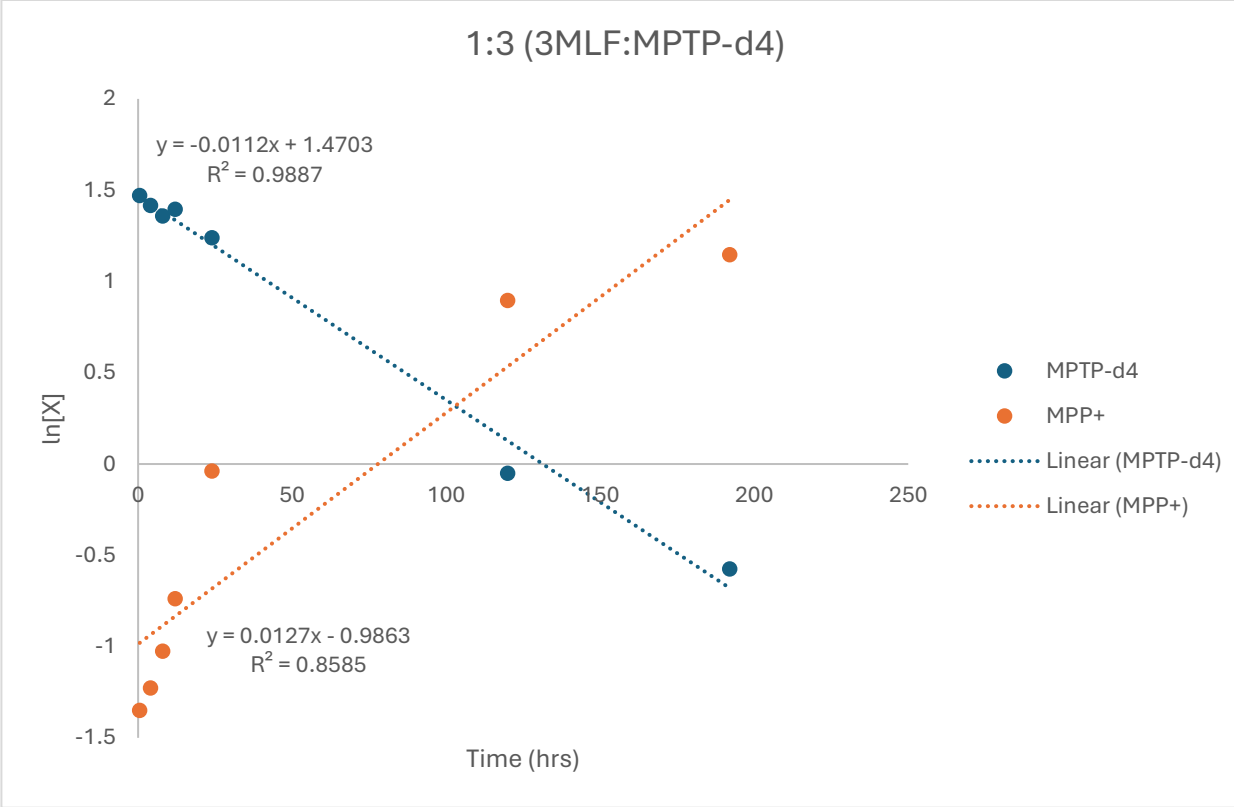

Figure B.16: Plot of ln[MPTP-d4] and ln[MPP^+] vs. time. Obtained from analysis of time-resolved ^1H NMR integrations with a benzene internal standard.

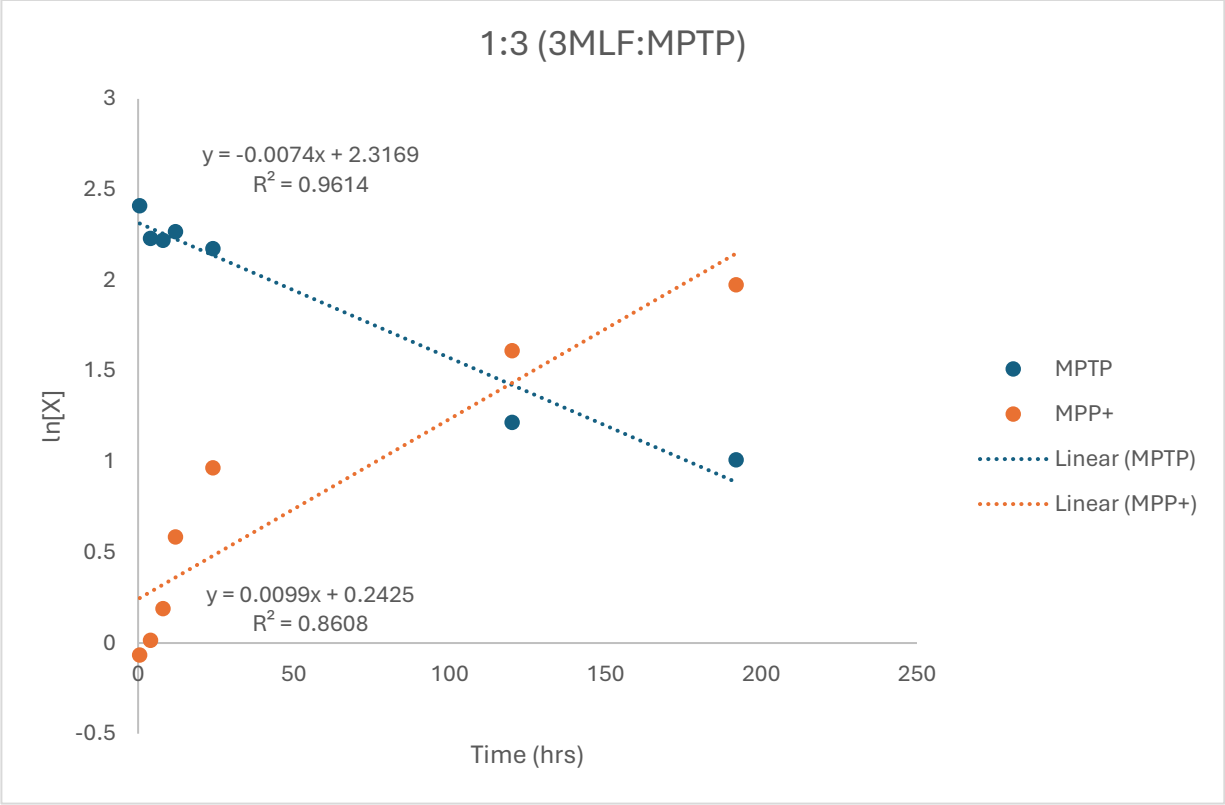

Figure B.17: Plot of ln[MPTP] and ln[MPP^+] vs. time. Obtained from analysis of time-resolved ^1H NMR integrations with a benzene internal standard.

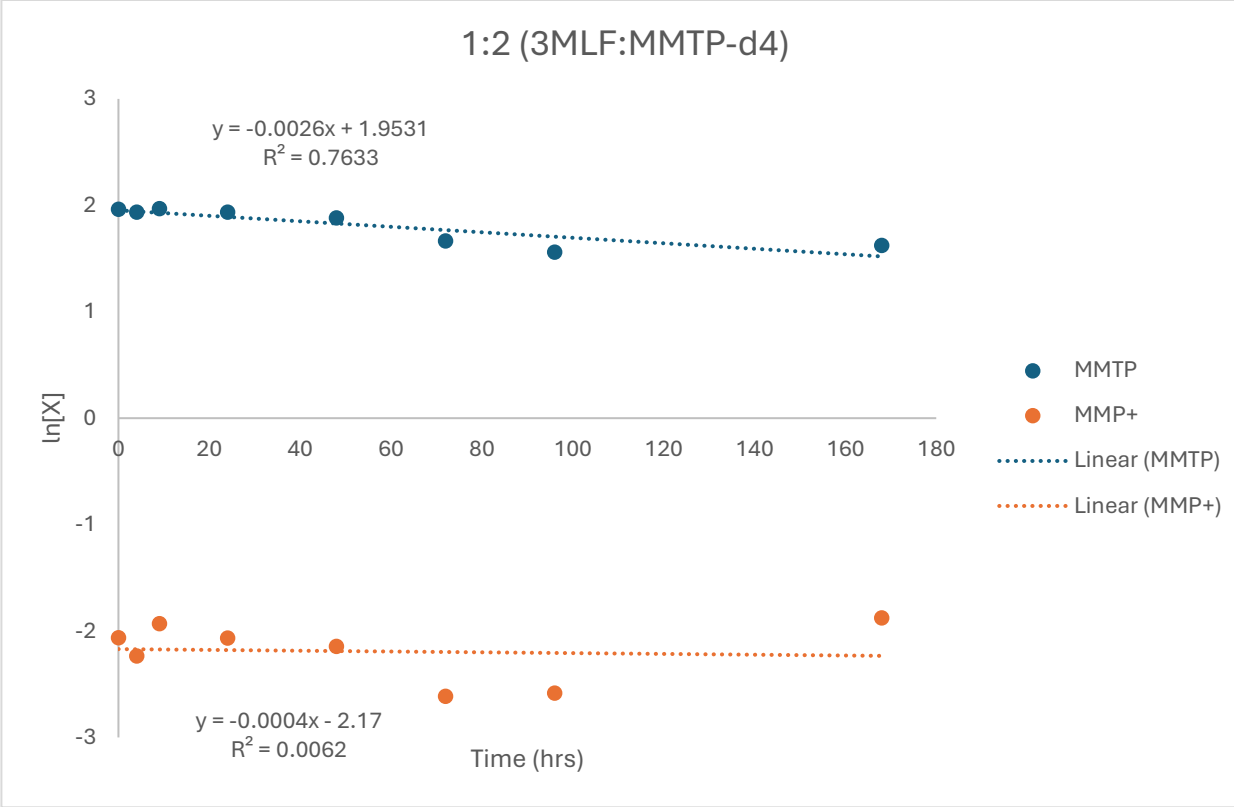

Figure B.18: Plot of ln[MMTP-d4] and ln[MMP^+] vs. time. Obtained from analysis of time-resolved ^1H NMR integrations with a benzene internal standard.

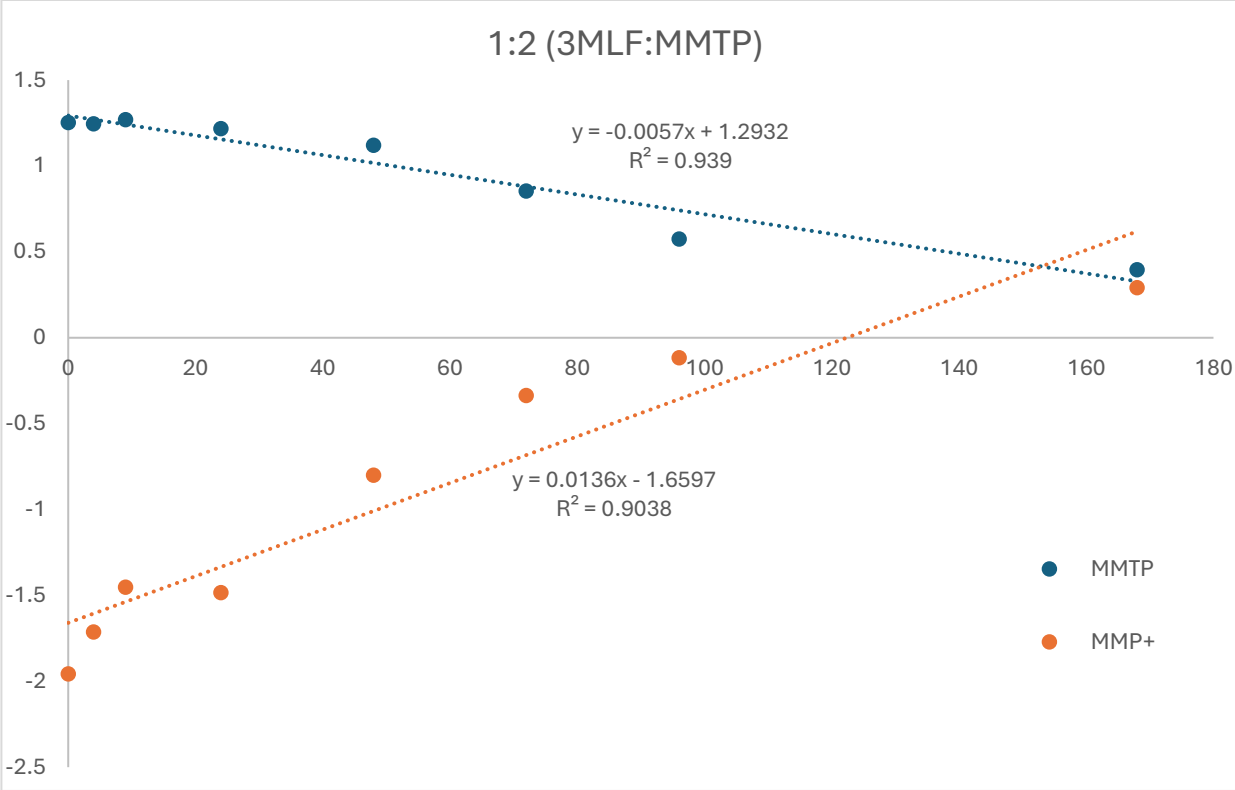

Figure B.19: Plot of ln[MMTP] and ln[MMP^+] vs. time. Obtained from analysis of time-resolved ^1H NMR integrations with a benzene internal standard.

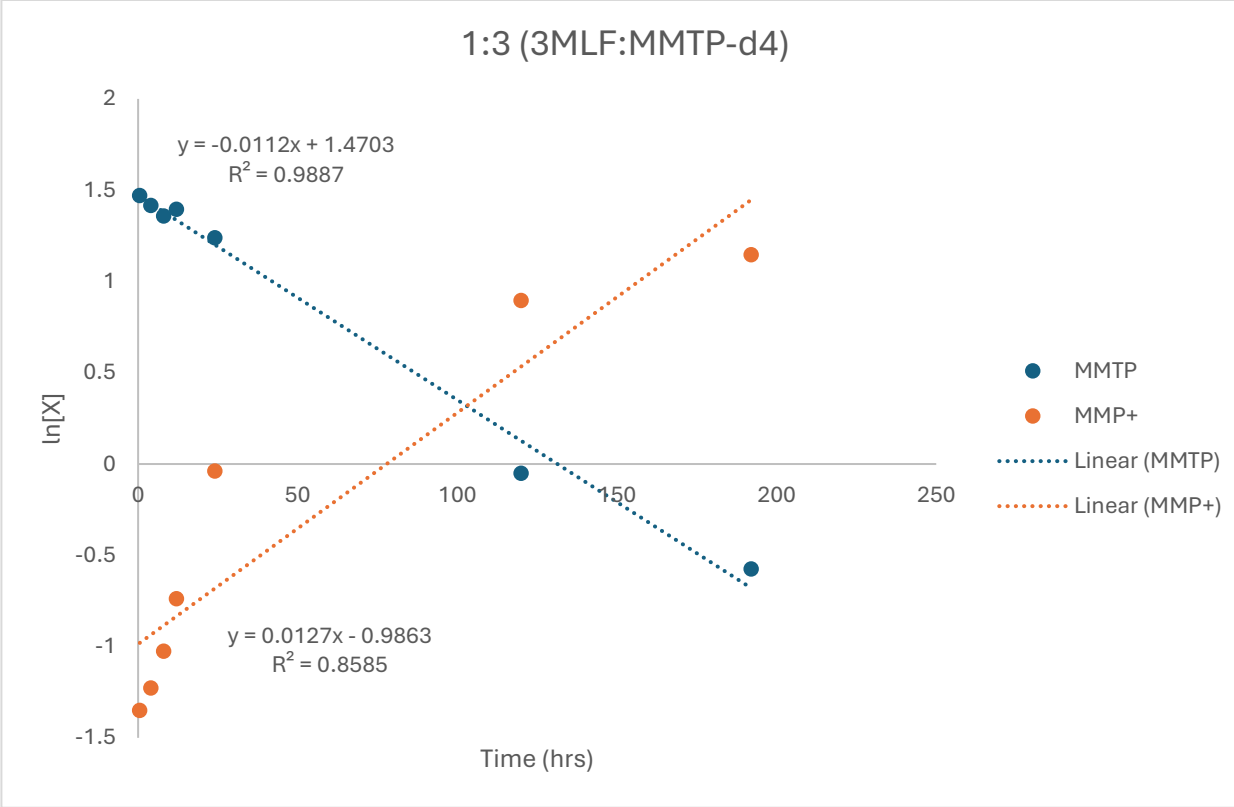

Figure B.20: Plot of ln[MMTP-d4] and ln[MMP^+] vs. time. Obtained from analysis of time-resolved ^1H NMR integrations with a benzene internal standard.

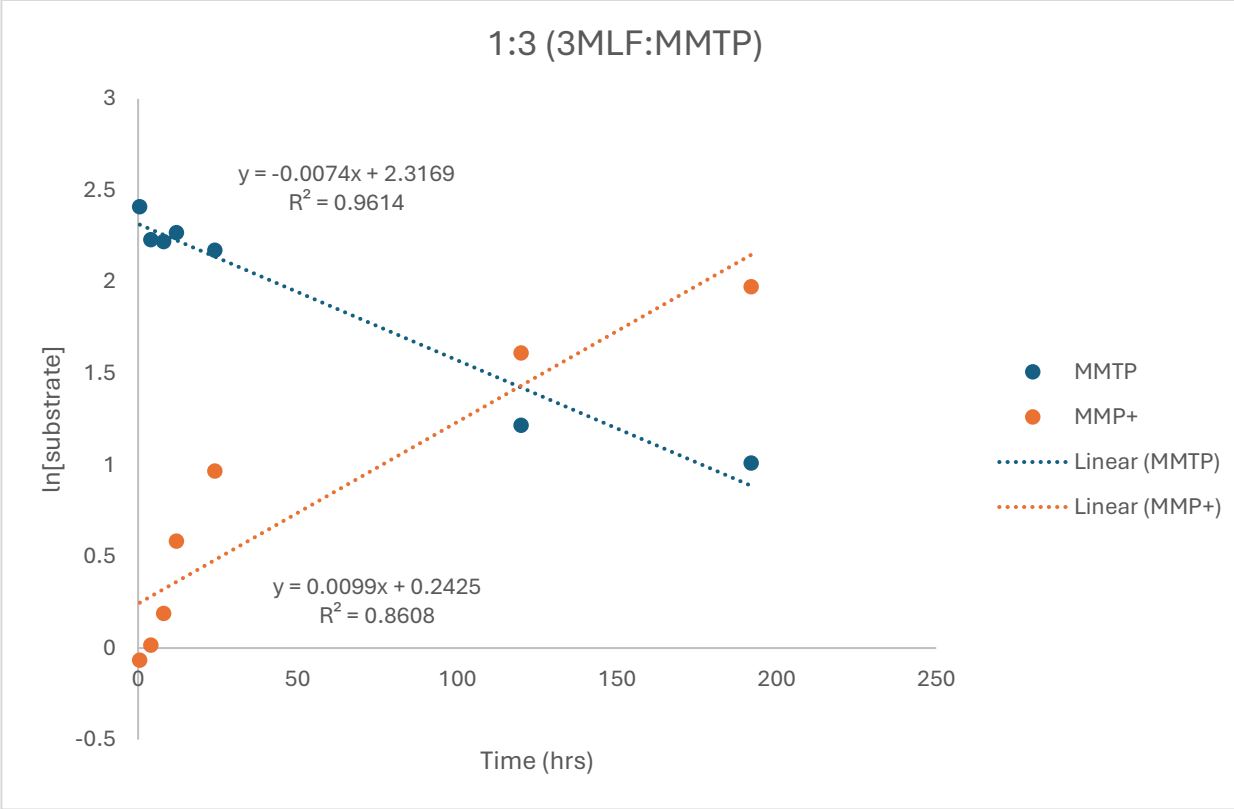

Figure B.21: Plot of ln[MMTP] and ln[MMP^+] vs. time. Obtained from analysis of time-resolved ^1H NMR integrations with a benzene internal standard.

Appendix C: Supporting Information for Exploration of Alternative Flavins for Biomimetic Studies

C.1 Synthesis of 5,10-diethyl-3,7,8-trimethyl-2,4-dioxo-2,3,4,10-tetrahydrobenzo[*g*]pteridin-5-ium perchlorate (ETDFl$^+$ ClO_4^-)

1) Formation of Reduced ETD

10-ethyl-3,7,8-trimethylbenzo[*g*]pteridine-2,4(3*H*,10*H*)-dione (429 mg; 1.51 mmol) was hydrogenated over Pd-C (135.8 mg) in a sealed flask containing ethanol (32.6 mL), water (37.6 mL), hydrochloric acid (4.0 mL), and acetaldehyde (4.0 mL) at room temperature and atmospheric pressure. The reaction mixture was degassed and hydrogenated using an H_2-containing balloon. The reaction was allowed to proceed for 24 hours. The catalyst was filtered out over a vacuum using Celite 545, producing a red filtrate. The filtrate was then evaporated using a rotary evaporator.

2) Conversion of Reduced ETD into 5-Et-ETD$^+$ ClO_4^-

The previous filtrate was dissolved in 2 M $HClO_4$ (25.4 mL) and 70% $HClO_4$ (7.4 mL). Solid $NaClO_4$ (2.16 g) was added followed by $NaNO_2$ (0.78 g) which produced a red-purple smoke. The mixture was stirred while submerged in an ice bath for 4 hours. The dark violet crystals were placed in a vial and dried in a desiccator. The mother liquid was stored in a refrigerator if any more 5-Et-ETD$^+$ ClO_4^- was needed. For the product isolated the yield was about 21%. ^{1}H NMR (400 MHz, cd_3cn) δ 8.21 (s, 1H), 7.95 (s, 1H), 6.08 (s, 1H), 4.84 (d, *J* = 5.4 Hz, 1H), 3.42 (s, 3H), 2.64 (d, *J* = 0.9 Hz, 3H), 2.57 (d, *J* = 1.0 Hz, 3H), 1.78 (t, *J* = 7.1 Hz, 3H), 1.46 (t, *J* = 7.2 Hz, 3H).

C.2 Preparation of Anhydrous Stock Solutions

Crystals of 5-Et-ETD$^+$ and MMTP were placed into a desiccator for 48 hours. Those crystals were removed from the desiccator and quickly covered to minimize air exposure. They were placed into a glove box within two minutes of being removed from the desiccator. Approximately 25 mL of anhydrous CD_3CN (>99%) was placed into a flask for degassing. The acetonitrile was freeze-pump-thaw degassed three times to ensure minimal air in solution. The degassed sample was then transferred into the glove box. To an empty scintillation vial, 31.3 mg of 5-Et-ETD$^+ClO_4^-$ was added and subsequently dissolved into 10.0 mL of the degassed CD_3CN in the glove box. In a separate scintillation vial, 17.6 mg of MMTP was dissolved in 10.0 mL of degassed CD_3CN. The stocks were verified to contain no water by ^{1}H NMR.

C.3 Experimental

NMR spectra were recorded using an Agilent U4-DD2 (400 MHz) or Bruker Avance II (500 MHz). Data analyses were performed using MestreNova. All reactions were prepared using degassed CD_3CN stock solutions. Stocks were kept refrigerated unless being actively used. This was done primarily to maintain consistency in sample preparation. Aerobic reactions were prepared directly in NMR tubes with a total reaction volume of 0.6 mL. To ensure proper and consistent aeration of the sample, the tubes were placed on a mixing table when not being analyzed. Anaerobic reactions were also prepared directly in NMR tubes, but were immediately freeze-pump-thaw degassed (the process started <1 minute after mixing). After degassing, the NMR tubes were flame-sealed. Although control experiments did not suggest that light plays a role in this reaction, tubes were stored in the dark to minimize the risk of photochemical side reactions.

C.4 Identification of 5-Et-ETD$^+$-OH Adduct

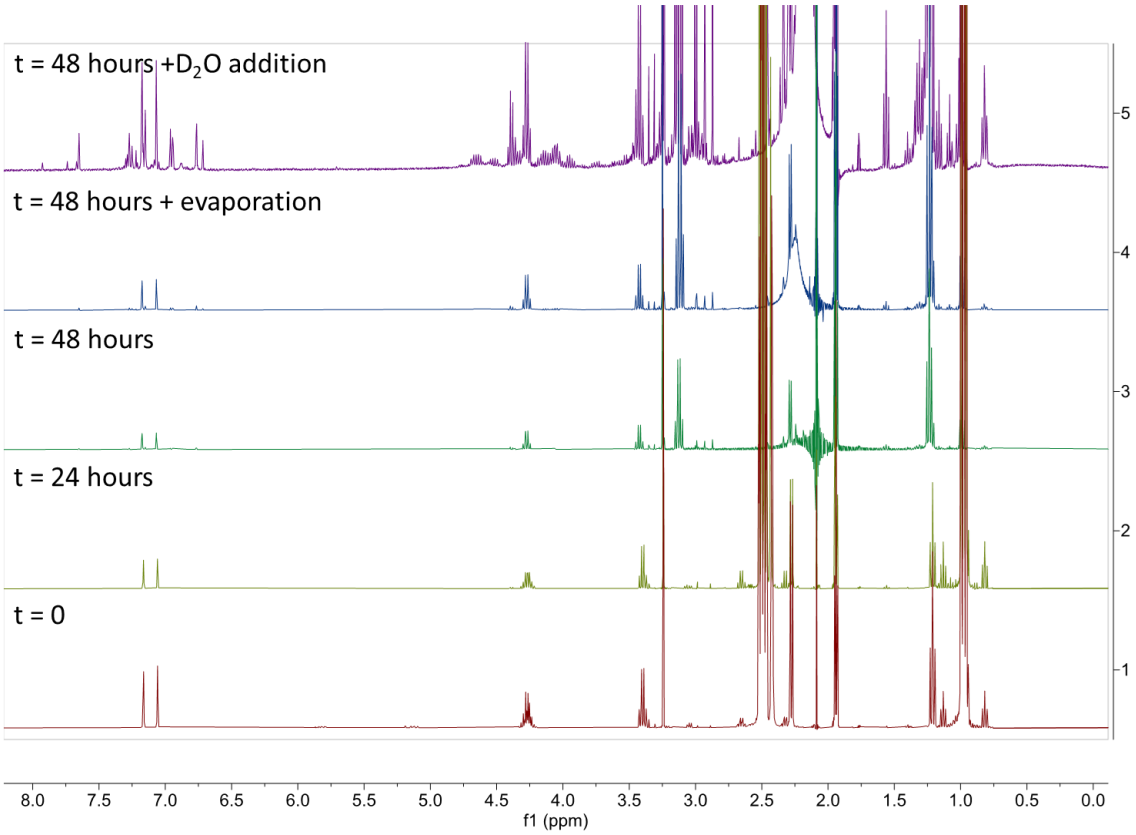

Figure C.1: Several ^{1}H NMR spectra for the 1:1 aerobic reaction of MMTP and 5-Et-ETD$^+$ in the presence of water are shown here. From bottom to top: the reaction at t = 0, t = 24 hours, t = 48 hours, t = 48 hours after the sample was evaporated to remove volatile compounds, and t = 48 hours after addition of D_2O to promote further addition of -OH to 5-Et-ETD$^+$.

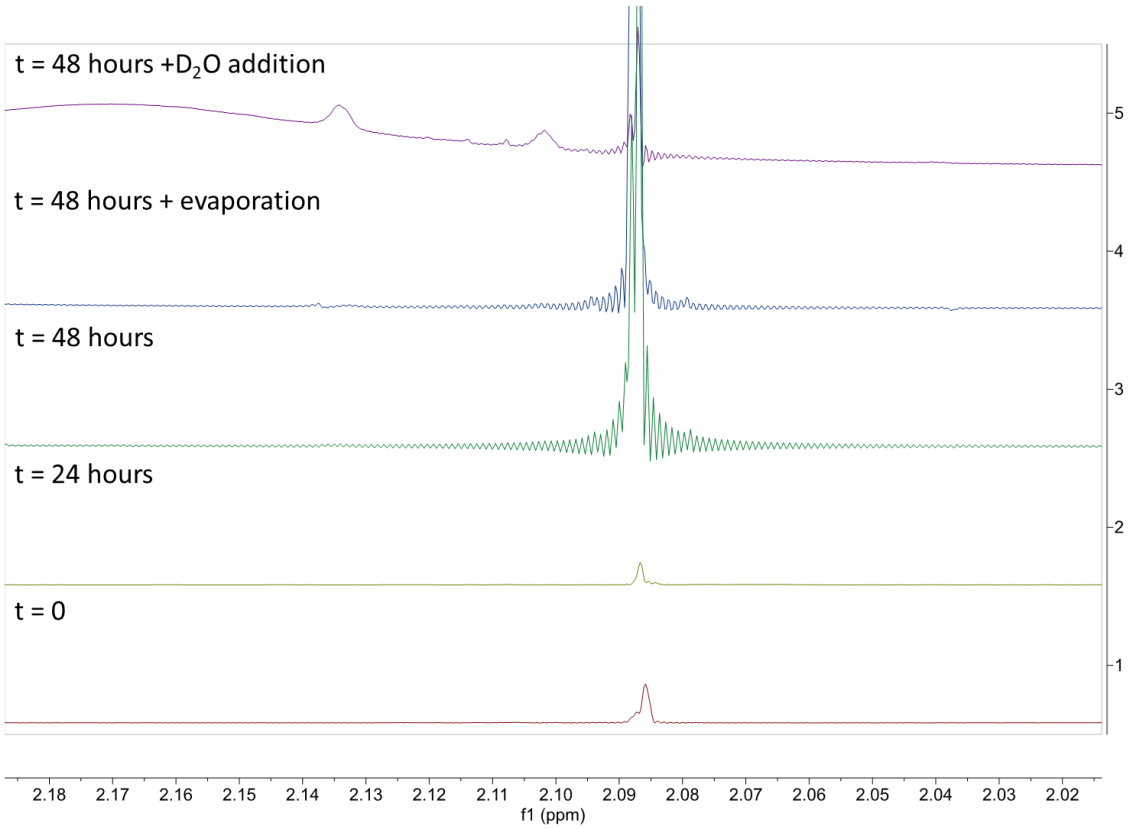

Figure C.2: Several ^{1}H NMR spectra for the aerobic 1:1 reaction of 5-Et-ETD^{+} and MMTP in the presence of water are shown here. From bottom to top: the reaction at t = 0, t = 24 hours, t = 48 hours, t = 48 hours after the sample was evaporated to remove volatile compounds, and t = 48 hours after addition of D_2O to promote further addition of -OH to 5-Et-ETD^{+}. These focus on the diagnostic peak for the -OH adduct at 2.086 ppm.